Joint Program in Molecular Biology

Insight into the degradation pathway of proteins produced by ribosomes stalled at the termination codon

PhD Student: Francesca Cesaratto

Laboratory of Molecular Immunology

ICGEB, Trieste

Supervisor: Dr Oscar R. Burrone

Laboratory of Molecular Immunology

ICGEB, Trieste

Co-supervisor: Dr Gianluca Petris

Laboratory of Molecular Virology

CIBIO, Trento

CONTENTS

ABSTRACT

Protein translation is an essential cellular process that must be efficient, accurate and appropriately regulated to guarantee the correct homeostasis and cell survival. When ribosomes fail to complete protein translation, cells developed mechanisms of quality control that target to degradation both the incomplete polypeptides and the mRNAs. However, more studies are necessary to understand how products originated from ribosome stalled at the ER membrane are recognised and targeted to degradation.

We found that imposing a conventional termination at the C-terminus of the Foot-and-Mouth Disease Virus (FMDV) peptide 2A induced translational stalling at the termination codon of both free and ER-bound mammalian ribosomes. Reporter proteins tagged at their C-terminus with this 2A sequence were highly less expressed in living cells, due to reduced rate of synthesis and proteasomal degradation.

In this PhD project, we exploited the 2A stalling mechanism in mammalian cells to investigate the degradation pathway of polypeptides translated by stalled ER-bound ribosomes. We found that ER-targeted 2A-stalled proteins are inserted in the ER lumen and recognised by the pivotal ER-resident chaperon BiP/GRP78. We hypothesised that BiP/GRP78 binding to peptides derived from stalling ribosomes is responsible of their targeting to degradation mainly via the ER-associated degradation (ERAD) pathway, as in the case of misfolded proteins. In fact, our findings strongly indicated that 2A proteins derived by ER-bound stalled ribosomes are retro-translocated from the ER lumen to the cytosol and processed by the AAA ATPase VCP/p97 and its associated deubiquitinase YOD1 before their proteasomal degradation. Interestingly, we found that also the ribosome-associated quality control E3 ubiquitin ligase Listerin is involved in 2A polypeptides poly-ubiquitination and degradation, suggesting a crosstalk between two different protein quality control systems at the ER membrane in case of ribosomes stalling of translation.

Surprisingly, we obtained indications that the products derived from ER-stalled ribosomes could be not misfolded or unfolded, suggesting that this multiple ER associated quality control system is able to specifically discriminate the products of stalled ribosome from those proteins normally translated with a mechanism different from canonical ERAD, in which the ribosome-associated quality control complex may also have an implication.

In the present study, we identified two C-terminal peptide sequences in the human proteome sharing the same three C-terminal amino acids of 2A, which similarly cause stalling at the STOP-codon and degradation of the associated protein by the ubiquitin-proteasome pathway. These results suggest that the termination codon-mediated stalling could affect a broad range of polypeptide sequences, representing a novel post-translational mechanism to control protein expression. A C-terminal sequence diverse from 2A, known to induce stall of ribosomes in the 3' UTR of the AMD1 mRNA, was also tested and revealed instead a mechanism of stalling different from the one induced by 2A.

INTRODUCTION

All instructions necessary for eukaryotic cells life are contained in their DNA. Genetic information is transferred from genes to messenger RNA (mRNA) in the nucleus and must be codified to generate all the proteins necessary for cellular structure and functions. mRNA is transcribed by RNA polymerases in the nucleus, then it is in most cases spliced, poly-adenylated at the 3' end and capped at 5' end and transferred from the nucleus to the cytosol. Only at this point, it is translated by ribosomes generating cytosolic, nuclear, secretory or membrane proteins. Ribosomes decode every codon contained into an Open Reading Frame into a specific amino acid, exploiting the complementation with the anti-codon in the transfer RNA (tRNA). During translation, codons read-through by ribosomes result in a polypeptide chain that is folded and released at the end of translation to perform its activity in the cell. Protein translation is delicate and complex and requires several quality control processes to avoid formation of toxic elements that can compromise cellular survival. When translation, proteins or ribosomes are damaged or do not work properly, cells are able to eliminate them.

In this introduction is presented an overview of the translational process of eukaryotic cells and the associated mechanisms of quality control and clearance.

1. PRICIPLES OF PROTEIN TRANSLATION IN THE EUKARYOTIC CELL

1.1 TRANSLATION IN EUKARYOTES

The translation process consists in the "conversion" of the message enclosed in the mRNA into a protein, the final product of the gene-expression pathway. The main actor involved is the ribosome, whose two subunits assemble on the mRNA to start and perform translation. The structure of the ribosome is treated in paragraph 1.3.
Protein translation can be divided into four steps: translation initiation, elongation, termination, and ribosome recycling.

Translation initiation

Translation initiation is a multistep process extremely complex that involves several proteins, such as the eukaryotic Initiation Factors (eIFs). As schematised in Figure 1, a protein complex containing eIF2-GTP-Met-tRNAi binds to a second complex composed by the small ribosomal subunit (40S) and eIFs 3, 1, 1A and 5, forming the cytosolic 43S pre-initiation complex. At the same time, the eIF4F complex constituted by eIF4A, E and G binds the mRNA 5'-cap, uncoils the 5'-UTR structures and cooperating with eIF3 and the poly(A) binding protein (PABP), it loads a molecule of mRNA into the 43S complex. At this point, the newly formed 48S complex scans the mRNA until the recognition of the initiation codon (AUG). In this way, it takes place the very first event of codon-anticodon base pairing between the AUG and the initiation tRNA (Met-tRNAi), already part of the 43S pre-initiation complex. This process triggers the eIF2-bound GTP hydrolysis with consequent dissociation between eIF2-GDP and Met-tRNAi and the eIFs release from the 40S subunit, leaving only the Met-tRNAi paired with AUG codon. Next, eIF5B-GTP modulates the binding of the large ribosome subunit (60S) to the 40S-Met-tRNAi-mRNA complex and dissociates from the

complex upon GTP hydrolysis, thus forming the 80S ribosome. The ribosome is now competent for polypeptide synthesis (Gebauer and Hentze, 2004; Kapp and Lorsch, 2004).

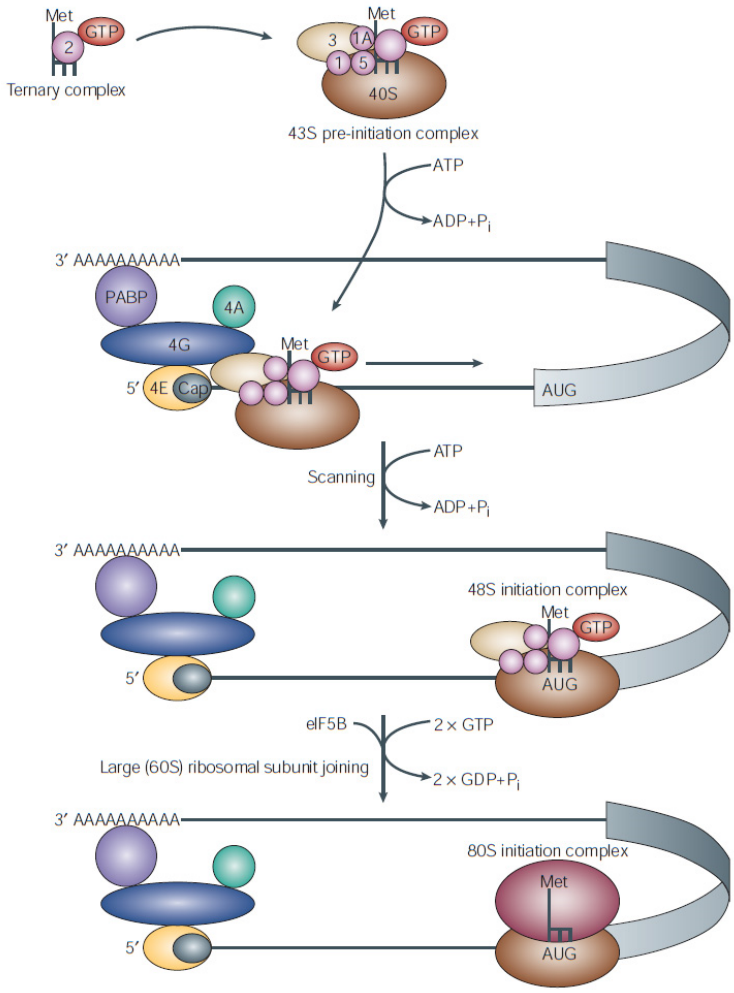

Figure 1. A scheme of the eukaryotic translation initiation: the ternary complex eIF2-GTP-Met-tRNAi binds the small ribosomal subunit (40S) and eIFs 3, 1, 1A and 5, forming the 43S pre-initiation complex, which is loaded with mRNA by the eIF4F complex (eIF4A, E and G), eIF3 and PABP (Gebauer and Hentze, 2004). The 48S complex scans the mRNA and, upon recognition of the AUG-codon, eIF5B regulates 60S joining to form the 80S initiation complex ready for polypeptide translation.

Translation elongation

As represented in Figure 2, at the end of translation initiation the peptidyl-tRNA is in the peptidyl (P) site of the 80S ribosome, with a free aminoacyl (A) site that can accommodate an amynoacil-tRNA-GTP-eEF1A complex (where eEFs stands for eukaryotic Elongation Factor). In this site, the pairing between the triplet on mRNA and the correct cognate tRNA

allows to proceed with elongation. Codon-anticodon interaction causes a shift of three bases in the 40S rRNA and their interaction with the mRNA-tRNA duplex, with GTP hydrolysis and the consequent release of eEF1A-GDP from the aminoacyl-tRNA into the A site. At this point, the nascent chain must be transferred from the tRNA in the P site to the aminoacyl-tRNA present in the A site, with formation of a new peptide bond, catalysed by the peptidyl transferase centre (PTC) of the ribosome. The remaining deacylated-tRNA is translocated by eEF2 from the P to the adjacent exit (E) site and the new peptidyl-tRNA from the A to the P site. The cycle is repeated until a STOP-codon (UAA, UGA or UAG) enters the A site of the translating ribosome (Gebauer and Hentze, 2004; Kapp and Lorsch, 2004).

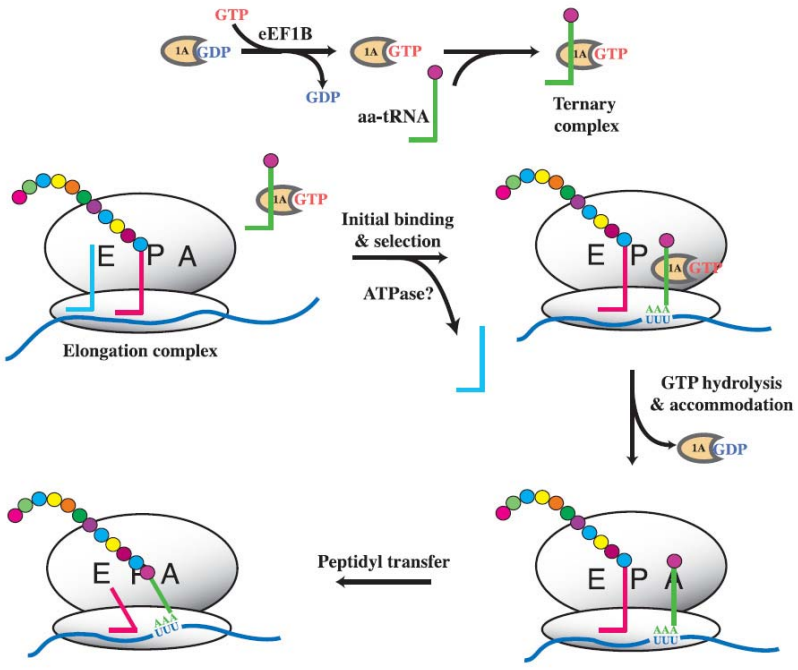

Figure 2. The eukaryotic translation elongation. An amynoacil-tRNA-GTP-eEF1A complex enters the A site to proceed with codon-anticodon pairing. The nascent chain is then transferred from the P site to the aminoacyl-tRNA in the A site. The new peptidyl-tRNA moves from the A to the P site, while the deacylated-tRNA is translocated from the P to the E site (Kapp and Lorsch, 2004).

Translation termination

When ribosomes recognise a STOP-codon, protein synthesis must be terminated. Translation termination is mediated by two classes of Release Factors (RFs), class I and class II. Eukaryotes have evolved to have only eRF1 for the class I and eRF3 for the class II. eRF1

recognizes all three STOP-codons and binds to the 40S A site to trigger hydrolysis of the ester bond between the nascent polypeptide and the tRNA in the P site of the 60S PTC, while class II eRF3 enhance the activity of eRF1 with its GTPase activity (Korostelev, 2011). eRF1 is composed by three domains: N, M and C. The first one carries the conserved NIKS and YxCxxxF domains for STOP-codons recognition, probably through a three-dimensional structure formed within the 40S decoding centre. The M domain contains the highly conserved GGQ domain, responsible of the peptidyl-tRNA hydrolysis and of enhancing the affinity for eRF3 by stimulating its GTPase activity. The C domain mediates in a highly specific manner the interaction with eRF3, whose function is to couple the eRF1-mediated codon recognition with the peptidyl-tRNA hydrolysis, and to efficiently release the polypeptide chain (Figure 3) (Alkalaeva et al., 2006; Cheng et al., 2009; Kononenko et al., 2008; Song et al., 2000). eRF1 and eRF3 form a stable long-lived complex and show a mutual interdependence, but their detailed functions still have to be completely understood. It was suggested that eRF1 promotes GTP but not GDP binding to eRF3 and induces eRF3 GTPase activity on the ribosome, while eRF3 stimulates peptide release by eRF1 (Cheng et al., 2009).

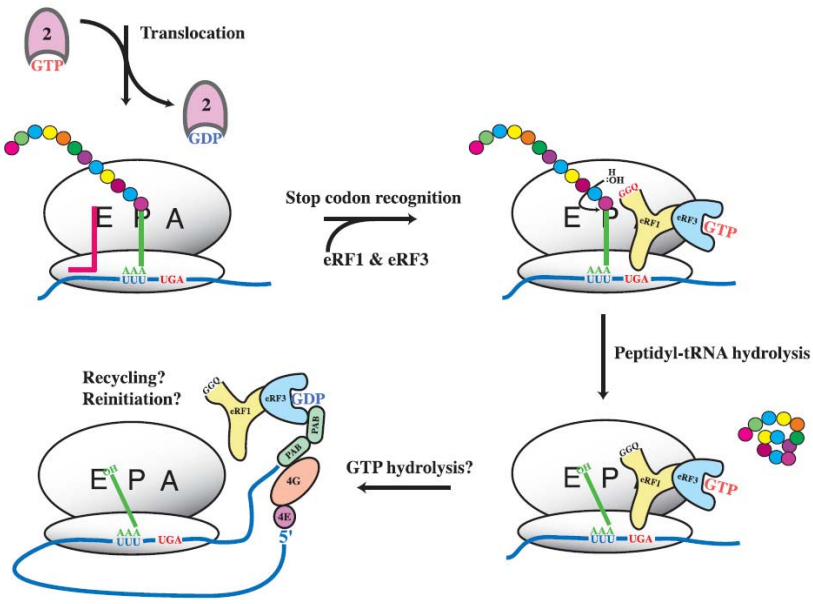

Figure 3. The eukaryotic translation termination. When a termination codon enters the A site, eRF1 in complex with eRF3 accommodates in the ribosome and induces the polypeptide hydrolysis from the tRNA, through eRF3 activity (Kapp and Lorsch, 2004).

Ribosome Recycling

Ribosome recycling takes place after translation termination, but it occurs also as a control mechanism when ribosomes assembly is not correct or when ribosomes are translationally stalled (see paragraph 4.2). The 80S ribosome is disassembled in the two large and small subunits to recycle them for other rounds of translation or to degrade aberrant components; however, this process is still unclear.

A recent work identified a member of the ATP-binding cassette (ABC) family, the ABCE1/Rli1, as the major player involved in 80S ribosome splitting *in vivo*, thus allowing to understand more the process. At first, it was thought that the recycling was promoted by the combination of eIFs 3, 1, 1A and 3j, because the eIF3 was able to split post-termination ribosomes by its own *in vitro* under certain conditions, and its function was enhanced by eIF3j and at a less extent by erF1 and 1A (Pisarev et al., 2010, 2007). Now, it was demonstrated that ABCE1 is recruited once the eRF3 dissociates from the termination complex and it stimulates 80S splitting by ATP hydrolysis (Figure 4). After 60S dissociation, how tRNA, eRF1, mRNA and ABCE1 itself are dismissed is not yet known, while the remaining 40S-eIF3-eIF1-eIF1A complex is thought to be recycled as a starting point for the assembly of the 43S pre-initiation complex (Kapp and Lorsch, 2004; Pisarev et al., 2007).

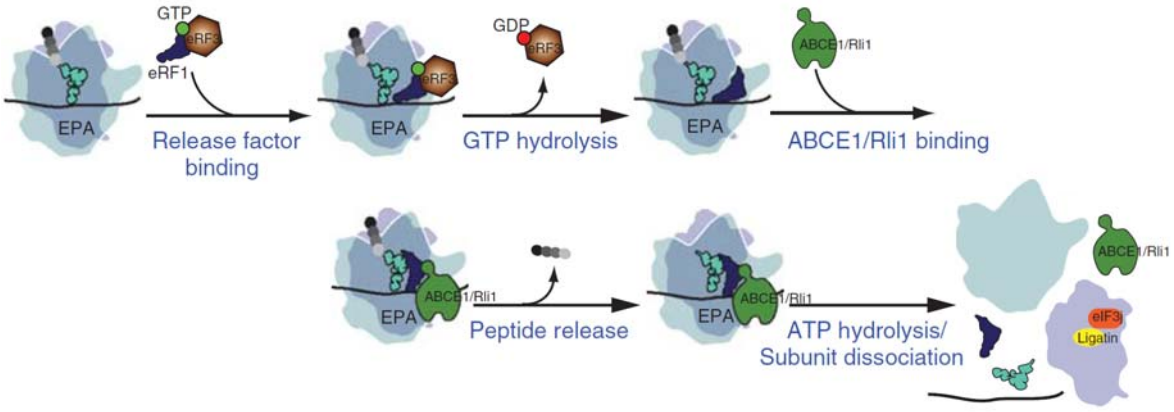

Figure 4. In the current model of the eukaryotic ribosome recycling pathway, the complex from by eRF1 and eRF3-GTP binds to the A site of the ribosome upon recognition of a STOP-codon. eRF3 is released after GTP hydrolyses and ABCE1/Rli1 binds eRF1 and favours its activity of tRNA hydrolysis and protein release. ABCE1 then stimulates 60S subunit separation by ATP hydrolysis (Dever and Green, 2012).

5 domains of ABCE1 have been identified and characterised by structural studies: the N-terminus, which contains two FeS domains, two Nucleotide Binding Domains (NBD) for ATP and two Hinge regions. ABCE1 binds the small subunit of the ribosome with the hinge domain and NBD and eRF1 with the FeS domain.

The binding of ABCE1 to eRF1, which remained in the A site of the 80S ribosome after eRF3 GTP hydrolysis, is thought to stimulate peptide release in an ATP-independent way that is not clearly understood yet (Nürenberg and Tampé, 2013).

STOP-codon-independent termination

Nevertheless, it was described a type of termination that did not depend on the presence of a STOP-codon and can therefore be considered a non-conventional termination. It concerns a viral peptide, known as peptide 2A. 2A was originally identified in Picornaviruses, which have a single stranded RNA genome of positive polarity that bears a single ORF. This ORF encodes a single polyprotein that needs to be processed to produce all viral proteins (Donnelly et al., 1997). Most of this processing is post-translational and mediated by viral and cellular proteases, while 2A allows the processing between the group of capsid proteins and the one of replicative proteins during translation, and not after. 2A is a highly conserved 19 amino acids-long peptide, particularly at the C-terminus, where the Asn-Pro-Gly amino acids with the downstream Pro are described to be essential for its activity. When the ribosome translates 2A, the peptide is accommodated within the RET as a α-helix with a turn at the C-terminus that induces a pause in translation, thus promoting hydrolysis of the ester bond between the nascent peptide and the tRNA, rather than the formation of the peptide linkage between the last Gly and the following Pro (Donnelly et al., 2001b; Ryan et al., 1999). In this way, the upstream protein is terminated without the participation of a STOP-codon and released from the ribosome leaving the Gly as the C-terminal amino acid. The ribosome then continues translation from the Pro, which remains as the N-terminal residue of the downstream protein (Figure 5) (Donnelly et al., 2001b; Ryan et al., 1999).

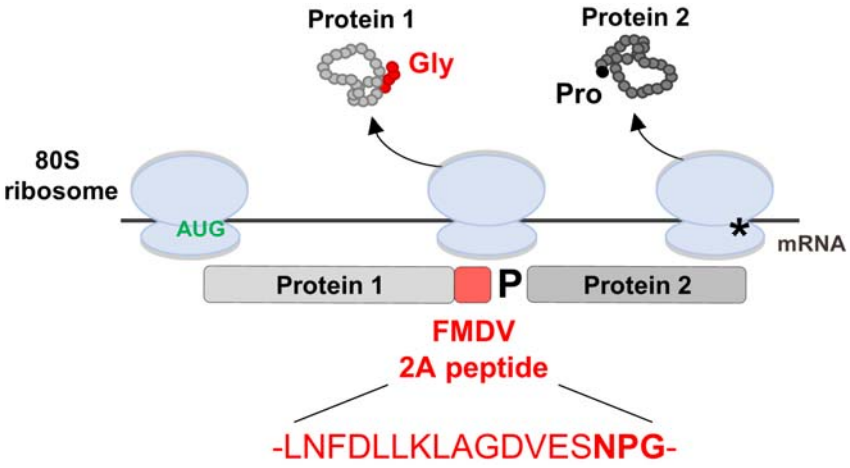

Figure 5. Schematic representation of the processing 2A peptide from the Foot-and-Mouth Disease Virus (FMDV). When ribosomes translate the amino acidic sequence of 2A, it causes a slowdown of translation, allowing the release of the upstream Protein 1 without ribosome's dissociation from the mRNA. Protein 1 terminates with NPG amino acids (indicated in bold red), while the downstream Protein 2 is translated starting to the following Pro codon (in black).

Although peptide 2A was first considered as an autonomous element, capable of self-processing at its C-terminus, there are evidences that suggest an involvement of both eRF1 and eRF3 (Figure 6) (Doronina et al., 2008b, 2008a). According to this model, the ribosomes stalled by the presence of peptide 2A in the RET should promote engagement in the A site of the eRFs instead of $tRNA^{Pro}$, thus inducing the release of the upstream protein, and subsequent dissociation of the eRFs should facilitate prolyl-$tRNA^{Pro}$ access to the A site to continue elongation of the downstream peptide chain (Luke et al., 2009). This mechanism, however, is not properly demonstrated and remains unclear.

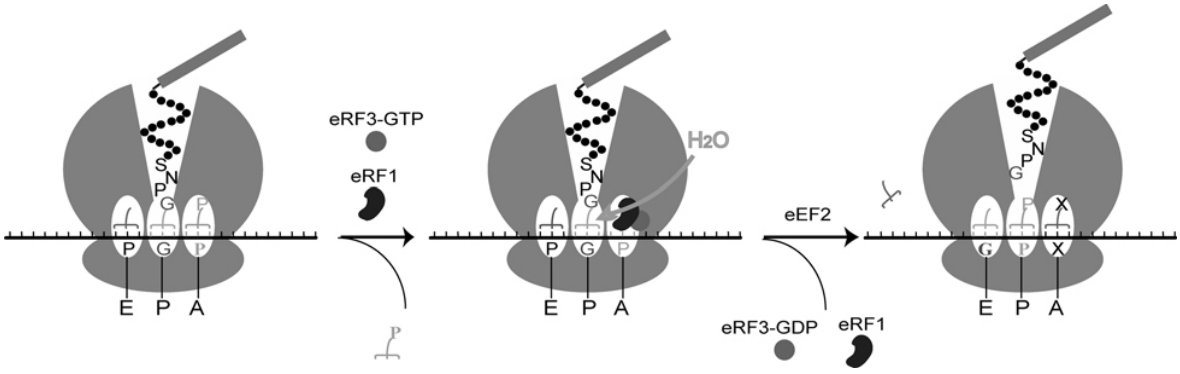

Figure 6. The current model proposed for 2A peptide STOP codon-independent termination, which is believed to require eRF1-3-mediated termination at the A site of ribosome, instead of forming the peptide bond between the $tRNA^{Pro}$ and the nascent chain (Yan et al, 2010).

1.2 TRANSLATION OF PROTEINS OF THE SECRETORY PATHWAY

The Endoplasmic Reticulum (ER) is a complex organelle of eukaryotic cells, discovered by Keith Porter, Albert Claude ed Ernest Fullam in 1945. The ER is essential for the correct folding and targeting of secretory and membrane proteins. In fact, in the ER lumen there are many enzymes that function as chaperones, favouring solubility of these proteins during the acquisition of their proper fold. The lumen differs from the cytosol for its oxidising environment and a higher ionic calcium concentration (Borghese et al., 2006).
Proteins targeted for secretion or to the plasma membrane are translocated into the ER lumen during their synthesis. It was estimated that about one third of all cellular proteins take this path (Aridor, 2007). Translation of the majority of these proteins begin in the cytosol with a short hydrophobic sequence encoded at the N-terminus called the signal peptide (SP). SP is co-translationally recognized and bound by a cytosolic Signal Recognition Particle (SRP). SRP binding with SP dramatically increases its affinity for the ribosome, pausing translation to allow the GTP-dependent dislocation of the whole complex to the cytosolic face of the ER membrane, where the SRP receptor (SR) is located (Johnson and van Waes, 1999; Nyathi et al., 2013). The interaction between SRP and SR causes conformational rearrangements that reduce the affinity of SRP for the translating ribosome, facilitating its transfer to the translocon, which co-localizes with SR (Nyathi et al., 2013; Rapoport et al., 1996; Shan and Walter, 2005). Once into the lumen, the SP is removed by a specific signal peptidase (Rutishauser and Spiess, 2002) and the ER resident chaperones allow the nascent proteins to acquire their right conformation (Ellgaard and Helenius, 2003).

The **translocon** is a protein channel formed by the Sec61 complex in eukaryotes and SecY in prokaryotes, by which native proteins can cross the ER membrane during translation to reach the lumen (Figure 7). Sec61 is composed by three subunits: the two essential and highly conserved α and γ subunits, and a less conserved and non-essential subunit β. It has an hourglass structure inserted within the ER membrane. A face of the hourglass is directed towards the ER lumen, while the other is in the cytosol and they are connected by a central pore, formed prevalently by the α subunit (Figure 6, right panel). It has been calculated that the inner channel can accommodate around 30 amino acids (Liao et al., 1997). The cytosolic

side of the channel has a funnel-like shape, with a diameter of 20-25 Å and a constriction in the membrane middle. This structure corresponds to a closed, impermeable pore, blocked at the bottom of the funnel by the so-called “plug”, a helix of the α subunit that separates the cytosolic environment from the luminal space. In its narrowest point, six hydrophobic amino acids form a “pore ring” of 5-8 Å that can reach 20 Å upon interaction between the SP and the translocon, thus allowing the channel opening and the passage of only stretches or partially assembled proteins. During the co-translational translocation, the ring forms a seal around the nascent peptide to avoid the entrance of other molecules. At the end of the translocation, the plug returns to block the channel (Berg et al., 2004; Li et al., 2007; Rapoport, 2007).

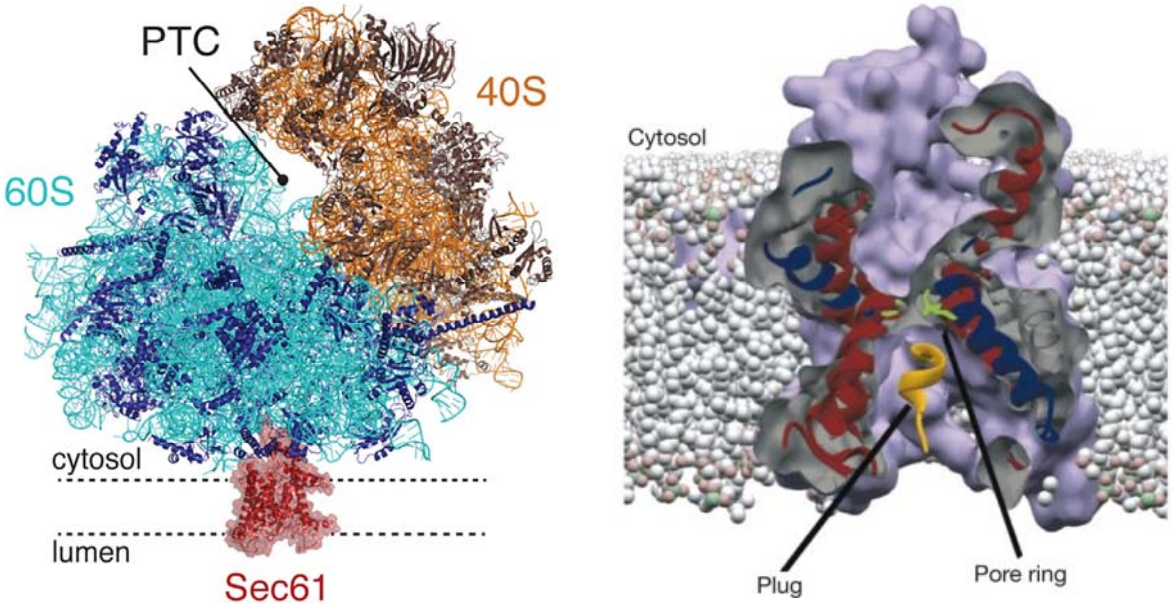

Figure 7. The translocation of nascent proteins trough the ER membrane. On the left panel, the structure of the ribosome in complex with the Sec61 translocon, the ribosome subunits and the PTC are indicated (Voorhees et al., 2014). On the right panel, the structure of the SecY channel within the ER membrane. In blue and red are indicated two transmembrane segments of the α subunits, in grey the β and γ subunits, in yellow the plug and the central hydrophobic residues are in green (Rapoport, 2007).

1.3 STRUCTURE OF THE EUKARYOTIC RIBOSOME

The ribosome is a large ribonucleoprotein complex that has different dimensions depending on the belonging species; in the case of humans, the 80S ribosome has a molecular weight of 4.3 MDa. The ribosome is in charge of translating the cellular mRNA into amino acidic sequences, the proteins. By complementarity of the anti-codon on the tRNA with a nucleic triplet on the mRNA, the corresponding aminoacyl-tRNA is selected thus allowing elongation of the polypeptide chain by the ribosome peptidyl transferase activity, until it recognises a termination codon. Translations at single-mRNA resolution demonstrated that a translating ribosome can incorporate a range of 3-10 amino acids per second (Kramer et al., 2009; Morisaki et al., 2016; Wu et al., 2016; Zhu et al., 2016).

The eukaryotic ribosome is characterised by a small and a large subunit, called 40S and 60S respectively, where "S" means the sedimentation rate upon ultracentrifugation expressed in Svedberg, defined as a measure of time ($1S = 10^{-13}$ seconds). To initiate translation, the two subunits interact with each other to form a unique complex, the 80S ribosome, through the formation of contact points known as inter-subunit bridges, formed by the binding of 60S proteins to a large part of the small subunit structure (Khatter et al., 2015; Melnikov et al., 2012).

The 40S subunit

The small subunit is a ribonucleoprotein complex composed by a single 18S RNA chain (1870 nucleotides long) and 33 proteins (Figure 8A) and is organised in seven regions (head, neck, body, platform, beak, shoulder and foots). This subunit is endorsed of the decoding function and contains three functional sites: the mRNA path, which drives mRNA during translation; the decoding centre, where occurs the codon-anticodon recognition and the translation fidelity is ensured; the three tRNA-binding sites, amino-acyl (A) site, peptidyl (P) site and exit (E) site. As described above, during the translation process the aminoacyl-tRNA enters at the A site, then it is conjugated at the nascent peptide forming the peptidyl-tRNA in the P site and, once in the E site, the tRNA dissociates from the ribosome (Melnikov et al., 2012; Rabl et al., 2011; Steitz, 2008).

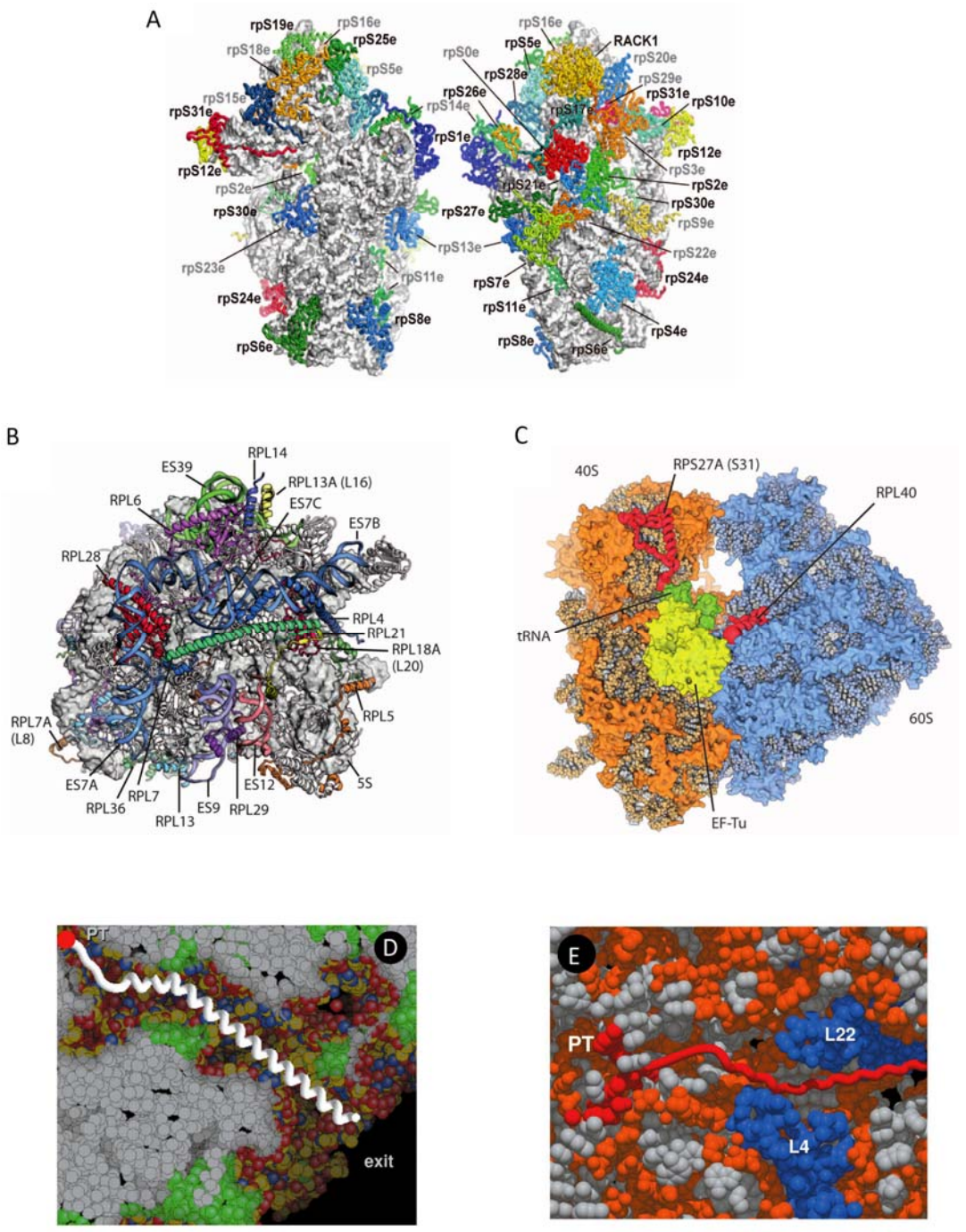

Figure 8. The eukaryotic ribosome. **A:** Crystal structure of the ribosome subunit 40S with the 18S rRNA as spheres and coloured according to each domain (5' domain, red; central domain, green; 3' major domain, yellow; 3' minor domain, blue; ESs, magenta), and the proteins as gray cartoons (abbreviations: H, head; Be, beak; N, neck; P, platform; Sh, shoulder; Bo, body; RF, right foot; LF, left foot) (Rabl et al., 2011). **B:** Overview of 60S ribosomal proteins (conserved proteins in white; eukaryotic-specific proteins or protein extensions color-coded) (Klinge et al., 2011). **C:** the 80S ribosome (EF-Tu in yellow, tRNA in green, 40S rRNA and proteins in orange, 60S rRNAs and proteins in light blue) (Klinge et al., 2011). **D and E:** the Ribosomal Exit Tunnel, with a particular of the tunnel restriction between L4 and L22 (coloured in green in D and blue in E) (Nissen et al., 2000).

The 60S subunit

The large ribosomal subunit is responsible of the ribosome's catalytic function. It is composed by 5S RNA, 5.8S RNA, 28S RNA (121, 156, and 5034 bases respectively) and 47 proteins (Figure 8B). Structurally, it is divided in three regions (the central protuberance, the L1 stalk and the P stalk) and is characterised by two main structures, the peptidyl transferase centre (PTC) and the ribosome exit tunnel (RET). Within the PTC, a peptidyl transferase catalyses the peptide bond formation between the nascent peptide chain and the next amino acid. At the termination codon, the ester bond between the tRNA and the nascent proteins is hydrolysed by the activity of mammalian eRF1 and eRF3, with the consequent release of the polypeptide chain.

The Ribosome Exit Tunnel

The RET is a complex tube-like structure, where the newly synthesised polypeptide is accommodated to exit from the ribosome and reach the solvent side (Klinge et al., 2011; Kramer et al., 2009; Melnikov et al., 2012). It originates at the level of the PTC and passes through the 60S subunit. In prokaryotes, RET was estimated to have a length of 80-100 Å and a diameter of 10 Å at its narrowest and 20 Å at its largest point (Nissen et al., 2000). However, eukaryotic ribosomes are larger and the RET was described to accommodate polypeptides from 30 to 60 amino acids, depending if their conformation is extended or α-helical. The tunnel's inner surface is negatively charged and constituted mainly by 28S rRNA, while the ribosomal proteins L4, L22 and L23 forming protruding loops. In particular, two β-hairpin loops that belong to L22 and L4A cause a constriction of the tunnel at a distance of 20 Å from the PTC, and not of 30 Å as observed for prokaryotic (Klinge et al., 2011) (Figure 8D and 8E). At the end of the tunnel, the RET enlarges because of the presence of a ring of four conserved ribosomal proteins (L25, L26, L35 and L39e), RNA and other proteins that are specific for the different kingdoms (L19e and L31e in eukaryotes) (Klinge et al., 2011; Kramer et al., 2009; Nissen et al., 2000).

It was proposed that the RET, thanks to its constricted part and its negative charged environment, can act as a discriminating gate by interaction with nascent chains, pausing or slowing the rate of translation. For example, translational elongation and termination can be affected by the nature of the amino acids side-chains located inside the RET, thus

forming stalled ribosome in complex with the peptide. Mutations inserted in the rRNAs or proteins of the exit tunnel prevent the formation of these complexes, inducing structural rearrangements of the ribosome. These findings suggest that stalling can be specifically trigger by the interactions between the RET and the nascent chain (Lu and Deutsch, 2008; Yap and Bernstein, 2009). The current model describes ribosomes not as passive conduits, but as active players capable of sensing the newly synthesised amino acidic chains and modulating translation as a response (Lu and Deutsch, 2008; Nakatogawa and Ito, 2002; Ramu et al., 2011; Wilson and Beckmann, 2011; Yap and Bernstein, 2009).

Translation regulation through the RET. In prokaryotes and eukaryotes there are several examples of translational control mediated by peptide sequences interacting with the RET: the upstream Open Reading Frames (uORFs), short ORFs found in the mRNA 5'-untranslated region (UTR). A ribosome is able to recognize and translate an uORF and, as a consequence, can modulate the expression of a primary ORF located downstream in several ways: it can remain associated with the mRNA and reinitiate the translation at the next start codon; or it can remain stuck during elongation or termination (ribosome stalling), blocking the scanning of the other ribosomes; or it can alter mRNA stability, inducing its degradation (Ruan et al., 1996; Spevak et al., 2010; Wang and Sachs, 1997). Some of the most well-characterised uORFs that encode sequences interacting with the RET that can cause ribosome stalling are the bacterial SecM (secretion monitor, regulatory peptide for secA gene expression) and TnaC (regulatory peptide for tryptophanase expression) (Yan et al., 2010). In eukaryotes, there are the fungal arginine attenuator peptide (AAP) and the uORF2 of human Cytomegalovirus (hCMV) glycoprotein gp48 (or UL4 uORF2), whose interactions with the RET are well characterised (Bhushan et al., 2010), and the S-adenosyl-L-methionine decarboxylase (AdoMetDC) uORF, found both in mammals and plants (Law et al., 2001; Uchiyama-Kadokura et al., 2014). Most of them, except for UL4 uORF2, modulate the activity of the translating ribosomes in response to the presence of a trans-acting effector element, such as tryptophan or arginine. However, even if there are many uORFs described, little homology was detected among their amino acidic sequences or their mechanisms to induce translation regulation (Bhushan et al., 2010; Morris and Geballe, 2000). For example, while UL4 uORF2 (MQPLVLSAKKLSSLLTCKYIPP), TnaC (MNILHICVTSKWFNIDNKIVDHRP) and AAP (MNGRPSVFTSQDYLSDHLWRALNA) codify

for 22-24 amino acid sequences, AdoMetDC uORF decodes only a short oligopeptide (MAGDIS).

Other peptides were described to cause only translational pausing or slowdown, such as the viral peptide 2A or the signal peptide (SP) for translocation to the Endoplasmic Reticulum (ER) translocon, which will be discussed later.

Of interest, a recent work suggested another level of translational control of AdoMetDC, modulated by an independent ORF found downstream the primary one, in the 3' end (Yordanova et al., 2018), suggesting that this mechanism of translation regulation is even more complex and diffused than expected.

2. CO-TRANSLATIONAL QUALITY CONTROL

Protein synthesis, protein folding and proteome homeostasis are crucial for cell survival. Aberrant or damaged mRNAs, in fact, may be translated into proteins that can have deleterious effects or ribosomes can remain stalled on such mRNAs during translation, without being able to continue protein synthesis or release of the peptide and dissociate, a behaviour known as stalling of translation. To safeguard and survey translational and folding processes, eukaryotic cells have evolved multiple co-translational quality control (QC) mechanisms, at the level of both, the translating mRNA and the nascent polypeptide.

2.1 QUALITY CONTROL AT THE mRNA LEVEL

Newly synthetized molecules of mRNA are tested in a first cycle of QC to avoid translation of truncated or non-functional transcripts. Aberrant mRNAs can cause translational stalling of ribosomes and this condition induce the degradation of the messenger, instead of its reuse for next cycles of protein synthesis. Based on the type of damage, stalling specifically triggers one of the following pathways (Lykke-Andersen and Bennett, 2014; Shoemaker and Green, 2012):

- the nonsense-mediated decay (NMD), for mRNAs containing a premature termination codon;
- the non-stop decay (NSD), which targets mRNAs lacking a termination codon;
- the no-go decay (NGD), which targets mRNAs containing various stalling sequences.

The **NMD** was the first surveillance pathway identified and is one of the most studied. The NMD machinery in yeast and mammals is composed by three highly conserved trans-acting factors, called up-frameshift (UPF) proteins UPF1, UPF2 and UPF3 and proteins of the SMG family, first recognised in yeast as Suppressor with Morphogenetic effect on Genitalia (Chang et al., 2007). While UFP2 and UPF3 are part of the exon-exon junction complex (EJC), UPF1 is an ATP-dependent RNA helicase recruited on the mRNA upon recognition of a premature termination codon to start the disassembly of the mRNA, thus allowing its

degradation. How UPF/SMG distinguish a normal STOP-codon from a premature one is not completely clear. A few models were suggested (Figure 9): in the 3' UTR model, the distance between a premature STOP-codon and the 3' UTR, and the absence of the poly(A)-binding protein (PABP), do not allow an efficient termination (Amrani et al., 2004); in the EJC model if the premature STOP-codon arises before an exon junction, the ribosome could not remove the complex from the mRNA and its presence results in a signal for NMD (Chang et al., 2007).

The NDM leads to degradation of aberrant mRNA by endonucleases activity and repression of ribosomes recruitment to this mRNA on one side, and to the targeting of native polypeptide to proteolysis on the other side.

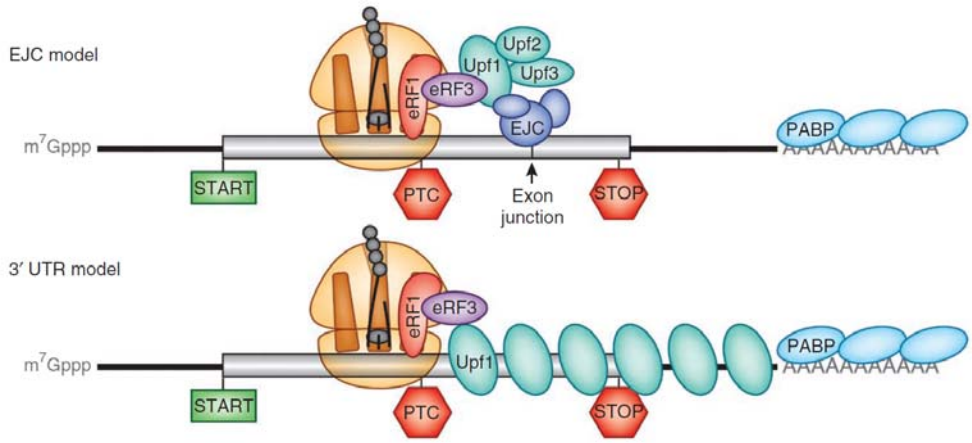

Figure 9. The eukaryotic NMD pathway can be triggered by a premature termination codon in proximity of a Exon Junction Complex (EJC model, upper panel) or far from the poly(A) (the 3'UTR model, lower panel) (Shoemaker and Green, 2012).

The **NSD** occurs in the cytosol when a translating ribosome reaches the mRNA 3' end without encountering a termination codon, thus extending translation into the poly(A) tail, which codes for a poly-Lysine C-terminal tail that causes ribosome stalling and consequently RNA decay. In fact, as explained previously, relatively long stretches of basic residues such as poly-Lys embedded in the negatively charged environment of the RET can block ribosome translation.

In yeast the most important factors involved are Ski7, which tags mRNA for 3'-to-5' degradation by the exosome, and the Dom34-Hbs1 complex, which is part of the

ribosome-associated quality control complex (discussed in chapter 4) and promotes ribosomes disassembly and nascent peptide degradation (Figure 10, left panel) (Klauer and van Hoof, 2012; Pisareva et al., 2011; Tsuboi et al., 2012).

In mammals the mechanism of NSD remains unclear, but there are indications of the involvement of the exosome Ski-complex and Pelota-Hbs1 (Aly et al., 2016; Saito et al., 2013).

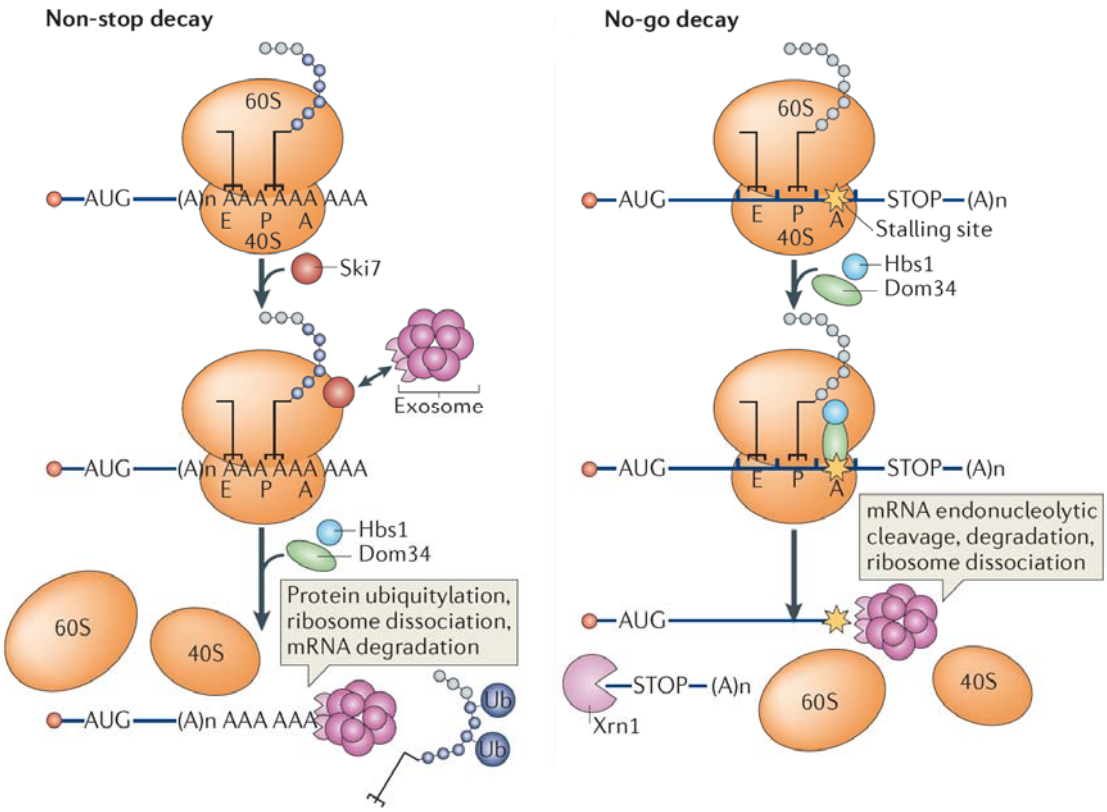

Figure 10. Models of the eukaryotic NSD pathway on the left side, and of NGD on the right side (Graille and Séraphin, 2012).

The **NGD** is triggered by different kinds of defects such as RNA structural elements, rare codons and mRNA depurination by viral enzymes. These damages cause ribosome stalling in the middle of translation, requiring 3'-to-5 'mRNA degradation by the exosome at the 5' fragment, and the 5'-to-3' degradation by Xrn1 at the 3' fragment (Figure 10, right panel). The Dom34-Hbs1 complex was found to play an essential role in this pathway as well, stimulating the initial mRNA endonucleolytic cleavage near the ribosome stalling site (Doma and Parker, 2006).

2.2 QUALITY CONTROL AT THE PROTEIN LEVEL

Protein folding is a delicate and error-prone pathway and nascent proteins that fail to acquire their proper structure are identified and eliminated. Eukaryotic cells evolved strategies to safeguard folding process, involving two groups of molecular chaperones: the chaperones linked to protein synthesis (CLIPS) that bind both the ribosome and the nascent peptide thus controlling the earlier folding steps, and the Hsp70/40 and Hsp60/10 chaperone families, cytosolic proteins not associated to the ribosome (Pechmann et al., 2013; Preissler and Deuerling, 2012). The main members of CLIPS are the nascent polypeptide-associated complex (NAC) and the ribosome-associated complex (RAC).

NAC is a widely conserved heterodimeric protein that associates with ribosomes in 1:1 stoichiometry and was characterized as the first cytosolic factor that binds nascent polypeptides emerging from the ribosome, preventing incorrect interactions with other factors (Wiedmann et al., 1994). It is composed by the subunits α-NAC (NACA) and a β-NAC (BTF3b) that dimerise through their homologous six-stranded β-barrel-like NAC domains. The BTF3b N-terminal ribosome-binding domain directly binds both the nascent polypeptide and the ribosome near the RET exit site, and this interaction is considered a prerequisite for NACA binding to the nascent peptide (Beatrix et al., 2000). NACA does not contact the ribosome and contains also a C-terminal ubiquitin-associated domain, suggesting different functions of the two subunits (Liu et al., 2010; Spreter et al., 2005).
It has recently been discovered that NAC interacts with the signal recognition particle (SRP): in particular, it seems that the presence of SRP is sensed within the RET to pre-emptively recruit SRP to the ribosome in a manner modulated by NAC, thus controlling the fidelity of protein translocation to the ER by increasing SRP specificity (Zhang et al., 2012).

RAC is a heterodimeric complex composed by the Heat Shock proteins (HSP) Hsp40 Mpp11 and the Hsp70L1 of the Hsp70 family. Mpp11 binds to the ribosome through a J-domain, while the function of Hsp70L1 is still poorly understood. Mammalian RAC cooperates with the cytosolic Hsp70, stimulating its ATP hydrolysis (Jaiswal et al., 2011; Otto et al., 2005).

2.3 THE ENDOPLASMIC RETICULUM QUALITY CONTROL

Proteins that undertake the secretory pathway undergo different co- and post-translational modifications to acquire their proper conformation. If they fail, they are recognised by the ER quality control (ERQC) machinery and tagged for degradation.

During the folding process, in fact, proteins are assisted by a wide range of chaperones and enzymes, which reside within the ER lumen thanks to a small C-terminal signal peptide, called KDEL because of the amino acidic sequence Lys-Asp-Glu-Leu. Among these chaperones, the proteins of the lectin family, such as calnexin, calreticulin, the mannosidase EDEM (ER degradation-enhancing α-mannosidase-like) and others, prevent the formation of aberrant proteins and protein aggregates. Calnexin is a membrane-bound lectin, while calreticulin is soluble and is retained in the ER due to the KDEL sequence.

Chaperones of the Hsp70 and 90 family interact with the hydrophobic portions of the nascent proteins allowing their solubilisation. Among the Hsp70, **BiP** (Binding immunoglobulin Protein) or GRP78 (Glucose-Regulated Protein) is an ER-resident chaperone with a KDEL tag at its C-terminus and well conserved in eukaryotes, which is structured with a nucleotide-binding domain (NBD) for ATP binding and hydrolysis and a substrate-binding domain (SBD) that allows BiP to associate and disassociate upon ATP hydrolysis with proteins exhibiting temporarily hydrophobic sequences (Wang et al., 2017) (Figure 11). Amino acidic mutations were reported to have a dominant negative phenotype causing protein retainment in the ER lumen, because ATP hydrolysis and the consequent substrate release by BiP was impaired (Awad et al., 2008; Wei et al., 1995). It was also noted that BiP alone is able to compensate for any lack of calnexin, which has a similar activity of solubilising native proteins (Zhang et al., 1997). Beyond protein folding, BiP has several other functions: it helps protein translocation inside the ER lumen, it retains misfolded or aberrant substrates and gives rise to the unfolded protein response (UPS, see next paragraph) and it also assists during the ER-associated degradation pathway (see chapter 3).

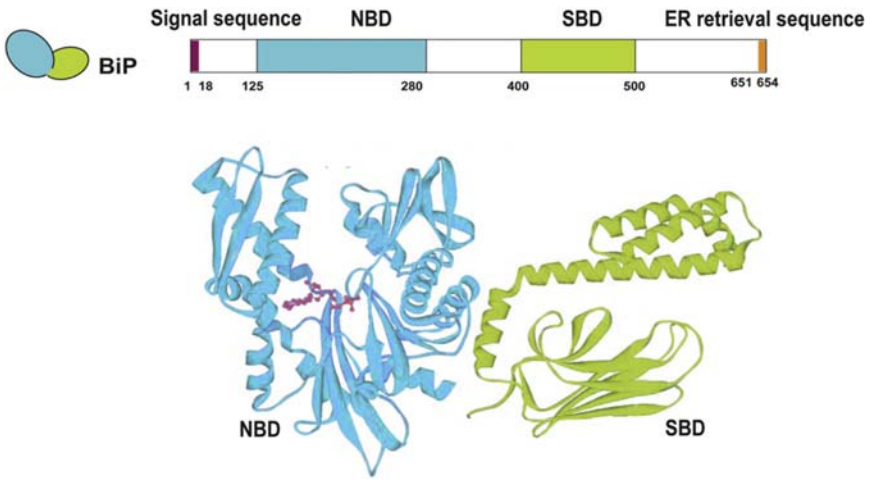

Figure 11. BiP structure. In the upper panel, BiP primary structure with the ER signal sequence at the N-terminus, the nucleotide-binding domain (NBD), the substrate-binding domain (SBD) and the C-terminus KDEL sequence. In the lower panel, the structures of NBD and SBD of human BiP (Wang et al., 2017).

Another chaperone, the Protein Disulphide Isomerase (PDI), catalyses the formation and breaking of disulphide bridges between cysteines, while peptidylprolyl isomerases (PPIs) mediate isomerisation of amino acids, thus facilitating the recruitment of the final conformation of the protein (Yoshida and Tanaka, 2010).

In addition, the ER lumen is provided of enzymes that catalyse the N-glycosylation, which allows the native protein to increase solubility, facilitates its assembly and may serve as a signal for its transport to the Golgi. Proteins whose glycosylation is not successful, in fact, are retained in the ER and eliminated (Bagola et al., 2011). Normally, the N-glycosylation takes place in parallel to protein translation and translocation upon recognition of the target sequence Asn-X-Ser/Thr (where X is any amino acid except proline). An oligosaccharyl-transferase catalyses the transfer of a preformed oligosaccharide ($NAcGln_2Man_9Glc_3$) linked to a dolichol triphosphate to the Asn residue of the target sequence (Yoshida and Tanaka, 2010). At this point, the glucosidases I and II remove, respectively, the last and the penultimate glucose on the oligosaccharide branch (Figure 12) (Takeda et al., 2009). In this form, the glycoprotein is recognized and bound by calnexin and calreticulin. The glucosidase II cleaves then the third and final glucose, thus reducing the affinity for calnexin/calreticulin and allowing the protein release from the ER. However, if the protein has not reached its correct conformation, it is retained in the lumen, where the enzyme UDP-Glucose:Glycoprotein Glucosyltransferase (UGGT) induces its

reglucosylation, conjugating again a glucose on the oligosaccharide. This enzyme specifically recognizes the molecular species with high energy state, named "molten globule" (Bagola et al., 2011). The mono-glucosylated protein enter again the calnexin cycle to gain its proper structure. If a protein is definitely not able to assume the right shape, it is directed towards degradation.

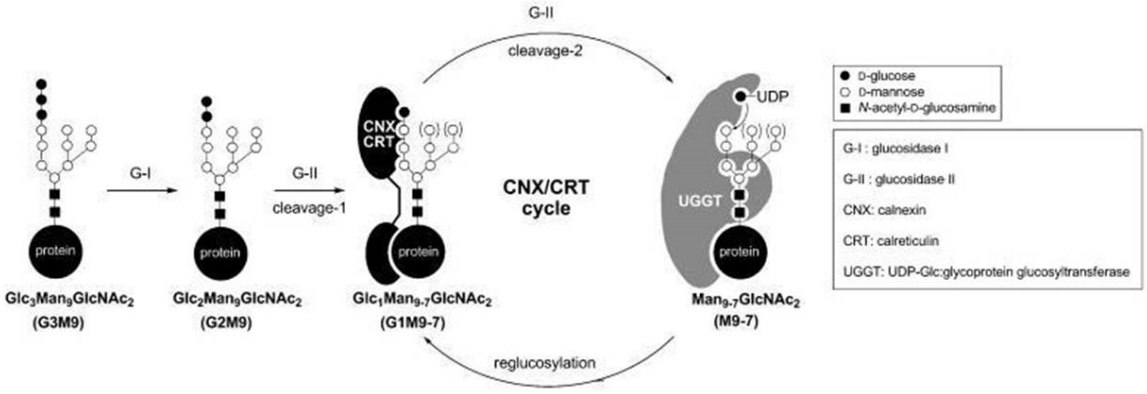

Figure 12. Glucosidases I and II remove external glucoses from the oligosaccharide tree added in the ER lumen. The protein enters the calreticulin/calnexin cycle and, if it doesn't acquire the right conformation, is then glucosylated again by UGGT and reintroduced in the cycle (Takeda et al., 2009).

The unfolded protein response

In case of aberrant proteins accumulation, the ER activates a specific response pathway known as Unfolded Protein Response (UPR). The UPR is specifically induced by stress conditions, such as alterations of ions concentration or oxidizing conditions, genetic mutations in ER residing or nascent proteins and environmental alterations. The ER is provided with a sensor system that has BiP as a key element. When misfolded or unfolded proteins accumulate in the ER, BiP dissociates from three UPR effectors, with which is normally linked, determining three different pathways to enhance transcription of chaperones and enzymes for protein folding, trafficking and degradation. The transducers are the inositol-requiring enzyme 1 (IRE1), the PKR-like ER kinase (PERK) and the Activating Transcription Factor 6 (ATF6) (Schröder and Kaufman, 2005).

IRE1 is a membrane kinase and ribonuclease that can be activated by BiP release or directly by the binding with poorly assembled proteins. In both cases, in fact, IRE1 association to unfolded proteins induces its oligomerisation and self-activation by trans-phosphorylation

of the cytosolic domain. Interestingly, this modification allows IRE1 to function as ribonuclease and to process the cytosolic mRNA of the X-box-binding protein 1 (XBP1). This spliced XBP1 mRNA codify for a longer C-terminus on the Xbp1 protein, which acts as a transcriptional modulator. Xbp1 stimulate transcription of genes codifying for ER chaperones and triggering growth arrest and apoptosis (Ron and Walter, 2007; Schröder and Kaufman, 2005). Moreover, IRE1 was reported to cleave also other mRNAs, probably to reduce ER overloading in a way faster than gene transcription (Hollien and Weissman, 2006).

ATF6 and PERK effector evolved only in mammals. ATF6 is a transmembrane protein complex composed by ATF6α and ATF6β. After release from BiP, the complex moves to the Golgi where, after the cleavage by proteases S1P and S2P, it releases a cytosolic dimeric fragment that acts at transcriptional level inducing expression of genes involved in stress response, like BiP and PDI, and in the ER-associated degradation (Schröder and Kaufman, 2005; Walter and Ron, 2011).

After dissociation from BiP, the transmembrane kinase PERK assumes its active conformation through *trans*-auto-phosphorylation. Its major effect is to reduce the rate of protein synthesis by inhibiting the translation initiation factor eIF2α through phosphorylation of the α subunit. The lack of an active eIF2 favours instead the translation of the transcription factor ATF4, which enhance expression of genes with a CRE-element in their promoter. Among these genes, there is one coding for the transcription factor C/EBP homologous protein (CHOP) that is involved in programmed cell death (Harding et al., 2000; Schröder and Kaufman, 2005). In fact, if the UPR is not able to solve the ER stress and the protein homeostasis is not restored, it can also lead to activation of the programmed cell death pathway.

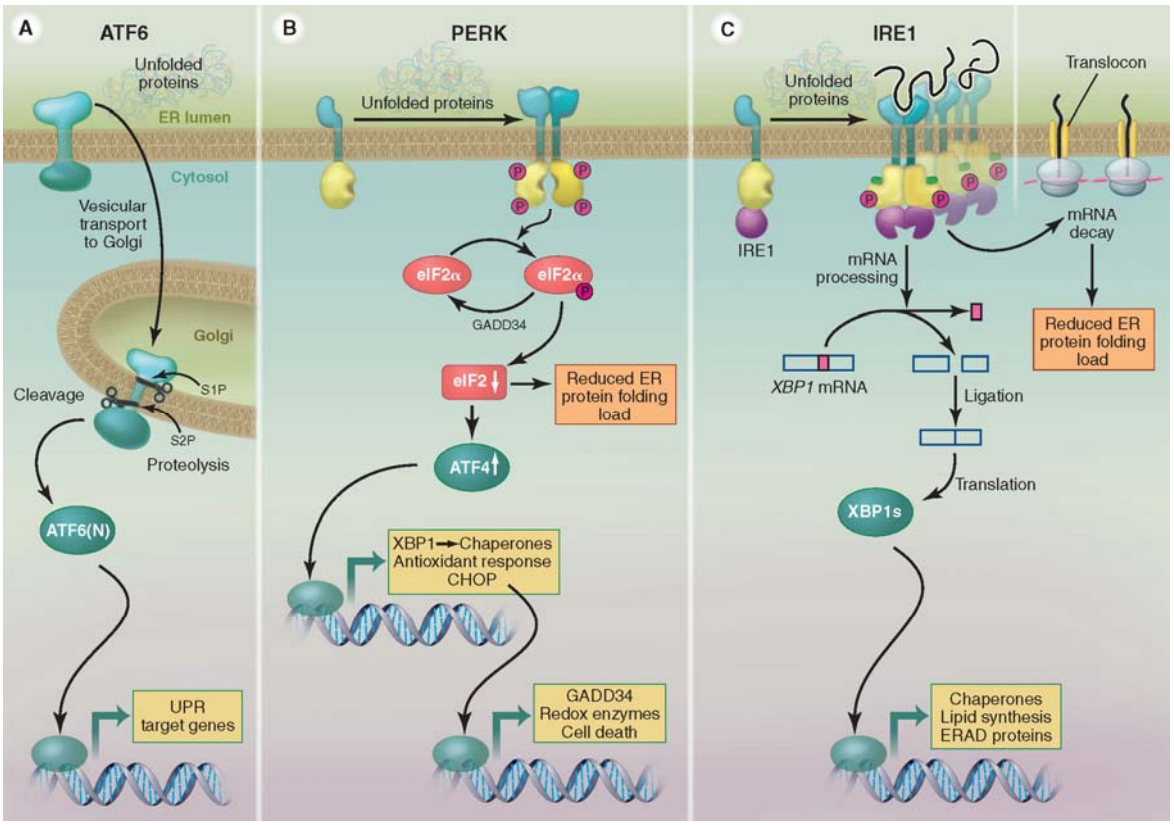

Figure 13. A scheme of the cascade of the three UPR transducers: ATF6 (A), PERK (B) and IRE1 (C). When BiP senses the ER stress due to unfolded proteins accumulation, they are release and, once activated, they modulate transcription of UPR target genes (Walter and Ron, 2011).

3. PROTEIN DEGRADATION THROUGH THE UBIQUITIN-PROTEASOME PATHWAY

Despite the activity of chaperones, it is possible that newly synthetized proteins remain misfolded or unfolded. This situation is potentially toxic for the cell, because proteins with erroneous folding can form aggregates or display aberrant functions. For this reason, they are recognised and targeted to degradation through the route of ubiquitin-proteasome pathway.

3.1 SUBSTRATE UBIQUITINATION

The ubiquitination reaction consists in the conjugation of a ubiquitin (Ub), a small 76 amino acids polypeptide, on a lysine present on the target protein catalysed by a ubiquitin ligase. Recently, it was observed that even cysteine, serine, tyrosine and threonine, as well as the N-terminus of the substrate protein, are potential ubiquitination sites available for ubiquitin-ligases (Shimizu et al., 2010). The first Ub conjugated on the substrate contains 7 lysines that can accept other Ubs, thus forming a larger chain. This acts as a signal for various cellular functions and the poly-ubiquitin chain extended preferentially on lysine at position 48 of Ub (but also on Lys11, 29 and 63) marks the protein for proteasome-mediated degradation (Baboshina and Haas, 1996; Chau et al., 1989; Finley, 2009; Komander and Rape, 2012).

As shown in Figure 14, the reaction involves the sequential action of three enzymes: the first one is the E1 or ubiquitin activator, which forms a thioester bond between its cysteine and the C-terminus glycine of ubiquitin; the second is the E2 or ubiquitin conjugator, which binds the activated ubiquitin to one of its cysteine through a trans-esterification reaction; the last enzyme of the pathway is an E3 or ubiquitin ligase, which moves ubiquitin from E2 to a specific substrate (Pickart and Eddins, 2004).

In humans, only eight E1 ubiquitin activator proteins are described to initiate the Ub conjugation, while there are 35 E2 ubiquitin conjugating enzymes available to receive the activated Ub and more than a thousand E3 ubiquitin ligases. The substrate-specificity of this pathway is given by E2-E3 complex (van Wijk and Timmers, 2010).

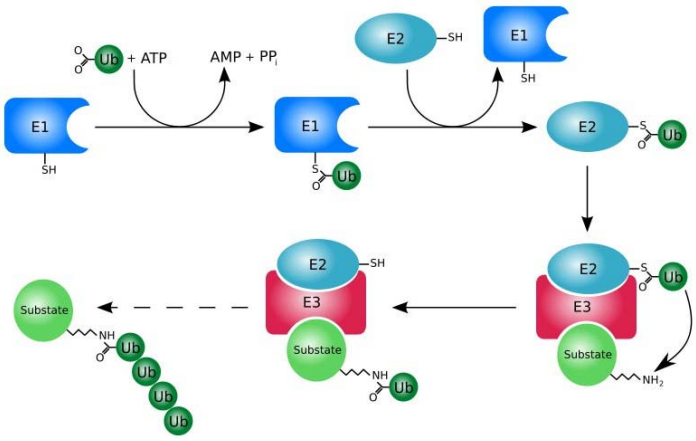

Figure 14. Schematic representation of a protein poly-ubiquitination. E1 or ubiquitin activator, which forms a thioester bond between its cysteine and the C-terminus glycine of ubiquitin; E2 or ubiquitin conjugator, which binds the activated ubiquitin to one of its cysteine through a trans-esterification reaction; E3 or ubiquitin ligase, which moves ubiquitin from E2 to a specific substrate (Roger B. Dodd).

Based on their structure and the mode of action, the E3s are classified in three families: HECT (Homologous to E6AP Carboxy Terminus), RING (Really Interesting New Gene) and U-box (UFD2 homology) (Pickart and Eddins, 2004).

After ubiquitination, either the substrate is released by the E3 ligase or the ubiquitin chain is elongated by further step of Ub conjugation. Poly-ubiquitination can be catalysed by the same E3 enzyme that performed the first conjugation, or by the E4 ubiquitin elongating factors, which can be other E3 or other cofactors (Koegl et al., 1999; Metzger et al., 2014).

3.2 THE p97/VCP ATPase

The AAA adenosine triphosphatases (ATPases) have multiple functions, such as cell cycle progression, membrane fusion, processing of transcription factors and degradation of proteins by poly-ubiquitination (Halawani and Latterich, 2006). The binding to various factors and co-factors modulates their activities determining the function specification in

the various cellular pathways. The p97 ATPase, also known as Valosin-Containing protein (VCP) in mammals or Cdc48p in yeast, belongs to this family of ATPases and is reported to localise mostly in the cytosol, soluble or associated to subcellular organelles like the ER and mitochondria, even if a small fraction was also found in the nucleus, where it is involved in chromatin regulation. It forms a homo-hexameric complex, where every monomer is structured with two concentric rings and is provided with two ATPasic domains (D1 and D2), a N-domain and a short C-terminal tail (Figure 15). Most of p97 interactors bind to the N-domain and only a small fraction to the C-terminal tail. Several proteins were reported to interact with the ATPase as adaptors, to link it to a specific subcellular compartment or substrate, or as cofactors that help to process substrates. Among the cofactors identified there are several enzymes, such as E3 ubiquitin ligases and deubiquitinases (Xia et al., 2016), which confirm its involvement in protein degradation.

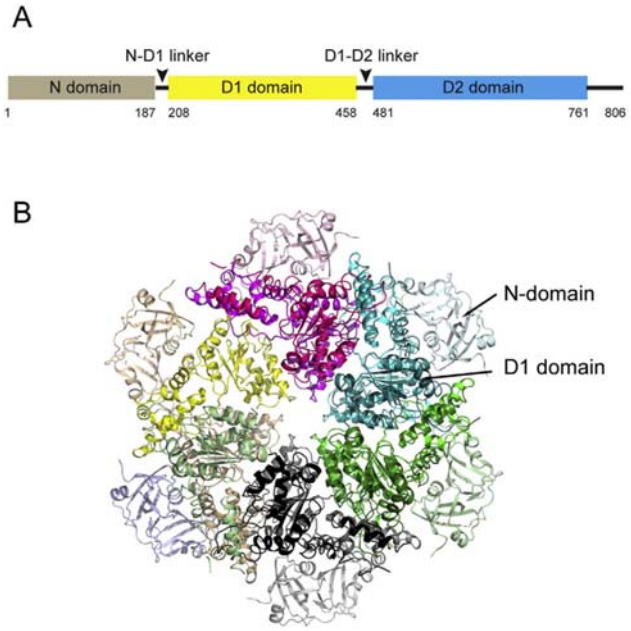

Figure 15. p97 structure. **A:** One monomer is structured in one N-domain, two ATPasic domain D1 and D2, a short C-terminal tail. **B:** The homohexameric structure of the VCP complex (Xia et al., 2016).

3.3 PROTEASOMAL DEGRADATION

The cellular machinery that carries out the degradation of the majority of proteins is the proteasome. It is localized both in the nucleus and in the cytosol of eukaryotic cells (Reits

et al., 1997). Degradation occurs with high specificity due to the ubiquitin-tagging system (Komander and Rape, 2012), to the unstructured regions where the proteasome initiate degradation (Prakash et al., 2004) and to the structure of the proteasome itself (Pickart and Cohen, 2004).

The proteasome consists of a multi-enzymatic complex (26S protease) composed of two subunits: the 20S core particle (CP) and the 19S regulatory particle (RP, Figure 16) (Díaz-Villanueva et al., 2015). The 20S is sealed from the external environment at both ends by the 19S regulator complex (RC). The 20S is composed by 28 subunits arranged into four seven-subunit rings organised to form a compact cylinder. The two inner rings are composed by different related β-subunits with the three main proteolytic activities that render the proteasome virtually able to degrade every kind of polypeptide: the caspase-like activity, performed by β1, the trypsin-like activity by β2 and the chymotrypsin-like activity by β5 (Borissenko and Groll, 2007; Finley, 2009). These β-rings, moreover, create an interior compartment of 84 nm^3, called "catalytic chamber" (Pickart and Cohen, 2004). The outer rings consist of the α-subunits, which can converge blocking the entrance to the channel when the CP is in a closed state or can open the channel with holoenzyme formation by binding of 19S to 20S (Groll et al., 2000; Smith et al., 2007). The catalytic site can be accessed only through axial pores, with a diameter of up to 2nM, thus allowing the entrance only of unfolded peptides (Pickart and Cohen, 2004). The α-rings as well, create two interior compartments, called "antechambers" (size of 59 nm^3), which may hold the mass of substrate or partial digestion products and regulate their passage in and out the catalytic chamber (Pickart and Cohen, 2004).

The RC complex instead contains 19 subunits and have two catalytic activities: ATP hydrolysis, mediated by the ATPases, and Ub proteolytic cleavage, performed by deubiquitinating enzymes (DUBs). The 19S is divided into two sub-complexes: the base and the lid (Figure 16). The base consists of six ATPases (Rpt1-6), which ensure the unfolding of the proteins to drive them towards the CP channel (Voges et al., 1999) and are involved in the 26S formation (Bar-Nun and Glickman, 2012), two subunits that mediate proteasome binding to a variety of factors (Rpn1 and 2) and two ubiquitin receptors (Rpn10 and 13).

The lid is composed by Rpn11, critical for proteasome function, its inactive binding partner Rpn8 and seven scaffolding subunits (Rpn3, 5, 6, 7, 9, 12, 15). Rpn11 is a Zn^{2+}-dependent DUB that cleaves K48- and K63-linked poly-Ub chains from substrates targeted to

proteasomal degradation (Yao and Cohen, 2002). In fact, the poly-ubiquitin chains must be removed from substrates in order to allow their degradation by the proteasome.

In addition, a large number of proteins associates with the 19S to modulate degradation, such as Rpn10, proteins containing Ub-like and Ub-associated domains and other DUBs (Finley, 2009; Glickman et al., 1998).

Alterations in this apparatus or in the ubiquitination pathway due, for example, to the use of chemicals such as the inhibitors MG132, Bortezomib or Epoxomicin, induce accumulation of proteasomal substrates in the cytosol.

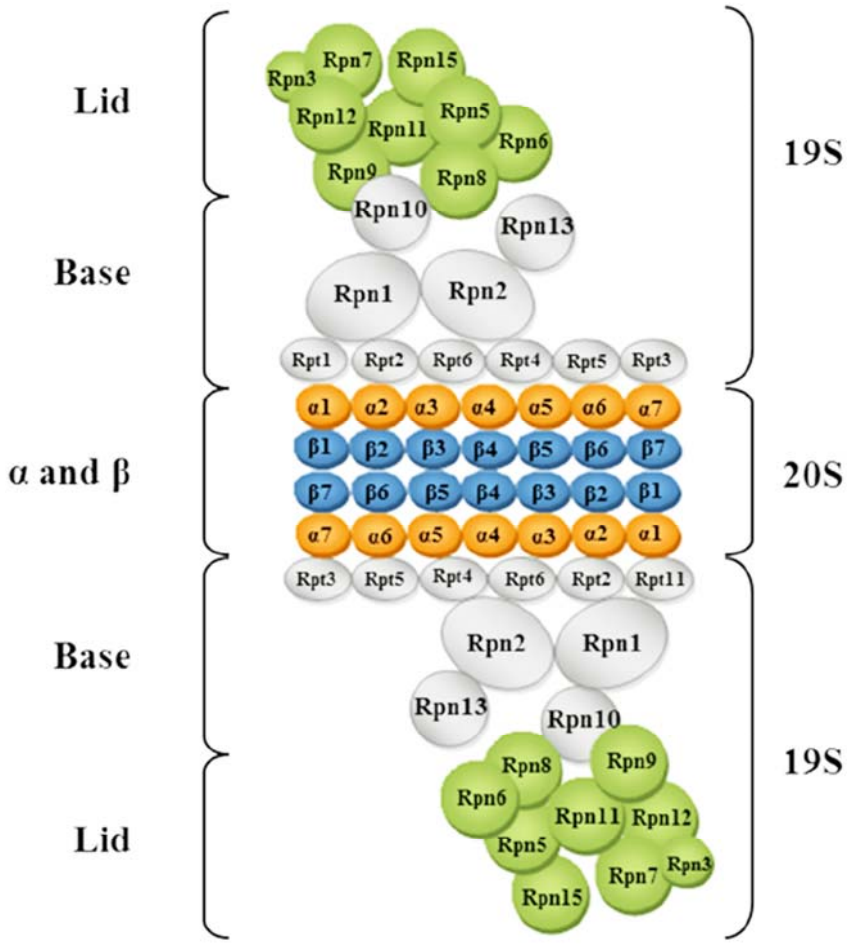

Figure 16. The 26S proteasome structure and components, with the core particle 20S and the two 19S regulatory particles (Díaz-Villanueva et al., 2015).

4. RIBOSOME-ASSOCIATED PROTEIN QUALITY CONTROL AND DEGRADATION

Ribosome-associated quality control during translation is the first check-point of both mRNA quality and efficient protein synthesis and folding. When it senses that translation is blocked, and ribosomes remain stalled on the mRNA, it gives rise to a multi-step process, known as ribosome-associated degradation that results in degradation of the native protein and disassembly of 80S ribosomes. This pathway requires the coordinated activity of many cellular enzymes and is extremely important to maintain protein homeostasis and cell viability. Failure in the quality control or degradation, in fact, is known to be involved in several pathological conditions, such as the Huntington disease (Yang et al., 2016) and other neurodegenerative diseases (Chu et al., 2009; Ishimura et al., 2014).

4.1 THE 80S RIBOSOME DISSOCIATION

In the NGD and NSD pathways, the yeast Dom34-Hbs1 complex and its mammalian counterpart Pelota-Hbs1 are responsible for the subunits split and recycling, together with the ATPases Rli1 and ABCE1 in yeast and mammals, respectively (Doma and Parker, 2006; Pisareva et al., 2011; Shoemaker and Green, 2011). Their roles in the subunits dissociation is thought to be due to their structure: Dom34 and Pelota N-terminal and middle domains resemble the termination factor eRF1 (Graille et al., 2008; Lee et al., 2007), while the GTPase Hbs1 belongs to the same family of eEF1A and eRF3 (Chen et al., 2010; Wallrapp et al., 1998). Based on a model recently proposed (Graille and Séraphin, 2012), the complex Dom34-Hbs1 is first recruited at the A site of stalling ribosome in a way that remind the complex eRF1-eRF3. Once in the ribosome, it mimics the tRNA conformation and stimulates mRNA degradation. Then, GTP hydrolysis by Hbs1 induces the release of Hbs1 itself from the ribosome, followed by the recruitment of Rli1/ABCE1 that, upon ATP hydrolysis, stimulates the dissociation of the 40S subunit from the 60S.

In contrast to this model, however, a recent work found that most of the complexes formed by translationally stalled ribosomes and the associated proteins were resolved by the yeast Release Factors Sup45-Sup35 (mammalian eRF1-3 homologues) and not by Dom34-Hbs1 complex (Shcherbik et al., 2016). In fact, the majority of proteins were already hydrolysed from the tRNA, while Dom34-Hbs1 seems not to have this activity.

4.2 THE 60S RIBOSOME-BOUND QUALITY CONTROL COMPLEX

As schematised in Figure 17, the 60S split subunit remains associated with the nascent peptide, exposing the tRNA in the P site at the interface. To stabilise this complex and to avoid its reassociation with a 40S subunit, a complex of multiple proteins associates with the 60S, forming the 60S-associated ribosome quality control complex (RQC). The first protein of the RQC is the mammal **NEMF** protein (yeast Rqc2, ribosome quality control protein 2), which associates with the 60S subunit at the exposed interface, contacting the 60S and the tRNA in three and two positions respectively, thus maintaining the tRNA in place (Lyumkis et al., 2014; Shao et al., 2015). The presence of NEMF favours the association of an E3 ubiquitin-ligase, Ltn1, first recognised in yeast and then in mammals as **Listerin** (Bengtson and Joazeiro, 2010; Malsburg et al., 2015). This Ub ligase is responsible for the nascent peptide poly-ubiquitination and consequent recruitment of the ATPase **p97/VCP** (Cdc48 in yeast) (Brandman et al., 2012; Defenouillère et al., 2013; Verma et al., 2013). p97 was found bound to the RQC with the ubiquitin binding proteins Npl4 and Ufd1 only after poly-ubiquitination of the nascent peptide. Consequently, it is thought to mediate the extraction of peptides from the RET for the last step of the pathway, the proteasome-mediated degradation (Brandman et al., 2012; Defenouillère et al., 2013; Verma et al., 2013).

The E3 Ub ligase Ltn1/Listerin was described to be essential for stalled peptides degradation mainly in NSD (Bengtson and Joazeiro, 2010) and for this reason is the most studied in co-translational ubiquitination. Interestingly, a mouse model carrying a mutated gene for Listerin resulted to be affected with a neurodegenerative phenotype (Chu et al., 2009), supporting the importance of Listerin-mediated quality control regulation.

This ligase is highly conserved among species and is characterised by a N-terminal and middle domains arranged in α-helix and super-helix, while the C-terminus contains the RING domain (Lyumkis et al., 2013). The N-domain is responsible of the binding to the ribosome thanks to NEMF (Lyumkis et al., 2013; Shao et al., 2015). Both the extremities are flexible, thus allowing the movement from E2 to the substrate protein emerging from the RET (Dimitrova et al., 2009).

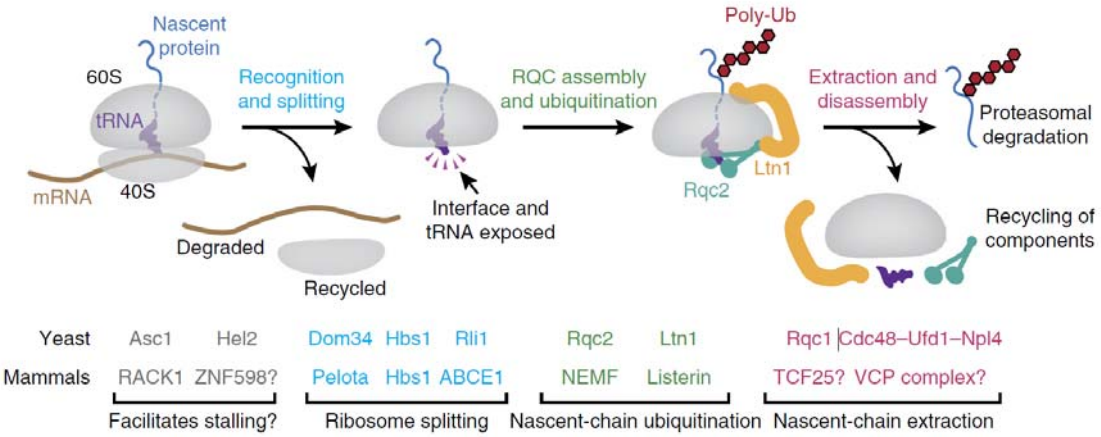

Figure 17. The current model of the ribosome-associated protein degradation in yeast and mammals that described a multistep pathway: after the ribosome stalling sensing, the 80S ribosome is split and the ribosome quality control complex (RQC) assembles on the 60S subunit, which remained associated with peptidyl-tRNA. The polypeptide chain is poly-ubiquitinated by Ltn1/Listerin, extracted by the RET and degraded by the proteasome (Brandman and Hegde, 2016).

Two other E3 ligases were found to be involved in the ribosome-associated degradation pathways in yeast: Not4 and Hel2. Not4 is a component of the Ccr4-Not deadenylase complex and was the first Ub-ligase identified in translational stalling, in particular in NGD and NSD (Dimitrova et al., 2009). At the N-terminus Not4 carries a Zn-binding RING domain that is important for ubiquitination activity. Two other domains, a coil-coiled domain and an RNA recognition motive (RRM), were predicted but their functions are still unknown (Panasenko, 2014). It associates with the NAC complex and some ribosomal proteins, suggesting its importance in co-translational quality control.

Hel2 is a ubiquitin ligase found in association with the yeast 80S ribosome, implicated in inhibition of translation by polybasic and poly-Arginine sequences (Brandman et al., 2012;

Letzring et al., 2013) and is believed to be implied in the earlier steps of stalling to stimulate peptides degradation, probably through ubiquitination of the 40S ribosome subunit (Matsuo et al., 2017; Sitron et al., 2017).

Other factors were identified to be implicated in stalling resolution, but their roles remain to be investigated: the yeast Rqc1, which co-immunoprecipitates with Ltn1, Cdc48 and Rqc2; yeast Asc1 or mammalian Rack1, probably involved in mRNA endonucleolytic cleavage or in stalling targeting together with Hel2 (Brandman et al., 2012; Ikeuchi and Inada, 2016; Sitron et al., 2017).

4.3 THE RQC AT THE ER MEMBRANE

Investigations on the degradation pathway of products originated from translational stalling regard so far predominantly cytosolic free ribosomes. In the case of polypeptides produced by ER-associated ribosomes, the way in which their degradation is induced is not clear, as they are already inserted in the Sec61 translocon and in the ER lumen. The current knowledge is poor and contradictory and there are only a few works in literature about.

In yeast, soluble proteins of the secretory pathway derived from non-stop mRNA were found glycosylated and only slightly affected by proteasome inhibitors indicating that these proteins were fully translated and inserted in the ER lumen (Izawa et al., 2012), while in the case of non-stop transmembrane reporters, the effect of proteasome inhibition can vary (Arakawa et al., 2016). Depletion of Dom34 induced non-stop soluble or transmembrane substrates accumulation and blocked the influx of other ER proteins due to translocon occupancy by non-stop proteins. Conclusions were that the complex formed by Dom34 and Hbs1 was indispensable to favour proteins insertion in the lumen and translocon clearance (Arakawa et al., 2016; Izawa et al., 2012). Another research demonstrated instead that soluble and transmembrane proteins co- or post-translationally translocated in the yeast ER from non-stop or poly-Lysin stalled ribosomes were inside the ER and glycosylated, and sensitive to Ltn1 as well as to proteasome inhibition, in contrast to the previous work (Crowder et al., 2015).

Regarding stalling at the ER membrane in mammals, microsomes from pancreatic tissue were purified and analysed for the presence of Listerin and NEMF. The data reported indicated that 60S ribosomes associated to Sec61 translocon, Listerin and NEMF (Malsburg et al., 2015). Reporter proteins expressed in the same purified system were found glycosylated and poly-ubiquitinated at the C-terminus, suggesting ER lumen insertion of the reporters and back-sliding through the translocon to extract the proteins and allow their ubiquitination and degradation.

The mechanism that drives degradation of peptide products of ribosomes translationally stalled at the ER membrane remain obscure; however, the RQC complex seems to be involved also in this case in ribosome splitting and Ltn1/Listerin is involved in the ribosome-associated polypeptides ubiquitination.

5. ER-ASSOCIATED DEGRADATION

It has been estimated that about 30% of the proteins enters the secretory pathway. If they fail to reach a proper folding when they are translated in the ER lumen, they are targeted to the ER-associated degradation (ERAD) (Schubert et al., 2000). The ERAD pathway is responsible for selection and displacement of the soluble and membrane substrates from the ER lumen to the cytosol, a retrograde movement called "retro-translocation" or "dislocation". Three different kinds of ERAD were characterized, depending on which domain is altered: ERAD-L, for proteins mutated in a soluble domain in the ER lumen; ERAD-M, which mainly concerns the integral proteins with mutations in the transmembrane portion and ERAD-C, which relates to the degradation of integral proteins that are altered in a cytosolic domain.

ERAD is characterised by three main steps (Figure 18):

1. Substrate recognition
2. Substrate retro-translocation from the ER lumen to the cytosol
3. Substrate degradation by the cytosolic proteasome.

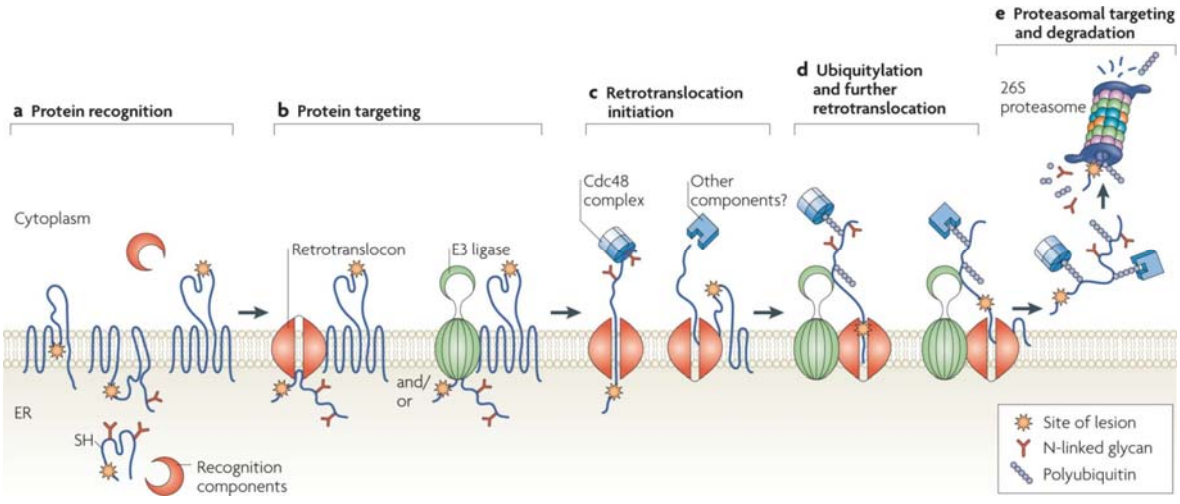

Figure 18. ERAD step by step. Proteins targeted for degradation are recognised by ER resident sensors (**a**) and driven at the ERAD apparatus (**b**). The protein is then retro-translocated across the membrane to reach the cytosol (**c**, **d**), where it is poly-ubiquitinated for the targeting to the proteasome (**d**, **e**) (Vembar and Brodsky, 2009).

5.1 SUBSTRATES RECOGNITION

The ERQC discriminates with high specificity between molecules that are properly folded from those that are not, discerning a protein in an initial or intermediate state of its assembly from an aberrant one. In recent decades, many studies have focused on the signals that allow the recognition of the substrates to be degraded. The question is fascinating, considering how different are between each other the proteins in the ER in terms of type, structure, post-translational modifications, size and function. Moreover, the causes that lead to the degradation can be many: genetic mutations, the ER or cellular stress, alterations in molecules that should assist the assembly, physiological mechanisms of turnover.

ERAD for glycoproteins is one of the most studied pathways. When these proteins remain too long in the calnexin/calreticulin cycle, they are recognized by a **mannosidase** resident in the ER, the α-mannosidase I in mammals (ERManI) (Mns1p in yeast), that removes one or more α(1,2)-mannose residues from the glycan, thereby exposing an α(1,6)-mannose and generating the glycans $NAc_2GlcMan_8$ and $NAc_2GlcMan_{5\text{-}7}$ (Aebi et al., 2010). With this structure the protein can no longer be recognized by UGGT, establishing the exit from the calnexin/calreticulin cycle. Moreover, the absence of an active mannosidase makes proteins that would normally be degraded more stable (Liu et al., 1999), while a greater expression accelerates mannoses removal and protein degradation (Hosokawa et al., 2003). These observations led to the hypothesis that the oligosaccharide modification is a signal for the ERAD pathway, although not the only one, as there are proteins at the initial stage of their maturation exposing the same α (1,6)-mannose. In fact, it was demonstrated that it may depend on the type and location of the oligosaccharide and on the conformation that this modification induces in the protein (Kostova and Wolf, 2005; Mbonye et al., 2006; Xie et al., 2009).

There are many ER resident proteins that can recognise and specifically bind the modified oligosaccharides present on glycoproteins targeted for ERAD. One of them recently identified is the lectin family of the **EDEM** (ER degradation-enhancing α-mannosidase-like) proteins. As suggested by its name, this group of integral proteins has the same characteristics of an α-mannosidase class I. While in mammals were found three isoforms

(EDEM1, 2, 3), in yeast it was only identified the ortholog Htm1p/Mnl1p, involved in ERAD-L pathway of glycoproteins (Vashist and Ng, 2004). In mammals, EDEM1 is able to interact with calnexin (Molinari et al., 2003) and was found associated with Delrin 2, 3 (Oda et al., 2006) and ERdj5 (Hosokawa et al., 2006), an oxide-reductase ER resident responsible for disulphide bonds reduction before retro-translocation and for BiP requirement to prevent aggregation. EDEM2 and 3 accelerate the degradation of glycoproteins targeted for ERAD and the over-expression of EDEM1 and 3 seems to have mannosidase activity *in vivo*, leading to the formation of $Man_{6-7}GlcNAc_2$ (Hirao et al., 2006; Olivari et al., 2006). Based on these observations, some researchers have speculated that EDEMs can act as chaperones, because they accelerate ERAD, prevent the formation of aggregates and the formation of disulphide bridges. Moreover, they could actively intervene in the termination of the calnexin/calreticulin cycle and therefore play an important role in addressing the substrates to ERAD.

The ERAD-labelled glycoproteins are recognized by the ERAD receptors Yos9p in yeast and its counterparts **OS-9** and **B-XTP3** in mammals. These lectins are glycoproteins residing in the ER and provided of MRH domains, as the mannose-6-phosphate receptor (Christianson et al., 2008). In yeast, Yos9p recognizes and binds to glycans through this domain (Szathmary et al., 2005) and is able to recognize α(1,6)-mannose terminals (Quan et al., 2008). In particular, Yos9p seems to be involved in the substrates recognition and/or targeting to ERAD-L and –M (Kim et al., 2005; Szathmary et al., 2005): it interacts with Hrd3, an ER trans-membrane protein associated to the ubiquitin ligase Hrd1p and Der3p, the major mediators of the yeast ERAD-L and -M.

Mammalian OS-9 e XTP3-B are characterised by one and two MRH domains, respectively, but differ from each other because of substrates recognition and association modalities. In analogy with Yos9p, both OS-9 and XTP3-B interact with the ubiquitin-ligase complex of Hrd1, through the glycoprotein SEL1L (the Hrd3 counterpart in mammals). It remains to be demonstrated if the MRH domain of OS-9 is required for the interaction with SEL1L (Christianson et al., 2008) rather than other N-glycans on the ERAD substrates (Hosokawa et al., 2009).

However, there are ERAD substrates that are not glycosylated and the literature in this field is still not very rich. The yeast Yos9p seems to be not involved in degradation of these substrates (Kim et al., 2005; Szathmary et al., 2005). However, mutations in the MRH domain do not hamper the lectin binding to glycans, as well as the interactions with non-glycosylated proteins. Other evidences highlighted that the ER membrane protein HERP binds only ERAD substrates with no glycosylation that are recognised by BiP, but not by calnexin (Okuda-Shimizu and Hendershot, 2007). Consequently, it was assumed that there are distinct ERAD pathways for glycosylated proteins and not, and perhaps the selection by these lectins depends on the characteristics of both the glycans and the peptides.

5.2 SUBSTRATE RETRO-TRANSLOCATION

Independently whether proteins are or not glycosylated, those targeted to degradation enter the retro-translocation step. The retro-translocation or dislocation is the process by which the ERAD substrates move from the ER lumen to the cytosol. It consists in the recruitment of ER-specific receptors that initiate the dislocation and the active extraction of the ERAD substrate from the ER membrane.

Receptors

It has been speculated that the receptors responsible of selecting ERAD substrates are also involved in the dislocation induction: **SEL1L** in mammals and its counterpart **Hrd3** in yeast have a large soluble domain exposed to the ER luminal side, which contains tetratricopeptide repetitions (TPR), known to mediate protein-protein interactions. As mentioned in the previous paragraph, both Hrd3 and SEL1L are associated to the ubiquitin ligase Hrd1 probably to initiate the retro-translocation. Moreover, they interact also with XTP3-B and OS-9 receptors (or Yos9 in yeast), recruiting them to the ERAD (Mueller et al., 2008). It can therefore be assumed that SEL1L and Hrd3 are responsible for the substrates recruitment and induction of retro-translocation.

Energy requirement

Substrates extraction from the ER membrane requires energy. In the cytosolic side, the ERAD ubiquitin ligases associated in a multimeric enzymatic complex that includes the ATPase **p97/VCP** (**Cdc48** in yeast) is thought to couple dislocation with ATP hydrolysis and found associated to ERAD Ub-ligases (Bagola et al., 2011). In yeast, Cdc48 is recruited by the ER membrane protein Ubx2 through UBX domains (a common features among ubiquitin-binding proteins) to associate with the Ub ligases Doa10 and Hrd1 (Neuber et al., 2005). A similar behaviour was detected also in mammals: the p97 C-terminus interacts with the ubiquitin ligase gp78 through Erasin, the Ubx2 homologue, involved in the degradation of some ERAD substrates (Ballar et al., 2006; Lim et al., 2009).

More in detail, p97 binds Ufd1 and Npl4 (ubiquitin-binding proteins), Ufd2 (an ubiquitin elongating factor) and some DUBs enzymes, such as Otu1 and Yod1 (Ernst et al., 2009; Rumpf and Jentsch, 2006). Inhibition of p97 ATPase activity causes degradation impairment of many ERAD canonical substrates, while non-functional Ufd1, Npl4 or Ufd2 are associated with defects in the proteasome-mediated degradation of some ERAD substrates, which remain associated to the ER membrane (Jarosch et al., 2002; Richly et al., 2005). Similar results were observed with alterations of DUBs (Ernst et al., 2009; Rumpf and Jentsch, 2006).

These evidences suggest that Cdc48/p97 facilitate the extraction of some ERAD substrates from the ER membrane, probably generating the driving force to the system. In this view, what induces the engagement of the ATPases to the retro-translocation apparatus might be the poly-ubiquitination of substrates (Flierman et al., 2003). In yeast, the complex could also be responsible for the mobilization of proteins dislocated by the ligases (Rape et al., 2001; Shcherbik and Haines, 2007), the prevention of substrates aggregation in the cytosol and their transport to the proteasome.

However, recent studies have shown that both p97 and Yod1 can be involved in diverse moments of ERAD and are not necessary for the extraction of all substrates (Sasset et al., 2015). For example, p97 activity is essential for retro-translocation of MHC-Iα and CD4, both well-known ERAD substrates, whose degradation are induced by CMV immunoevasins US2 and US11 and the HIV Vpu, respectively. However, different ERAD substrates that spontaneously retro-translocate, like BST-2/Tetherin, the Ig κ light chain NS1 and the Null

Hong Kong (NHK) mutant of α1 anti-trypsin, were efficiently dislocated without requiring p97 or Yod1 activity, which were instead involved in the downstream steps for degradation. It was suggested that p97 recruitment may depend on hydrophobicity: proteins with multiple trans-membrane domains prefer a pathway dependent on p97/Cdc48, while proteins with polar or charged amino acids were found to interact preferentially with the 19S subunit of the proteasome, which has AAA ATPase domains (Nakatsukasa and Brodsky, 2009).

In conclusion, based on the experiments reported, p97 participates in the extraction of some ERAD substrates by actively dragging the molecules into the cytosol and/or segregating in the cytosol those that have already been extracted.

Protein retro-translocation across the ER membrane

The mechanism responsible for aberrant proteins dislocation, however, is still unknown. There are several theories in the literature that span from the existence of a protein channel to a role of lipid droplets.

The hypothesis of the translocon. Considering that proteins are co-translationally translocated into the ER lumen through the Sec61 translocon, it was speculated that the retro-translocation also requires the presence of a similar channel. Although there is still no conclusive evidence of its existence, several proteins that could form the pore were identified (Figure 19). The first potential candidate is Sec61 itself. There are some experiments that suggest its involvement in the ERAD pathways in yeast (Kalies et al., 2005; Pilon et al., 1997; Plemper et al., 1997; Schäfer and Wolf, 2009) and mammals (Fisher and Ginsberg, 2002; Oyadomari et al., 2006; Schmitz et al., 2000; Wiertz et al., 1996). However, according to Bagola and colleagues, it is difficult to know whether the aberrant proteins are completely dissociated from the translocon after their import in the ER: structural aberrations that take place in the very early stages of protein maturation, even during translocation, can immediately activate the ERAD apparatus. In addition, the wrong protein folding may induce a prolonged association with Sec61 complex. The binding of the ERAD substrates to the translocon highlighted in some experiments can therefore be due to a

translocation slowdown, rather than to an active substrate re-targeting by the channel (Bagola et al., 2011).

Finally, it must be considered the Sec61 channel structure: first, the pore allows the passage of only stretches or partially assembled proteins (Berg et al., 2004; Rapoport, 2007); second, the channel can be opened only from the cytosolic side and the insertion of a peptide from the luminal side should lead to its closure, blocking the transport of proteins (Li et al., 2007).

Folding, disulphide bridges and N-glycosylation of certain ERAD substrates, moreover, are maintained during the retro-translocation, and the translocon pore is not wide enough to allow their passage (Fiebiger et al., 2002; Kario et al., 2008; Misaghi et al., 2004; Petris et al., 2014b). To support these observations, the deglycosylating enzymes of the ERAD pathway (NGLY1, see paragraph 5.3) are expressed exclusively in the cytoplasm, despite the fact that their intervention was reported as not necessary to degrade proteins. In fact, this is the case of BST-2/Tetherin and Vpu-induced CD4 retro-translocation: both were found in the cytosol partially folded, still glycosylated and with oxidised cysteines during the early steps of dislocation. N-glycosylation and disulphide bridges were removed in a second moment, prior to proteasome degradation (Petris et al., 2014b).

Taken together, these observations indicate that there could be other factors and/or different mechanisms that govern the transport of an ERAD substrate across the ER membrane.

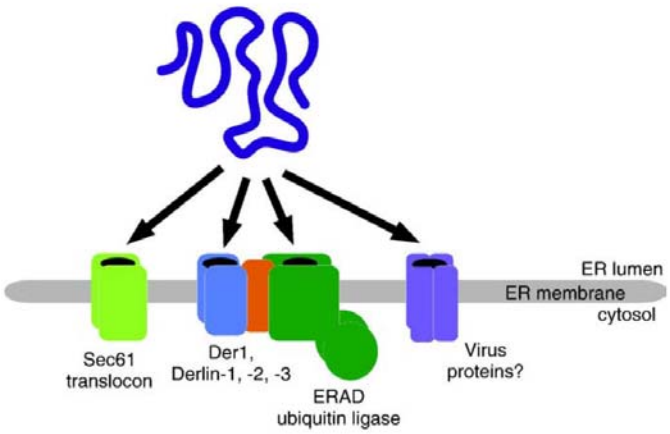

Figure 19. The components of a putative retro-translocation channel: the Sec61 translocon, ERAD ubiquitin ligases in association with Derlin proteins, or viral proteins like HIV Vpu (Bagola et al., 2011).

Other proteins that are possible candidates for the formation of retro-translocation channel are viral proteins, like the HIV protein Vpu itself, responsible of inducing dislocation and degradation of newly synthesized endogenous CD4 through ERAD machinery (Margottin et al., 1998), which can oligomerise and form ion channels that may export part of the luminal CD4 in the cytosol (Ewart et al., 1996), also indicating how ERAD is used electively during pathogen infection.

Other possible candidates for a channel formation are the ubiquitin ligases Doa10 and Hrd1p (Horn et al., 2009; Swanson et al., 2001; Walter et al., 2001) in yeast and Hrd1 and gp78 in association with the proteins of the Derlin family in mammals (Baldridge and Rapoport, 2016; Schulze et al., 2005; Zhong et al., 2004).

The yeast Der1 is a small protein that is associated to the ligase Hrd1p. Its inhibition reduces the turnover of proteins with large soluble domains in the ER lumen, while it does not affect the degradation of membrane proteins (Taxis et al., 2003; Vashist and Ng, 2004). Three homologous proteins were identified in mammals: **Derlin 1, 2 and 3**. As Der1, they associate with ERAD ligases, but are involved in the degradation of both soluble and integral proteins (Huang et al., 2013; Lilley and Ploegh, 2004; Oda et al., 2006; Zhong et al., 2015). Some experiments seem to demonstrate Derlin 1 involvement in retro-translocation at the expense of Sec61 (Bernardi et al., 2008; Wahlman et al., 2007).

The yeast Der1 and the mammalian Derlin 1 are actually able to form oligomers in the ER membrane (Goder et al., 2008; Ye et al., 2005). Greenblatt and colleagues discarded this hypothesis, demonstrating a homology between Derlin1 and the protein GlpG of the rhomboid family and therefore arguing that, as GlpG, Derlin 1 would not be able to form channels (Greenblatt et al., 2011).

Transient channel hypothesis. Considering that the existence of a protein channel has not been yet demonstrated and that the pore size of a Sec61 channel is reduced, it is possible that it should adapt dynamically to allow the passage of glycosylated and/or partially folded proteins. Consequently, it was taken into consideration the existence of a transient channel, on the basis of similar discoveries related to peroxisomal Pex5/Pex14 channel that allow whole complexes to cross the membrane (Meinecke et al., 2010).

Lipid droplets hypothesis. Identified initially as a lipids storage system, the lipid droplets originate by budding from the ER and form a real independent organelle, deputy to the synthesis of neutral lipids. They are involved in the ubiquitin-mediated degradation of ApoB (Ohsaki et al., 2006). In case of ER stress, these lipidic formations increase, probably to facilitate the elimination of incorrect proteins from the ER (Fei et al., 2009; Ploegh, 2007). Therefore, it is not clear if this system represents a stress-induced mechanism, rather than a pathway of degradation regularly implemented by the cell.

5.3 THE SUBSTRATES DEGRADATION

According to current models, once the proteins are extracted from the membrane and are located in the cytosolic environment, they must be poly-ubiquitinated and/or deglycosylated before being degraded by the proteasome.

Poly-ubiquitination

The ubiquitination was described as an essential step to induce protein dislocation initiation: mutations that prevent Ub chain polymerization inhibit the ER export of some integral and soluble proteins (de Virgilio et al., 1998; Kikkert et al., 2001; Yu and Kopito, 1999). Deletion of the E2 enzyme in yeast gave similar results (Jarosch et al., 2002).

In yeast, there are two important ubiquitin E3 ligases, **Hrd1p** and **Doa10**, that are involved in almost all the pathways associated with ERAD. Hrd1p immunoprecipitates with other components of ERAD that are generally required for degradation of ERAD-L and -M substrates. Doa10, instead, mediates the turnover of components of the ERAD-C pathway (Carvalho et al., 2006).

Both Hrd1p and Doa10 have a structure with a RING domain on the cytosolic side of the ER membrane and they count respectively 6 and 14 transmembrane domains. The Hrd1p N-terminal domain that contains these trans-membrane segments is very hydrophobic, while the C-terminal RING is hydrophilic. Mutation of one amino acid in this C-terminal domain with a hydrophobic one irreparably alters Hrd1p activity, in particular for ERAD-M substrates (Sato et al., 2009).

In mammals, the situation is more complex because there are many ubiquitin-ligases involved in ERAD that often have interconnected or even overlapping functions. Among these, there have been characterized Hrd1, Teb4/MARCHIV (counterpart of Doa10), a cytosolic CHIP, RMA1/Rnf5, gp78 and SCF-Fbs1/FBS2 (Yoshida and Tanaka, 2010).

In analogy with its homologous in yeast, mammal Hrd1 is involved in ERAD-L and -M pathways. Along with gp78, it is one of the most well characterized E3 associated within the ER membrane. It is structured with 6 trans-membrane segments and a RING domain exposed in the cytosolic side.

It is believed that the trans-membrane domains of Hrd1 (and presumably those of other ligases) are involved in the selection of membrane-associated proteins by binding to SEL1L, which in turn binds XTP3-B and OS-9 (Christianson et al., 2008; Mueller et al., 2008).

In conclusion, ubiquitination is important in the initial steps of ERAD not only to start protein dislocation, but also for the substrate recognition. However, many aspects of these mechanisms have yet to be investigated. It was hypothesized that these Ub chains may facilitate the protein extraction through the binding with factors with Ub-binding domains (p97/Cdc48), which accumulate in proximity of the dislocation site. Moreover, the poly-ubiquitination that the ERAD substrates undergo in the cytoplasm is essential for targeting to the proteasome.

De-glycosylation

As reported before, the removal of oligosaccharides from glycosylated ERAD substrates is performed by specific enzymes found only in the cytosol: the PNG1 in yeast and the N-glycanase 1 (NGLY1) in mammals. Both these proteins belong to the superfamily of trans-glutaminases and their catalytic activity is due to the Cys-His-Asp triad that resides in a deep fissure, accessible only by an already denatured protein (Lee et al., 2005). Unlike PNG1, NGLY1 developed a PUB domain on the N-terminal side, while the C-terminal portion is very similar to the α(1,6)-mannose binding domain (Suzuki, 2007) (Figure 20). It was shown that the NGLY PUB domain interacts with Derlin1 and p97/VCP (Yoshida and Tanaka, 2010).

In yeast, PNG1 is able to associate with the proteasome through the Rad23p protein and a similar situation was also found in mammals, where NGLY1 associated with Rad23p orthologs, HR23A/HR23B (Suzuki et al., 2001). Rad23p and HR23 contain an Ubl domain

responsible for the proteasome interaction and two UBA domains for the binding to ubiquitin (Yoshida and Tanaka, 2010).

Consequently, it was hypothesized that NGLY1 is able to recognize glycans with high mannose content, as the case of glycoproteins targeted to ERAD, and can be enrolled at the ER membrane during retro-translocation.

The deglycosylation, therefore, is an important reaction and can be used to identify a protein when it has reached the cytosol even if, however, deglycosylation is not essential for degradation (Kario et al., 2008; Misaghi et al., 2004).

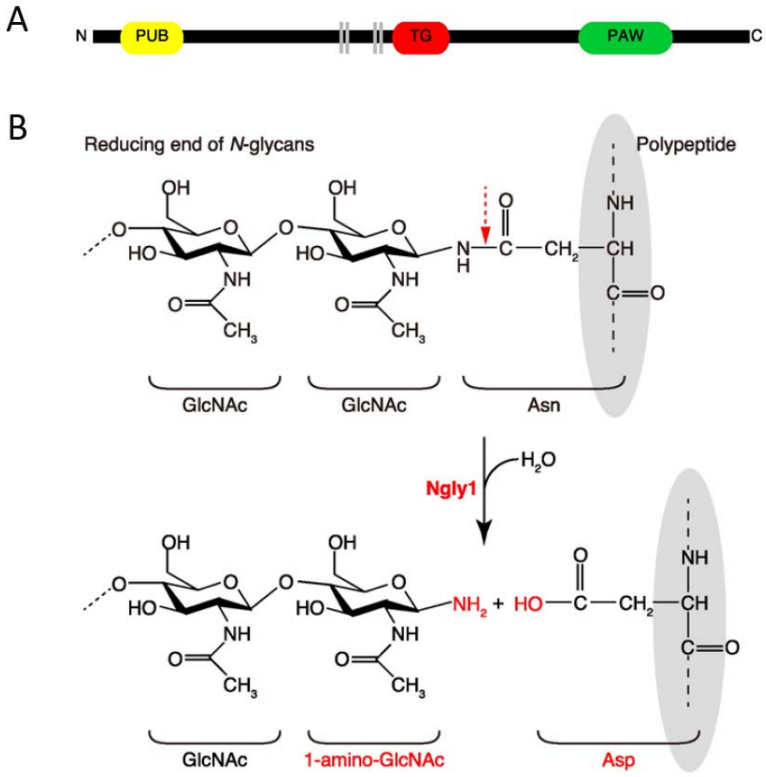

Figure 20. The human NGLY1. **A:** The structure with the main domains. **B:** A scheme of its enzymatic activity (Suzuki et al., 2016).

Proteasome degradation

The most widely accepted hypothesis is that the protein dislocation occurs independently on the proteasome, although the degradation of some specific membrane proteins seems to be coupled with their displacement, indicating that the proteasome can actually be directly involved in this process (Walter et al., 2001). Supporting this observation, *in vitro*

studies have demonstrated an interaction between Sec61 and the RC subunit of the proteasome (Kalies et al., 2005). It was suggested that in situations of reduced proteasome activity, the degradation of trans-membrane regions is mainly altered, while the proteolysis of soluble regions is less affected (Bagola et al., 2011). Integral proteins have cytosolic domains that can be ubiquitinated before retro-translocation. Assuming that extraction and degradation processes can be coupled, the degradation of integral proteins can take different forms: it can start from one of the extremities during or after extraction from the ER membrane or it may start from a cytosolic domain, following an endoproteolytic cleavage mediated by the proteasome itself. In contrast, however, there are strong evidences that ERAD substrates accumulate in the cytosol upon proteasome inhibition (Petris et al., 2014b, 2011; Sasset et al., 2015; Vecchi et al., 2012), suggesting that the transmembrane domains would be solubilised before the degradation (Johnston et al., 1998; Wiertz et al., 1996). Other experiments indicate that some ERAD substrates may be released into the cytosol before the degradation in a p97-dependent way (Nakatsukasa et al., 2008).

However, it is not yet clear whether the degradation takes place simultaneously with the retro-translocation, and how membrane proteins, especially the integral ones, are extracted from the membrane.

MATERIALS AND METHODS

Constructs

Plasmids used are all cloned into pcDNA3 vector (LifeTechnologies). The 2A-P and 2A coding sequences were previously described (Sasset, 2013). CD99L2, POTE, TBCA, SPIRE2 and C-Tail coding sequences were inserted by digestion with enzymes KpnI and EcoRI (New England BioLabs) in frame at the C-terminus of previously described scFv anti-coronavirus 6A.C3 mAb (Bestagno et al., 2007), already present in the laboratory, using oligoes listed below.

When indicated, Pro-codon (CCT), STOP-codon (TAG), SV5-tag (GKPIPNPLLGLD), BAP-tag (GLNDIFEAQKIEWHE), roTag-tag (SISSSIFKNEG) (Petris et al., 2014a), HA-tag (YPYDVPDYA) and N-glycosylation site (NGT) were inserted by cloning from existing sequences or by site-directed mutagenesis (QuikChange Site Directed Mutagenesis Kit, Stratagene).

Plasmids encoding secretory proteins were engineered with an immunoglobulin secretion leader peptide at the N-terminus (Li et al., 1997) as previously described (Petris et al., 2014a).

The coding sequence of BioID2 was previously reported (Kim et al., 2016). Plasmid encoding the MHC-Iα, cyt-BirA, wild type BiP and BiP mutant T37G were previously described (Sasset et al., 2015).

Plasmid encoding the sequence of a TEVp active in the ER-lumen was recently developed in our laboratory (Cesaratto et al., 2015).

CCHFV-L OTU plasmid was kindly provided by Adolfo García-Sastre, the N-terminal FLAG-tagged human and YOD-C160S plasmids by Christian Schlieker, the His6-tagged rat p97QQ and Myc-tagged Hrd1 C291S plasmids by Linda Hendershot.

Engineered new constructs were checked through enzymatic digestion and Sanger sequencing (Eurofins Genomics) after transformation of *Escherichia coli* DH5α competent

cells and single clone DNA plasmids purification using EUROGOLD Plasmid Miniprep Kit (EuroClone). DNA plasmids used to transfect HEK-293T cells and for *in vitro* protein expression were obtained by single clone expansion in overnight cultures of *E. coli* DH5α and DNA was purified using QIAGEN Plasmid Midi kit.

Sequences of Oligos:

FCAMR for:	CAAGATGCTCCAGGATGACTCTCTTCCTGCTGGGGCCAGCCTGACTGCCCCA GAGAGAAATCCAGGACCCTG
FCAMR rev:	AATTCAGGGTCCTGGATTTCTCTCTGGGGCAGTCAGGCTGGCCCCAGCAGGA AGAGAGTCATCCTGGAGCATCTTGGTAC
FCAMR ΔP for:	CAAGATGCTCCAGGATGACTCTCTTCCTGCTGGGGCCAGCCTGACTGCCCCA GAGAGAAATCCAGGATG
FCAMR ΔP rev:	AATTCATCCTGGATTTCTCTCTGGGGCAGTCAGGCTGGCCCCAGCAGGAAGA GAGTCATCCTGGAGCATCTTGGTAC
CD99L2* for:	CCCTTTCTGTGTCTCTCTCCTTTCTCTTACAAAGATGCTTGTTAGTGGGTTT AAGGCCCACCTGGATAATCCAGGATG
CD99L2* rev:	AATTCATCCTGGATTATCCAGGTGGGCCTTAAACCCACTAACAAGCATCTTT GTAAGAGAAAGGAGAGAGACACAGAAAGGGGTAC
CD99L2-P* for:	CCCTTTCTGTGTCTCTCTCCTTTCTCTTACAAAGATGCTTGTTAGTGGGTTT AAGGCCCACCTGGATAATCCAGGACCATG
CD99L2-P* rev:	AATTCATGGTCCTGGATTATCCAGGTGGGCCTTAAACCCACTAACAAGCATC TTTGTAAGAGAAAGGAGAGAGACACAGAAAGGGGTAC
POTE* for:	CGTAATTTGCCAGTTACTTTCTGACTACAAAGAAAAACAGATGCTAAAAATC TCTTCTGAAAACAGCAATCCAGGTTG
POTE* rev:	AATTCAACCTGGATTGCTGTTTTCAGAAGAGATTTTTAGCATCTGTTTTTCT TTGTAGTCAGAAAGTAACTGGCAAATTACGGTAC
POTE-P* for:	CGTAATTTGCCAGTTACTTTCTGACTACAAAGAAAAACAGATGCTAAAAATC TCTTCTGAAAACAGCAATCCAGGTCCATG
POTE-P* rev:	AATTCATGGACCTGGATTGCTGTTTTCAGAAGAGATTTTTAGCATCTGTTTT TCTTTGTAGTCAGAAAGTAACTGGCAAATTACGGTAC
POTE-P-rT* for:	CTGAAAACAGCAATCCAGGTCCATCTATTTCTTCTAGTATCTTTAAAAATGA AGGTTGAATTCTAGAGGGCCCTATTC
POTE-P-rT* rev:	GAATAGGGCCCTCTAGAATTCAACCTTCATTTTTAAAGATACTAGAAGAAAT AGATGGACCTGGATTGCTGTTTTCAG
TBCA* for:	CGCCGATCCTCGCGTGAGACAGATCAAGATCAAGACCGGCGTGGTGAAGCGG CAGAGATCCTACAAGAATCCAGGATG
TBCA* rev:	AATTCATCCTGGATTCTTGTAGGATCTCTGCCGCTTCACCACGCCGGTCTTG ATCTTGATCTGTCTCACGCGAGGATCGGCGGTAC

TBCA-P* for:	CGCCGATCCTCGCGTGAGACAGATCAAGATCAAGACCGGCGTGGTGAAGCGG CAGAGATCCTACAAGAATCCAGGACCATG
TBCA-P* rev:	AATTCATGGTCCTGGATTCTTGTAGGATCTCTGCCGCTTCACCACGCCGGTC TTGATCTTGATCTGTCTCACGCGAGGATCGGCGGTAC
SPIRE2* for:	CGGGGTACCGGGCTGCGGGGCTCGCCGGGCCGGCGCCTGCGGGATACCGGGG ACCTCCTGCTGCGCGGGGACGGCTCGGTCGGGGCGCGG
SPIRE2* rev:	CGGAATTCATCCTGGGTTTCTGACCTCTTCAACCGCGGCCTCGGGCTCCCGC GCCCCGACCGAGCCGTCCCCGCGCAGCAGGAGGTCCCC
SPIRE2-P* for:	CGGGGTACCGGGCTGCGGGGCTCGCCGGGCCGGCGCCTGCGGGATACCGGGG ACCTCCTGCTGCGCGGGGACGGCTCGGTCGGGGCGCGG
SPIRE2-P* rev:	CGGAATTCATGGTCCTGGGTTTCTGACCTCTTCAACCGCGGCCTCGGGCTCC CGCGCCCCGACCGAGCCGTCCCCGCGCAGCAGGAGGTC
C-Tail* for:	CATGCACAGTGTAATATTTCTCCAAGTATCATCCAAAATTCCCCACAGACAA GGCTTTCGTCCTCATTAG
C-Tail* rev:	AATTCTAATGAGGACGAAAGCCTTGTCTGTGGGGAATTTTGGATGATACTTG GAGAAATATTACACTGTGCATGGTAC
C-Tail-P* for:	CATGCACAGTGTAATATTTCTCCAAGTATCATCCAAAATTCCCCACAGACAA GGCTTTCGTCCTCATCCTTAG
C-Tail-P* rev:	AATTCTAAGGATGAGGACGAAAGCCTTGTCTGTGGGGAATTTTGGATGATAC TTGGAGAAATATTACACTGTGCATGGTAC
C-Tail ΔPH for:	CCACAGACAAGGCTTTCGTTGACCTCATTAGAATTCTAGAGG
C-Tail ΔPH rev:	CCTCTAGAATTCTAATGAGGTCAACGAAAGCCTTGTCTGTGG
C-Tail-P-rT* for:	CAGACAAGGCTTTCGTCCTCATCCTTCTATTTCTTCTAGTATCTTTAAAAAT GAAGGTTAGAATTCTAGAGGGCCCTATTC
C-Tail-P-rT* rev:	GAATAGGGCCCTCTAGAATTCTAACCTTCATTTTTAAAGATACTAGAAGAAA TAGAAGGATGAGGACGAAAGCCTTGTCTG
N^N for:	TGCATGGCTCCTCAGGAAATGGCACTTCTGGAG
N^N rev:	TGCACTCCAGAAGTGCCATTTCCTGAGGAGCCA

Cell culture and transfection

Human embryonic kidney (HEK)-293T cells were cultured in Dulbecco's modified Eagle's medium (DMEM, Life Technologies), supplemented with 10% fetal calf serum (FCS, Life Technologies).

Transfection of 293T were performed in 6-well, 12-well or 10 cm plates (about 5×10^5, 2.5×10^5 and 2.5×10^6 cells respectively) with standard calcium-phosphate technique. Medium was changed 18 hours post-transfection and cells were further incubated for at least 7–8 hours, before medium and/or cell harvesting. Where indicated, the proteasome

inhibitor MG132 (Sigma) or Chloroquine (Sigma) were added at a concentration of 20 µM and 50 µM, respectively, for 4 hours.

24 hours post transfection, cells were washed with PBS and lysed with SDS lysis buffer (100 mM Tris–HCl, pH 6.8, 6% SDS, 30 mM NEM (Fluka), 1% protease inhibitors cocktail (Sigma) and sonicated or, where required for the following experiments, lysis was performed using TNN lysis buffer (Tris HCl 100 mM pH 8, NaCl 250 mM, NP-40 0,5%, 1% protease inhibitors cocktail).

Silencing

For silencing experiments, HEK-293T cells were grown in 12-wells plates. Irrelevant (UCGUCUUCUACAACGUCAA) and Ltn-specific (GCAGUGGUGUGAAGAAUUA) siRNAs (Sigma) were transfected with Lipofectamine RNAiMAX reagent (Life Technologies) according to manufacturer's instruction. 48 hours post-siRNA transfection, medium was discarded, and cells transfected with DNA plasmids and a transfection control plasmid encoding EGFP (pEGFP, Clontech) by standard calcium-phosphate procedure and lysed 24 hours post-transfection.

SDS-PAGE and Western blotting

For SDS-PAGE, samples were boiled 10 minutes in SDS-loading buffer (25 mM Tris–HCl, pH 6.8, 1% SDS, 10% glycerol) with reducing agent β-mercaptoethanol (175 mM) before gel loading. Gels were blotted onto PVDF membranes (Millipore) and membranes were blocked with 5% milk diluted in PBS, then reacted with mouse anti-SV5 (Life Technologies) or mouse anti-roTag mAbs (Petris et al., 2014a), followed by incubation with a HRP-labelled anti-mouse whole IgG antibody (KPL) and developed by ECL reaction (Pierce™). Where indicated blots were incubated with mouse anti-BiP (BD Bioscience), mouse anti-GFP (Santa Cruz Biotechnology), Streptavidin-HRP (Sigma) and anti-HA-HRP (Sigma) and the appropriate HRP-conjugated anti-mouse secondary antibody (Jackson). As loading control, blots were developed with mouse anti-β-tubulin (Calbiochem) or HRP-labelled anti-actin (clone AC-15, Sigma-Aldrich) antibodies.

Quantification of protein amounts was performed on serial diluted samples run with a reference sample. Bands intensity was detected with the image processing software ImageJ

v1.43 (National Institutes of Health) or UVItec Alliance (UVItec, Cambridge) and the values were normalised on actin.

In vivo biotinylation and Western blot-retardation assay

BirA is 35.5 kDa biotin-protein ligase (BPLs) from *E. coli* that conjugate biotin, a small molecule of 244.3 Da, to a substrate protein bearing the 14 amino acids-long biotin acceptor peptide (BAP) (Beckett et al., 2008; Chapman-Smith and Cronan, 1999; Schatz, 1993). The reaction catalysed by BirA is irreversible and stable, because it consists in the formation of an amide bond between one biotin and the residue of a specific and unique lysine present in the BAP-tag. The BAP-tag can be engineered to other proteins and successfully recognized by BirA and biotinylated (Cronan Jr., 1990) and this render this approach highly interesting to study protein-protein interactions (Choi-Rhee et al., 2004; Roux et al., 2013) and *in vivo* cellular localisation (Chapman-Smith and Cronan, 1999; Petris et al., 2011). In our laboratory it was developed a protocol for the *in vivo* biotinylation applied to the study of protein retro-translocation: the BAP-tag fused at the N- or C-terminus of several ERAD substrates allows to monitor and selectively biotinylate only the fraction of molecules that reached the cytosol, where the BirA is expressed (Petris et al., 2014b, 2011; Predonzani et al., 2008; Sasset et al., 2015).

Based on our protocol, HEK-293T cells were transfected as previously described and 20 hours after transfection, 0.15 mM of Biotin (Sigma) was added to the media for at least 4 hours. Cell were lysed in SDS lysis bugger always supplemented with 30 mM NEM.

For Western blot-retardation assays (WB-ra), cell lysates were incubated after boiling with 1 µg streptavidin (StrAv) (Sigma) or an equivalent volume of H_2O in negative controls for at least 20 minutes at room temperature before loading. The bond between biotin and avidin/streptavidin is one of the strongest non-covalent bonds in nature, characterised by high specificity and affinity (Kp = 10^{-15} M, calculated by Green in 1963) and resists to SDS detergent conditions, adding an apparent molecular weight of 30-40 kDa that slows protein electrophoretic migration.

In vitro protein expression and biotinylation

Protein expression *in vitro* was performed using the TNT® Quick Coupled Transcription/Translation System based on rabbit reticulocyte lysate (Promega) and 1-Step Human Coupled IVT Kit - DNA of HeLa cell lysate (Thermo Fisher Scientific) following manufactures' instruction.

To perform biotinylation of HeLa lysate, plasmid encoding cytoplasmic BirA was expressed in HEK-293T cells. 24 hours post transfection, cells were lysed in a hypotonic buffer (Tris HCl 20 mM pH 8, Sucrose 250 mM). The lysate was supplemented with BirA Reaction buffer (10 mM ATP, 10 mM MgOAc, 50 µM d-Biotin) and incubated with HeLa lysate in a 1:1 ratio for 1 hour at 37°C.

[^{35}S]-Methionine labelling

HEK-293T cells were starved for 30 minutes in Methionine/Cysteine-free medium supplemented with 10% dialyzed FCS, then labelled for 15 minutes with 200 µCi/ml of [^{35}S]-Methionine/Cysteine (Perkin Elmer) and 0.15 mM biotin where indicated. Cells were lysed in 100 µl of SDS lysis buffer and diluted with 400 µl of TNN for the subsequent immunoprecipitation of the SV5-tagged proteins with anti-SV5 mAb immobilized on Protein A agarose (Repligen). Proteins were eluted by boiling in SDS lysis buffer. Samples were resolved on a reducing SDS-PAGE and gels were fixed in 10% acetic acid and 10% methanol, incubated for 20 minutes in Amplify fluorographic enhancer (GE Healthcare), dried and exposed for autoradiography on Kodak BioMax XAR films.

Sample treatment with PNGase or RNAse

For enzymatic digestion with glycosidase PNGase (NEB), and RNase ONE™ (Promega), transfected HEK-293T cells were lysed in TNN-lysis buffer without Protease Inhibitors and treated following manufacturers' instructions. After incubation with PNGase, samples were boiled with reducing SDS loading buffer and resolved on SDS-PAGE as described above, while samples treated with RNase were not boiled to avoid tRNA ester bond hydrolysis.

Sample preparation for Mass Spectrometry analysis

HEK-293T cells were transfected with BioID2 encoding plasmids in presence of Biotin, 18 hours post-transfection media was replaced with fresh one and cells were lysed 24 hours

post-transfection using TNN lysis buffer with 30 mM NEM. Pull-down of biotinylated proteins was performed using Streptavidin Mag Sepharose™ (GE Healthcare).

RNA isolation, RT-PCR and qRT-PCR

Total RNA from HEK-293T cells was isolated with RNeasy mini Kit (Qiagen) following manufacturer's instructions. DNA was removed by treatment with RNAse-free DNAse I (Fermentas Inc, Massachusetts, USA). Total RNA was then retro-transcribed to cDNA by Moloney murine leukaemia RT (M-MLV-RT, Invitrogen) in the presence of random hexamers (IDT). qRT-PCR was based on SYBR Green Master Mix technology (Applied Biosystems) and the levels of target gene expression were normalized to those of endogenous GAPDH or the transfection control α-Globin.

Sequences of Primers:

NGLY for:	TCGTGACCTGATTGCCATAGAGAG
NGLY rev:	CTGCTTATTAAGCCCATTAATAGTGTC
Ltn for:	TGGTGCTGCGGAAACTTTCAAAG
Ltn rev:	GCAGCTGGTGTGTAAGTATCAC
scFv for:	CAAACAGACTCTCAACTT
scFv rev:	ATTTAGGTGACACTATAGAATA
EGFP-for:	TCAAGGAGGACGGCAACATC
EGFP-rev:	TTGTGGCGGATCTTGAAGTTC
α-Globin for:	GCCGACAAGACCAACGTCAA
α-Globin rev:	AGGTCGAAGTGCGGGAAGTA
GAPDH for:	GGGCGCCTGGTCACCAGGGCTGC
GAPDH rev:	GAGCCCCAGCCTTCTCCATGGTGG

Chemical crosslinking

24 hors post-transfection, HEK-293T were washed with PBS and incubated 30 minutes at room temperature with a solution of dithiobis(succinimidylpropionate) (DSP, Thermo Fisher Scientific) at the concentration of 1 mM. Reaction were quenched 15 minutes with Tris 20 mM and cells were lysed in TNN buffer.

Silver Staining

After Western blot electrophoresis, gels were incubated with shaking 30 minutes in Fixing solution A (50% methanol, 10% acetic acid), 15 minutes in Fixing solution B (5% methanol, 1% acetic acid) and washed for 3 times in ddH_2O for 5 minutes each. Gels were next incubated with shaking with the Sensitizer solution (0.02% $Na_2S_2O_3 \cdot 5H_2O$) for 90 seconds and stained at least for 60 minutes with Silver solution (0,2% $AgNO_3$), wash 3 times in ddH_2O for 30 seconds each and developed with Developing solution (3% $NaCO_3$, 0.05% formalin, 0.000016% $Na_2S_2O_3 \cdot 5H_2O$). Once the bands reached the desired intensity, reaction was blocked with Stop solution (6% acetic acid) for 5 minutes and gels were washed in ddH_2O.

Stable HEK^{NGLY-} cell line

HEK-293T cells were transfected with pX330-U6-Chimeric_BB-CBh-hSpCas9 (Addgene plasmid # 42230) (Cong et al., 2013) bearing one guide against the NGLY1 gene cloned with BbsI (New England BioLabs). Several guides were tested and transfected in combination to delete genomic DNA from exon 3 to 6 and avoid expression of alternatively spliced isoforms of NGLY1. As controls, HEK cells were transfected also with pX330 without hSpCas9 and pX330-hSpCas9 with no guides. 48 hours post-transfection cells media was discarded and replaced with fresh DMEM with antibiotics for selection (puromycin, 2 µl/ml) for 4 days. Cells were next resuspended and counted for limiting dilution in DMEM. Single clones were expanded, and exon deletions were tested by RT-PCR.

Sequences of Oligos:

```
guide exon3 for:  CACCGACACCATCTTCAAATCCCAG
guide exon3 rev:  AAACCTGGGATTTGAAGATGGTGTC
guide exon6 for:  CACCGCAGCACAGTGTAAAACAAT
guide exon6 rev:  AAACATTGTTTTACACTGTGCTGC
```

Sucrose gradients

10^7 HEK-293T cells were transfected with desired constructs as already explained. 48 hours post-transfection cells were treated with the translation inhibitor cycloheximide (Sigma) 100 µg/ml for 5 minutes, harvested and dropped into a flask containing frozen media at -20°C in an amount of 30% of the volume of cell suspension. Cells were washed and

collected by centrifugation at 1000 rpm for 10 minutes at 4°C. Cells were then resuspended in a hypotonic buffer (10 mM Tris-HCl pH7.4, 10 mM KCl, 1 mM Mg Acetate in DEPC treated water) and leaved at 4°C for 10 minutes. One volume of a solution of 70 mM Tris-HCl pH 7.4, 150 mM KCl, 100 mM NH_4Cl, 7 mM Mg Acetate, 10 mM DTT and 0.5% NP40 was added to the cell suspension and leaved for 10 minutes at 4°C. Cells were centrifuged at 5000 rpm for 10 minutes at 4°C and the supernatants were collected for analysis on sucrose gradients.

Sucrose was dissolved in a buffer solution of Tris-HCl 10 mM pH 7.4, KCl 50 mM, Mg Acetate 5mM and DEPC water. Linear gradients of 15% to 40% sucrose were prepared in 5 ml tubes of a SW 55 swinging rotor using a gradient-maker.

Cell lysates were loaded on the top of the gradient and centrifuged for 45 minutes at 45000 rpm at 4°C. Gradients were then manually divided from the bottom to the top into 12-15 fractions that were analysed on SDS page.

RESULTS

1. 2A-INDUCED RIBOSOME STALLING AT THE STOP-CODON TRIGGERS DEGRADATION OF THE NASCENT PROTEIN

The *in vivo* study of translational stalling is difficult because of the high rate of degradation of both mRNAs and/or peptides that renders complicated the identification of natural stalling mRNAs. For this reason, one of the best characterised model inducing ribosomal stalling is the presence of a poly(A) sequence that is translated in a poly-Lys tract that interacts with the negatively charged RET during translation elongation, thus imitating a NSD pathway (Amrani et al., 2004). Nevertheless, some upstream ORFs (uORFs) as AAP, uORF2 of CMV gp48 and tNAC encode amino acidic sequences that cause stalling of ribosomes once they reach a STOP-codon, instead of starting the translation termination, in order to modulate expression of the downstream ORF (Cao and Geballe, 1996a; Spevak et al., 2010; Uchiyama-Kadokura et al., 2014).

It was also reported that manipulation of the viral peptide 2A can induced translational stalling (Doronina et al., 2008b; Sharma et al., 2012): imposing a conventional termination codon after the C-terminal Gly of the Foot-and-Mouth Disease Virus (FMDV) 2A peptide caused the formation of prolyl-tRNAs translational products in *in vitro* wheat germ and rabbit reticulocyte translation systems (Doronina et al., 2008b; Sharma et al., 2012). This observation was explained with the hypothesis of ribosome stalling. Nevertheless, no further investigations were carried on to understand the mechanism or the biological consequences.

In parallel in our laboratory, it was noticed for the first time that engineering a reporter protein at the C-terminus with the 2A peptide followed by a STOP-codon strongly abrogated expression of the upstream protein in living human cell lines (Sasset, 2013). A similar behaviour of a translating ribosome remaining blocked at a canonical termination

was previously described only as a regulatory mechanism of uORFs. We thus decided to characterise this model of stalling in living cells for ribosomes translating proteins translocated in the ER lumen or in the cytosol.

1.1 EFFECT OF 2A PEPTIDE ON PROTEIN EXPRESSION

To study the effect of peptide 2A on the upstream protein translation in human cell lines, we used the sequence APVKQTLNFDLLKLAGDVESNPG* (2A*, where "*" indicates the STOP-codon) derived from the FMDV, which consists of the last 5 amino acids of the viral upstream protein VP1 (APVKQ) and 18 amino acids of peptide 2A.

As a secretory reporter protein, it was chosen a single chain variable fragments (scFv) of an immunoglobulin previously described (6A.C3) (Bestagno et al., 2007). The scFv is a fusion formed by the variable domains of the antibody light and heavy chains (V_L and V_H) separated by an 18 amino acids long flexible linker (Figure 21).

The scFv was engineered at the N-terminus with an immunoglobulin-derived secretion signal sequence (sec) to target the translation product into the ER (Li et al., 1997; Petris et al., 2011), and at the C-terminus with the SV5-tag (GKPIPNPLLGLD), followed by the FMDV 2A peptide with the last Proline mutated into STOP-codon (construct sec-2A*). As a control, the same reporter construct was engineered with a Proline upstream the STOP-codon (construct sec-2A-P*), reconstituting in this way the viral peptide 2A that undergoes non-conventional termination of the upstream protein, which will terminate with the NPG amino acids exactly like sec-2A. A scheme of both the constructs is reported in Figure 21 (left panel).

Constructs were cloned into pcDNA3 vector for CMV-driven expression in mammalian cells and were transiently transfected in human embryonic kidney cell line (HEK-293T) as described in Material and Methods. The total level of protein expression was analysed by Western blot. Cellular supernatants and/or total cell extracts were resolved under reducing conditions, blotted and developed with anti-SV5 antibody.

The molecular weight of the scFv is about 27 kDa, while, including the SV5-tag and the C-terminal 2A, the expected total mass of the reporter protein is around 31 kDa.

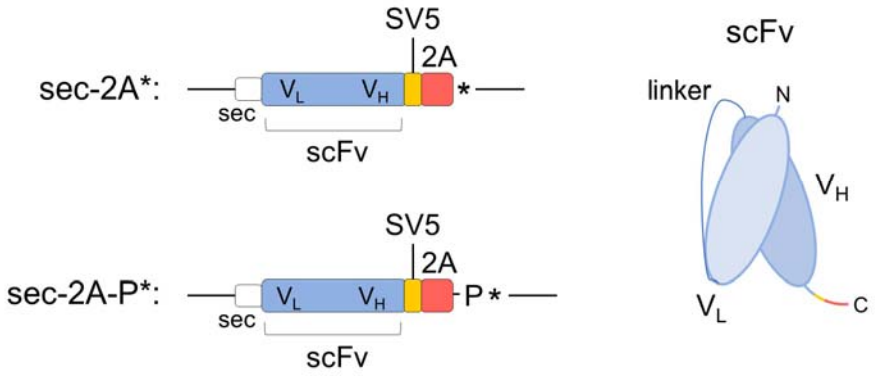

Figure 21. Scheme of the constructs used. The scFv 6A.C3 reporter protein was engineered with a secretory signal (sec) for targeting to the ER, an SV5-tag for SDS-page detection and the FMDV-derived 2A* or 2A-P* as a control. On the right, a representation of scFv domains V_H and V_L and their assembly. N-terminus (N) and C-terminus (C) are indicated.

The Western blot experiments clearly showed that proteins bearing 2A at their C-terminus were extremely less represented in the cellular supernatants in comparison with sec-2A-P, which was instead actively secreted (Figure 22, left panel). The analysis of proteins produced in cellular extracts confirmed the previous observation: the amount of sec-2A proteins is strongly reduced in comparison with the control sec-2A-P (Figure 22, right panel). Moreover, a comparable impairment in protein expression mediated by C-terminal 2A was observed also using a trans-membrane reporter protein, the major histocompatibility complex class I protein MHC-Iα (Sasset, 2013).

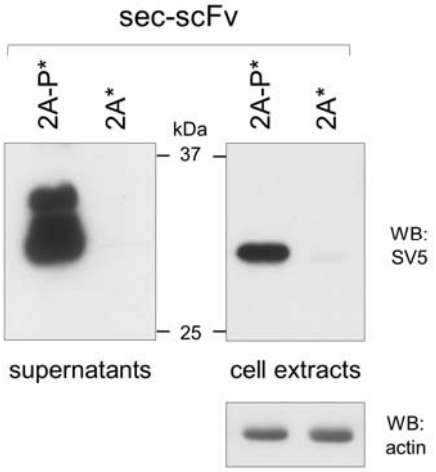

Figure 22. Secretory protein expression is impaired by 2A. Western blots of HEK-293T supernatants (on the left) and cell extracts (on the right) previously transfected with constructs expressing the reporter proteins sec-2A and sec2A-P, as schematised in figure 21. Western blot analysis is representative of at least 3 independent experiments.

The difference in expression between sec-2A-P and sec-2A was quantified in Western blot by densitometry and serial dilutions of samples (extracts or supernatants) from cells expressing construct sec-2A-P compared with the related reference sample derived from cells expressing sec-2A. Protein levels of cell lysates were also normalised on actin.

Extracts of cells expressing reporter proteins contained an amount of sec-2A of about 5.3% ± 0.86 with respect to sec-2A-P (Figure 23A), while only 1.1% ± 0.04 was secreted in comparison with sec-2A-P (Figure 23B).

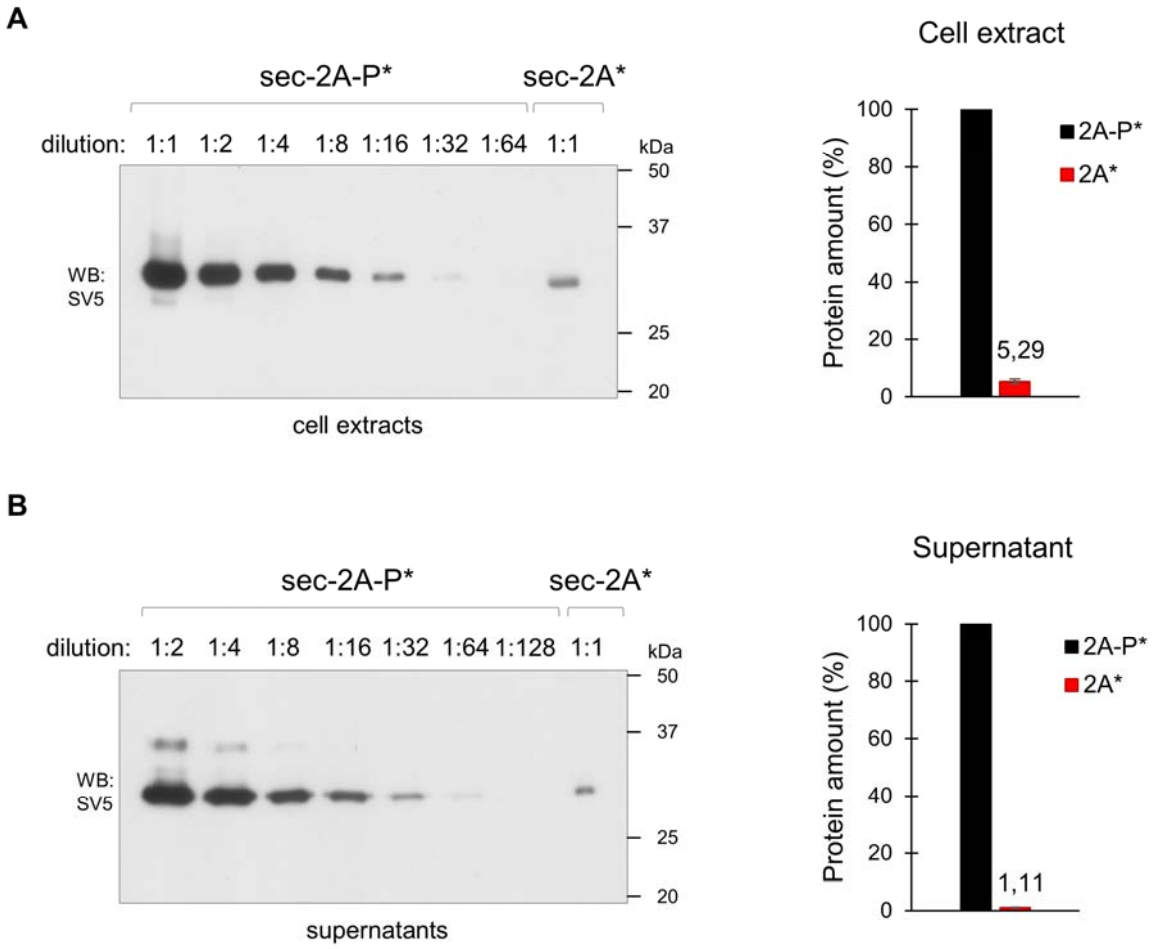

Figure 23. Relative quantification of protein expression. **A:** Quantification of protein amount in lysates of HEK-293T transfected with construct sec-2A* or sec-2A-P*. Proteins bearing C-terminal 2A (red bar) are expressed 5.3% ± 0.86 if compared to the control proteins with 2A-P (black bar). **B:** quantification of protein amount secreted in supernatant of HEK-293T transfected as in A. Proteins with C-terminal 2A are expressed 1.1% ± 0.04 in comparison to the control proteins with 2A-P. Quantification analysis was performed on n=4 experiments and images are representative of the results.

To see whether 2A causes a similar effect on translation of proteins expressed in the cytosol, the same scFv reporter constructs were designed to be translated only by free ribosomes in the cytosol, so the secretion signal at the N-terminus was removed (Figure 24, left panel). The corresponding plasmids were then transfected in HEK-293T cells and cell lysates were collected 24 hours post-transfection. Samples were resolved under reducing conditions in SDS-PAGE.

As reported in Figure 24 (right panel), the cytosolically expressed reporter engineered with 2A at the C-terminus was less expressed in comparison to cyt-2A-P control proteins.

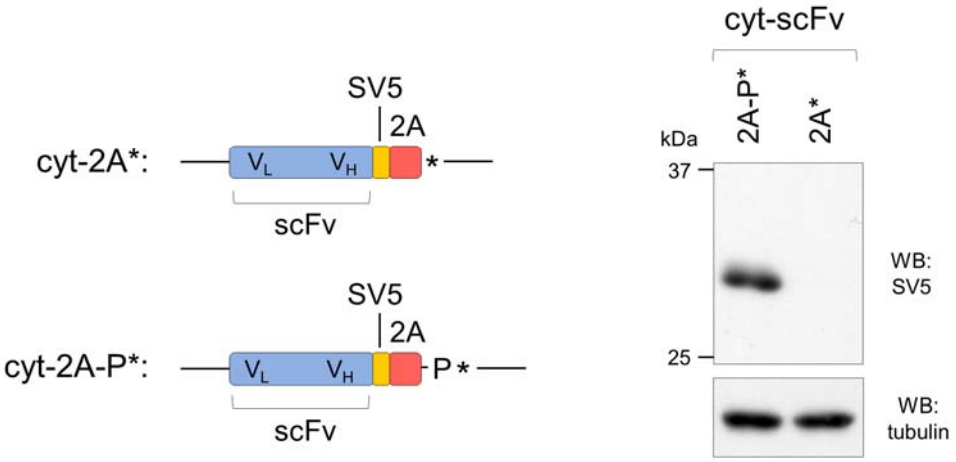

Figure 24. Cytosolic protein expression is impaired by 2A. On the left, the scheme of the constructs encoding the cytosolic reporter protein scFv 6A.C3 engineered with the SV5-tag and the FMDV-derived 2A or 2A-P as a control. On the right panel, a Western blot representative of their expression in HEK-293T 24 hours after transfection.

Similar results were obtained using EGFP as a reporter protein (Sasset, 2013). These findings confirmed that impairment of expression is 2A-dependent and regardless whether the protein is translated by ER-bound or free ribosomes.

The total amount of proteins expressed in HEK-293T cells from construct cyt-2A* was quantitated as described above and it consisted of 3.04 ± 1.21% in comparison with the same protein expressed from construct cyt-2A-P* (Figure 25).

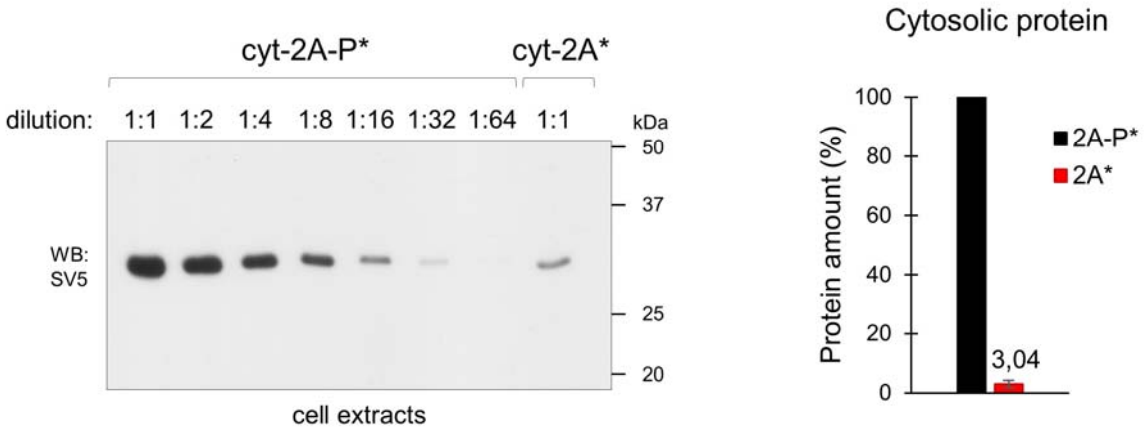

Figure 25. Quantification of protein amount in lysates of HEK-293T transfected with cyt-2A* or cyt-2A-P* plasmids. Proteins bearing C-terminal 2A (red bar) are expressed 3.04 ± 1.21% in relation to the control proteins with 2A-P (black bar). Quantification analysis was performed on n=3 experiments and Western blot is representative of the results.

Expression of the same construct in an *in vitro* transcription and translation system based on reticulocyte lysates showed a similar outcome, with a more modest reduction of about 3.5-fold for cyt-2A proteins, in comparison with the control cyt-2A-P (Figure 26). This is an indication that *in vivo* there are probably other mechanisms operating that produce a larger difference in expression.

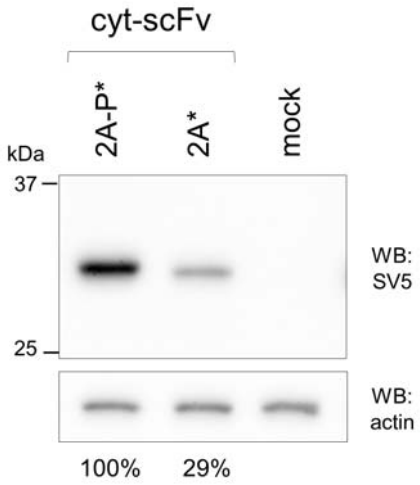

Figure 26. Expression of cyt-2A is impaired in *in vitro* transcription and translation system of reticulocytes. cyt-2A amount is 29% in comparison with control cyt-2A-P. Relative quantification was performed by densitometry normalising on actin levels. Quantification analysis was performed on n=3 experiments.

1.2 2A INDUCES RIBOSOME STALLING AT THE STOP-CODON

The difference in protein expression observed for 2A reporters can be reasonably explained by ribosome stalling. In fact, we found that the rate of protein synthesis in the case of sec-2A was reduced (Sasset, 2013). To quantify the rate of protein translation, HEK-293T cells were transfected with secretory reporters and labelled with a pulse of [^{35}S]-Methionine for 15 minutes. SV5-tagged proteins were then purified from total cell extract by immunoprecipitation, run in SDS-PAGE under reducing conditions and detected by autoradiography. The results obtained indicate a reduction in 2A synthesis of 15-folds in comparison with sec-2A-P (Figure 27). We deduced that this slowdown of ribosome synthesis is an indication of ribosomes stalled during translation. However, this finding didn't fully explain the difference observed between the total amount of 2A and 2A-P proteins.

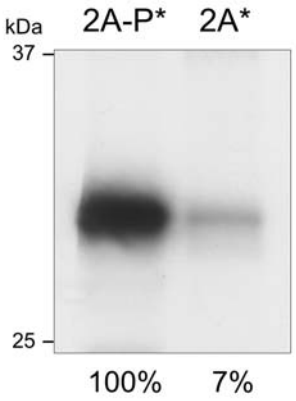

Figure 27. Autoradiography of anti-SV5 immunoprecipitated proteins obtained from extracts of HEK-293T transfected with the indicated constructs and labelled with [^{35}S]-Methionine for 15 minutes. Quantification is indicated at the bottom of each lane. Representative of n=2 independent experiments. From Sasset, 2013.

We reasoned that the prolonged stalling of ribosomes could depend by the presence of the termination codon after 2A. To confirm this point, we engineered two bicistronic constructs A and B (schematically shown in Figure 28, left panel). Both A and B are designed to produce the upstream protein (pr1) by 2A non-conventional termination, as pr1 is followed by the Pro-codon in both constructs. The downstream protein (pr2, same as pr1 with an extra tag) terminates in 2A* in the case of construct B (pr2-2A*) or in 2A-P* in the case of construct A (pr2-2A-P*), used as a control. In this way, we expected to observe impaired expression

of pr1 in construct B only if ribosomes stall at the termination codon downstream of pr2-2A. If not, pr1 should be equally expressed from constructs A and B. Constructs A and B were independently expressed in HEK-293T cells, and as controls we transfected as well monocistronic plasmids encoding only for pr1-2A-P, pr2-2A or pr2-2A-P.

The results reported in Figure 28 (right panel) show that pr1 and pr2 are both expressed from construct A, but not from construct B. Thus, compromised expression of pr1, as well as pr2, was consistent with ribosome stalling at the 2A-STOP-codon of construct B.

The difference between pr1 and pr2 produced from construct A is due to peptide 2A non-conventional termination, which is not always efficient in restarting translation from the downstream Pro (Sasset, 2013).

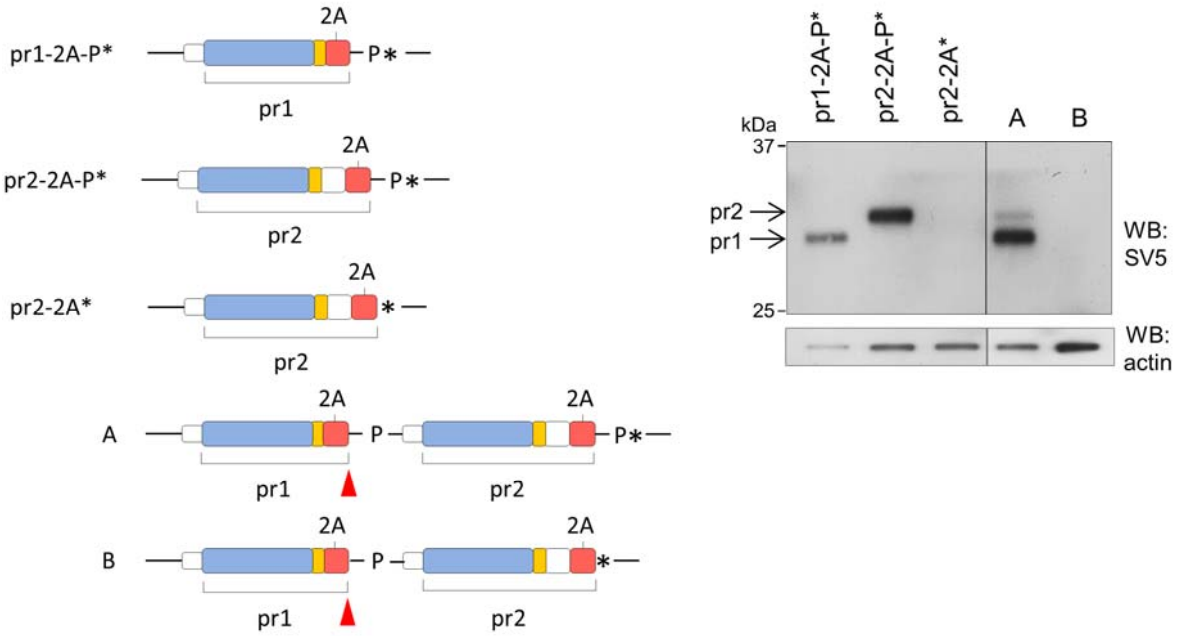

Figure 28. On the left panel, scheme of mono- and bicistronic constructs, with red arrowheads indicating non-conventional termination of pr1 in constructs A and B. On the right panel, Western blots of extracts of HEK-293T cells, transfected as indicated with constructs represented alongside. Western blot is representative of 3 independent experiments. Modified from Sasset, 2013.

To further confirm that stalling depends on termination codon after 2A and considering that the simple addition of a terminal Pro rescued the upstream protein expression, we decided to test the effect of the addition of an amino acid different from Pro before the STOP-codon. As showed in Figure 29, we found that Glu, Gly, Leu, Arg and Trp rescued

protein expression in a way comparable to Pro, strongly indicating that stalling is totally due to the presence of the STOP-codon in that precise position.

Moreover, the effect mediated by the presence of 2A amino acidic sequence at the C-terminus of any reporter proteins was demonstrated to be not dependent on nucleotide sequences or on the STOP-codon used, but exclusively on the peptide sequence LLKLAGDVESNPG (Sasset, 2013). For all these reasons, we refer to the 2A-mediated stalling as “stalling at the STOP-codon”.

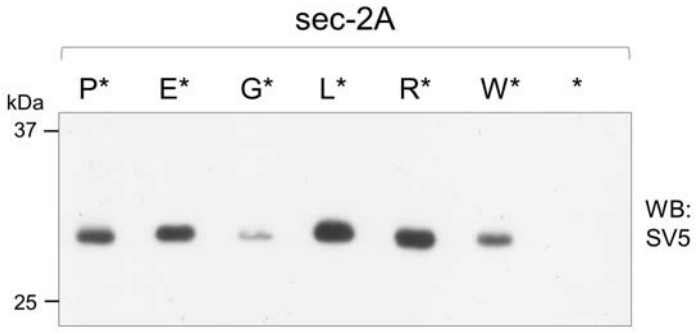

Figure 29. Western blot of HEK-293T cell extracts expressing sec-scFv reporter with the NPG C-terminus mutated with the addiction of the Pro or a different amino acid, as indicated.

As several sequences that cause translational stalling activate mRNA decay, we checked the mRNA levels present in cells after transfection with sec-2A* or sec-2A-P* plasmids by quantitative RT-PCR (qRT-PCR) and normalising on endogenous GAPDH or the co-transfected α-Globin-expressing construct.

As reported in the graphs of Figure 30, no significant difference was detected between mRNAs produced from sec-2A* and sec-2A-P* constructs (Sasset, 2013).

A similar qRT-PCR analysis performed on total mRNA from cells transfected instead with cytosolic 2A-tagged EGFP indicated that mRNA can be slightly affected by degradation.

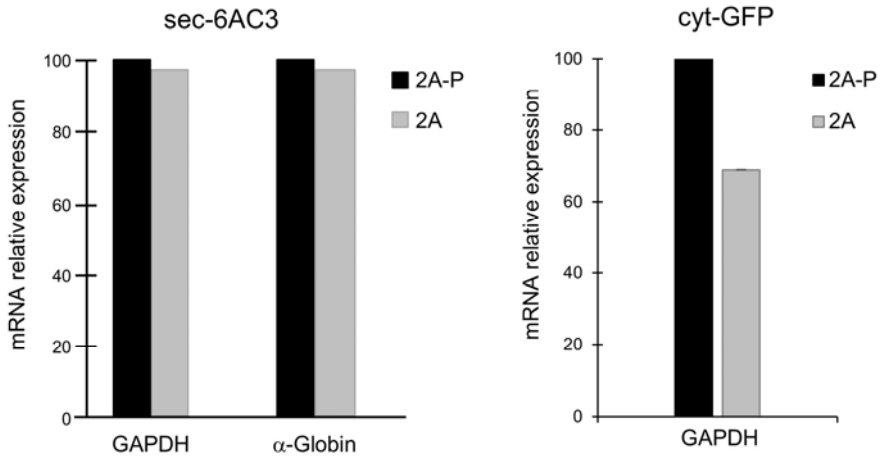

Figure 30. On the left panel, quantitative RT-PCR of mRNA levels in HEK-293T transfected with constructs sec-2A-P* (black) or sec-2A* (grey) and normalized to the endogenous GAPDH mRNA or to a co-transfected α-Globin encoding control plasmid. Representative of n=3 independent experiments. The graph is adapted from Sasset, 2013. On the right panel, a similar experiment performed on cells transfected with cytosolic EGFP constructs bearing 2A or 2A-P at their C-termini indicate a reduction in mRNA of 30% (n=4).

It was previously reported that in *in vitro* translation systems, the mutation of the FMDV Pro-codon with a STOP produce a polypeptide that remains associated to $tRNA^{Gly}$ (Doronina et al., 2008b; Sharma et al., 2012). Indeed, in similar experiments of cyt-2A expressed in an *in vitro* transcription-translation system based on reticulocyte lysate, we observed a small fraction of 2A proteins migrating below 50 kDa that was sensitive to treatment with RNAse, confirming that it was peptidyl-tRNA (Figure 31).

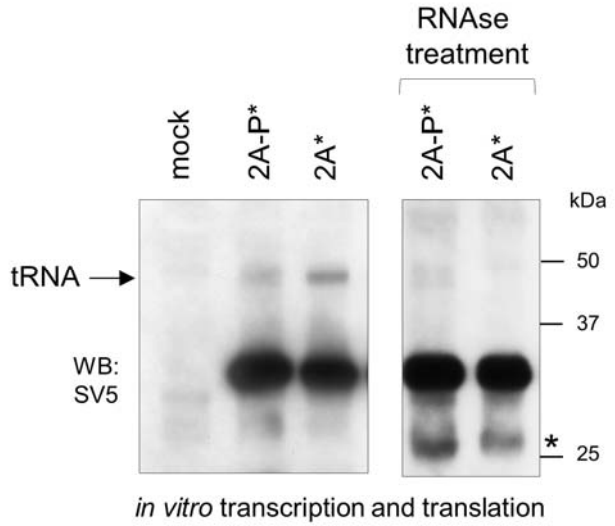

Figure 31. Western blot of *in vitro* reticulocyte-based system of transcription and translation expressing constructs cyt-2A-P* or cyt-2A*. After *in vitro* reaction, samples were divided and treated or not with RNAse A and were run without boiling in reducing condition. Asterisk indicates nonspecific signal due to the presence of the RNAse.

1.3 PROTEASOMAL DEGRADATION OF 2A POLYPEPTIDES DERIVED FROM ER-STALLED RIBOSOMES

Considering the strong differences in protein expression previously observed between sec- or cyt-2A and 2A-P, we speculated that 2A-tagged polypeptides were substrates of protein degradation. In fact, the reduced synthesis rate in translation doesn't completely justify such a difference and in literature there are examples of other polypeptides that are degraded because inducing translational stalling.

To determine the pathway of degradation of sec-2A reporter proteins, HEK-293T cells were transfected with the constructs shown in Figure 21. 20 hours after transfection, cells were treated with the proteasome inhibitor MG132. In this way, if this is the proper degradation pathway, its substrates should accumulate because their clearance is prevented.

As represented in Figure 32, sec-2A-P control proteins were not affected by the use of the compound, because they are efficiently translated and secreted, and not targeted to degradation. However, sec-2A proteins accumulated when proteasome activity was

impaired, indicating that degradation occurred through the proteasome. This was further confirmed by impairment of the autophagic pathway with Chloroquine, which did not induced accumulation of the secretory 2A reporters (Sasset, 2013).

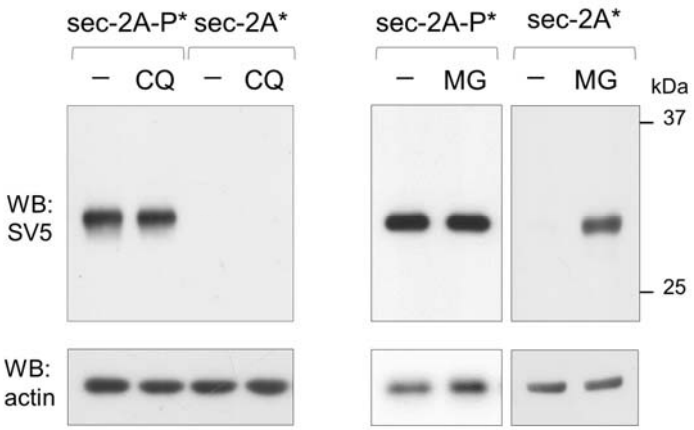

Figure 32. Lysates of HEK-293T cells expressing scFv reporters with sec-2A and sec-2A-P. 20 hours post-transfection, cells were treated as indicated with Chloroquine 50 µM (CQ, left panel) or MG132 20 µM (MG, right panel) for 4 hours. Equal volumes of DMSO were used as a control. Western blot results are representative of at least 2 independent experiments.

Proteasomal degradation requires conjugation of the substrates with poly-ubiquitin chains. So sec-2A should be first poly-ubiquitinated as well in order to be engaged by the proteasome. To demonstrate ubiquitination of these proteins, plasmids encoding sec-2A or sec-2A-P reporters were co-expressed with the deubiquitinase (DUB) OTU. This enzyme, derived from the OTU domain of the N-terminus of the Crimean Congo haemorrhagic fever virus-L protein (CCHFV-L), removes K48- and K63- linked poly-ubiquitin moieties from a broad range of proteins because of its low substrate specificity, thus preventing their degradation (Capodagli et al., 2011; Frias-staheli et al., 2007). As a result, deubiquitinated proteasome substrates accumulate (Sasset et al., 2015).

As shown in Figure 33, sec-2A proteins are stabilised as a consequence of OTU activity, while control sec-2A-P was not affected, indicating that degradation occurred predominantly for scFv proteins derived from ribosomes stalled at the STOP-codon.

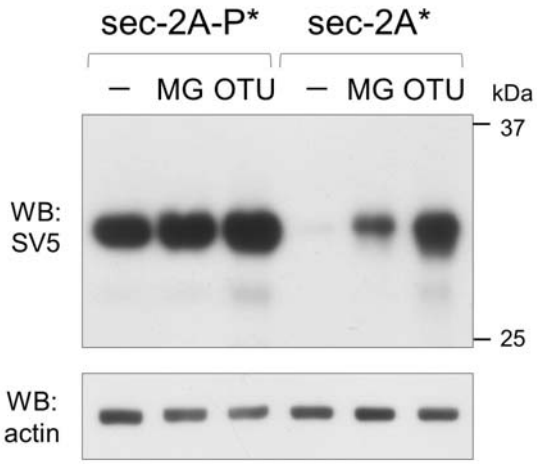

Figure 33. Cell lysates of HEK-293T transfected with plasmid expressing the reporter protein sec-2A or sec-2A-P and the deubiquitinase OTU or treated with proteasome inhibitor MG132 (MG) as indicated. Result is representative of n=3 experiments.

Poly-ubiquitination of 2A polypeptides targeted to the ER

To further confirm that ubiquitination occurred specifically for sec-2A reporters and not for sec-2A-P, corresponding plasmids were co-transfected with a plasmid encoding HA-tagged Ub. In this way, if sec-2A is a substrate of the ubiquitin-proteasome pathway, HA-Ub will be incorporated into poly-ubiquitin branches on sec-2A proteins, but not on sec-2A-P, which is mostly secreted. 20 hours post-transfection, cells were also treated with MG132 to avoid degradation of poly-ubiquitinated proteins and induce their accumulation. After 4 hours of proteasome inhibition, cells were lysed, and SV5-tagged proteins were immunoprecipitated, resolved on SDS-PAGE and immunoblotted with an antibody specific for HA-tag (Figure 34).

Poly-ubiquitination of proteins engineered with C-terminal 2A was easily detectable upon proteasome inhibition and was highly represented, whilst only a small amount of sec-2A-P proteins were found poly-ubiquitinated (Figure 34A), despite the fact that they were expressed at much higher levels, in line with our previous observations indicating they are not degraded.

To confirm that the signal observed in Western blot analysis is specifically due to poly-ubiquitinated sec-2A, the same experiment was carried out in presence of OTU. When the deubiquitinase was expressed, sec-2A was found definitely not ubiquitinated (Figure 34B).

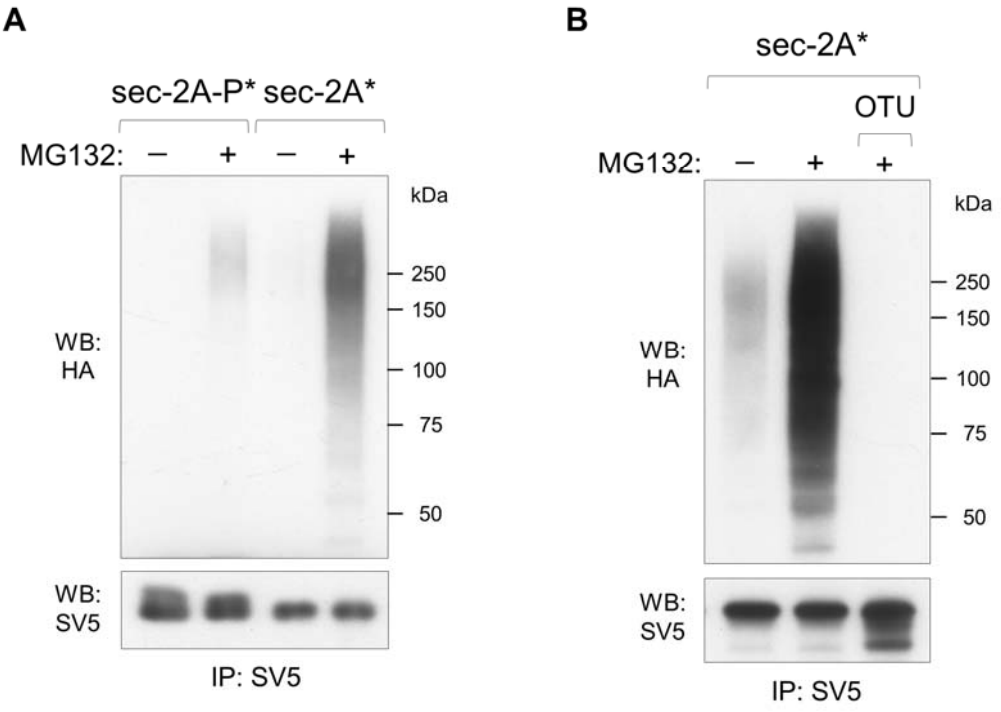

Figure 34. A: Immunoprecipitation of SV5-tagged sec-2A-P and sec-2A reporter proteins co-expressed in HEK-293T cells with HA-tagged Ub and treated or not with MG132 where indicated. **B:** Immunoprecipitation of SV5-tagged sec-2A reporter proteins co-expressed with HA-tagged Ub and OTU, with cells treated or not with MG132. Experiments are representative of n=2.

Taken together, these data strongly demonstrated that the reporter proteins bearing 2A and not 2A-P at their C-terminus, which resulted in stalling at the termination codon, are recognised for degradation, poly-ubiquitinated and targeted to the proteasome.

Considering that the ER-translated sec-2A products are substrates of degradation, we wondered if this corresponded to activation of the ER-associated degradation (ERAD). ERAD substrates are generally poly-ubiquitinated by E3 ubiquitin ligases specific for this pathway, like Hrd1.

To investigate if Hrd1 is the enzyme responsible of ubiquitination of 2A polypeptides, we co-transfected constructs sec-2A* or sec-2A-P* with the dominant negative version of the ERAD ubiquitin ligase Hrd1, with the RING domain C291 mutated with S to abolish binding to ubiquitin-conjugating enzymes E2 (Nadav et al., 2003; Okuda-Shimizu and Hendershot, 2007). The expected result is that if Hrd1 is the responsible of sec-2A ubiquitination, co-expression of the dominant negative mutant should impair 2A polypeptides degradation. The results obtained indicated accumulation of sec-2A under these conditions (Figure 35A,

upper panel). To confirm that the effect observed was specifically due to Hrd1, the same experiment was performed on cytosolically expressed 2A, as Hrd1 should not have activity on cytosolic proteins. Some accumulation, however, was observed for cyt-2A as well (Figure 35A, lower panel), suggesting that Hrd1 could be not the major ubiquitin ligase involved in sec-2A ubiquitination, as the accumulation observed with Hrd1 C291S might be non-specific and probably due to cellular stress.

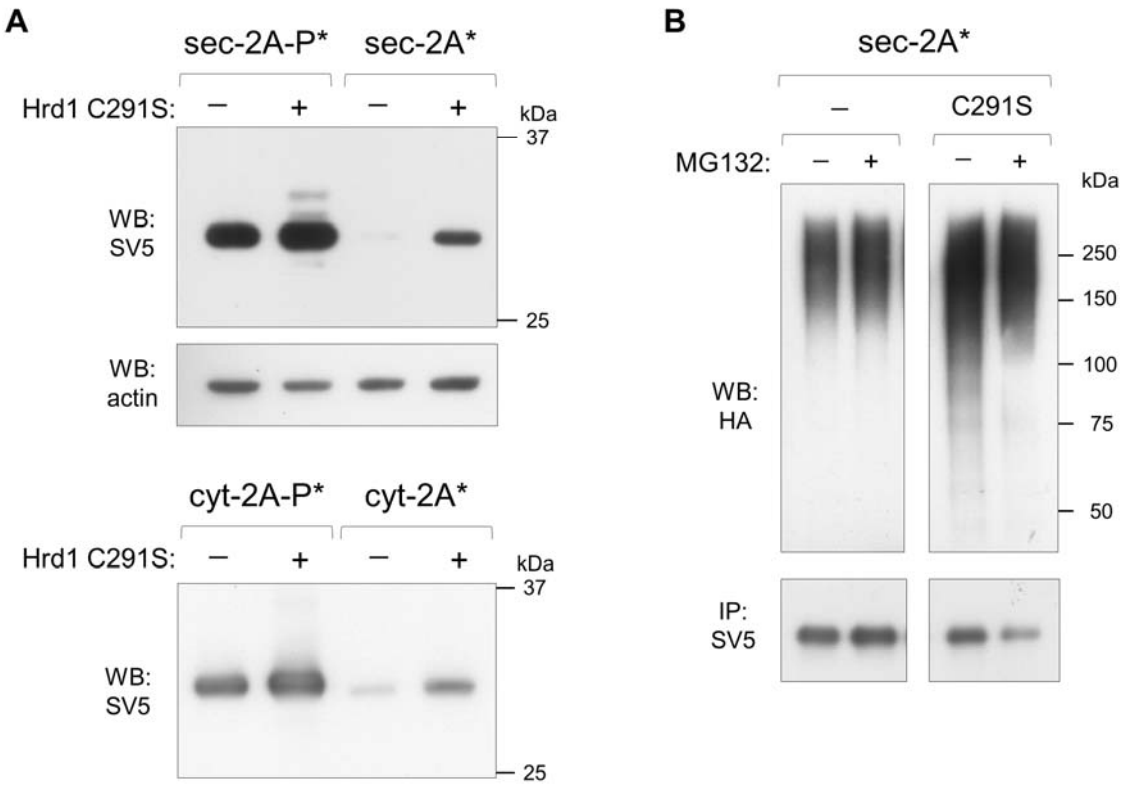

Figure 35. Poly-ubiquitination of sec-2A polypeptides. **A:** Upper panel, co-transfection of sec-2A and sec-2A-P reporters with the ERAD ubiquitin ligase Hrd1 dominant negative C291S. Lower panel, control of Hrd1 dominant negative specificity upon its co-transfection with cytosolic proteins. Results are representative of at least two experiments. **B:** Immunoprecipitation of SV5-tagged sec-2A and sec-2A-P co-expressed with HA-Ub and without or with Hrd1 C329S as indicated. The experiment was performed once.

To better understand if Hrd1 was involved or not, the same secretory constructs were co-transfected with plasmids encoding HA-Ub and with or without Hrd1 C291S. Cells were treated with MG132 as previously described and after lysis, SV5-tagged reporter proteins were immunoprecipitated. Samples were resolved on reducing SDS-PAGE and

immunoblotted against HA-tag to detect poly-ubiquitinated proteins. As reported in Figure 35B, there was an increase in secretory 2A molecules with shorter poly-ubiquitin chains as a consequence of Hrd1 impairment, however overall sec-2A appeared highly ubiquitinated upon co-expression with Hrd1 C291S, suggesting the involvement of at least one other main E3 ubiquitin ligase.

In case of stalling of translation, the E3 ubiquitin ligase Listerin was reported to be part of the ribosome quality control (RQC) complex and to ubiquitinate polypeptides associated to stalled ribosomes to target them to the proteasome (Bengtson and Joazeiro, 2010; Brandman et al., 2012; Saito et al., 2013; Shao et al., 2013). It was also described to be involved in ubiquitination of peptides derived from stalled, ER membrane-bound ribosomes in yeast and mammals (Arakawa et al., 2016; Crowder et al., 2015; Izawa et al., 2012; Malsburg et al., 2015). We then decided to check if Listerin was also involved in degradation of polypeptides originated from ribosomes stalled at the STOP-codon. Listerin expression in HEK-293T cells was transiently silenced using a specific siRNA as reported in Material and Methods. Cells were transfected with constructs sec-2A and sec-2A-P and cell extracts were analysed by Western blot.

As shown in Figure 36, upon Listerin silencing, sec-2A accumulated in cell extracts. Silencing was confirmed by RT-PCR performed on total mRNA extracted from HEK-293T cells after Listerin-specific or irrelevant silencing.

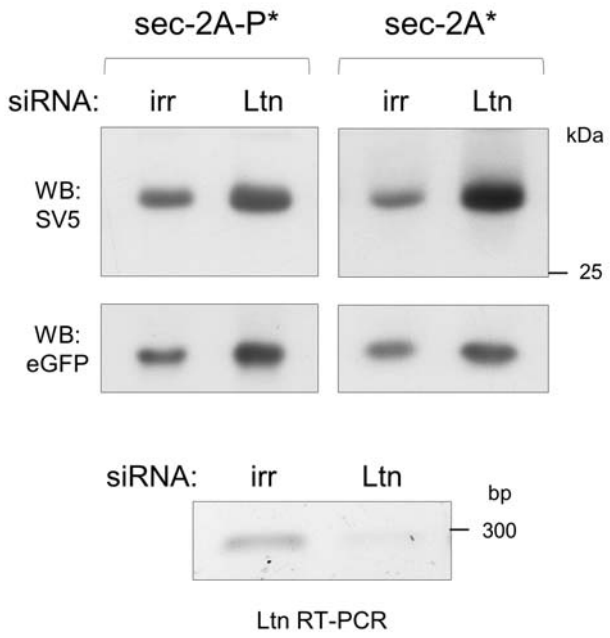

Figure 36. Upper panel, Western blots of extracts of HEK-293T cells transfected with siRNA for Listerin (Ltn) or irrelevant (irr) and followed by transient transfection with construct sec-2A* or sec-2A-P*. Plasmid pEGFP was used as control of transfection. Lower panel, ethidium bromide stained agarose gel showing RT-PCR amplification of a 290 bp fragment of Ltn mRNA from cells transfected as above. Representative of n=2 independent experiments.

AAA ATPase VCP/p97 and deubiquitinase YOD1 are involved in the degradation of 2A polypeptides

The AAA ATPase valosin containing protein (VCP) p97 was described to play important roles in extraction from the RET of stalled peptides and their degradation (Brandman et al., 2012; Defenouillère et al., 2013; Verma et al., 2013). However, it is involved as well in the extraction from the ER lumen and/or degradation of proteins substrates of ERAD (Carvalho et al., 2006; Jarosch et al., 2002; Neuber et al., 2005; Sasset et al., 2015). Moreover, VCP/p97 association to the cytosolic DUB YOD1 is required for some ERAD substrate retro-translocation and/or degradation (Bernardi et al., 2013; Ernst et al., 2009; Sasset et al., 2015). YOD1 belongs to the same DUB family of the otubain (OTU-domain Uba-binding) proteases as OTU.

Considering that secretory 2A-tagged reporters are intended for proteasomal degradation, we decided to study if they are also substrates of the AAA ATPse VCP/p97 and YOD1, as we

began to hypothesise that polypeptides derived from ER-stalled ribosomes are targeted to degradation by ERAD. For this reason, the sec-2A-expressing plasmid was co-transfected in HEK-293T cells with (i) a construct encoding a p97 with E305 and E578 mutated into Q (p97QQ) to abrogate ATPase activity, which is reported to have a dominant negative effect on endogenous p97 (Ye et al., 2001) or (ii) a construct encoding the dominant negative variant of YOD1, with C160 mutated into S to abrogate its catalytic activity (Ernst et al., 2009). In this way, if 2A polypeptides are normally recognised by VCP/p97 or YOD1, they should be stabilised when their activity resulted impaired.

As shown in Figure 37, sec-2A proteins accumulated when co-expressed with either of the dominants negative proteins p97QQ or YOD1 (C160S).

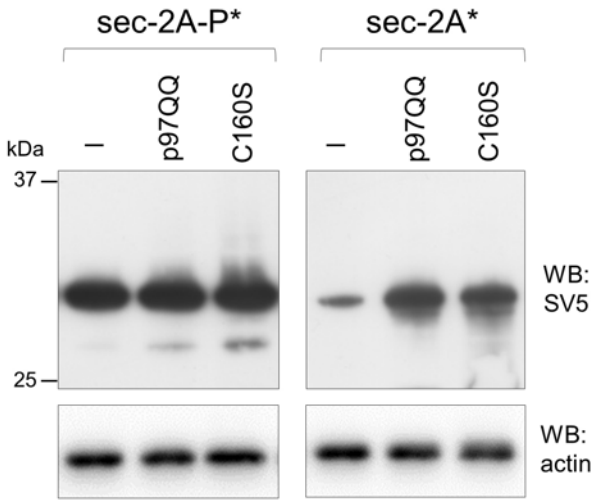

Figure 37. HEK-293T transient transfection of constructs sec-2A-P* or sec-2A* with dominant negatives of VCP/p97 (p97QQ) or deubiquitinase YOD1 (C160S), as indicated. Western blot is representative of n=3 independent experiments.

1.4 DEGRADATION PATHWAY OF CYTOSOLICALLY EXPRESSED 2A POLYPEPTIDES

Our next step was to analyse if cytosolically expressed 2A reporter proteins are degraded by the ubiquitin-proteasome pathway as well. For this reason, plasmid expressing cyt-2A-P or cyt-2A (represented in Figure 24) were transfected in HEK-293T cells in the presence or absence of the DUB OTU or proteasome inhibition. As reported in Figure 38, 2A

polypeptides cytosolically translated were clients of the proteasome, as they accumulated upon treatment with the proteasome inhibitor MG132, and their degradation resulted compromised because of OTU, indicating their ubiquitination. In contrast, the amount of protein produced from the control construct cyt-2A-P was much less influenced (Figure 38, left panel).

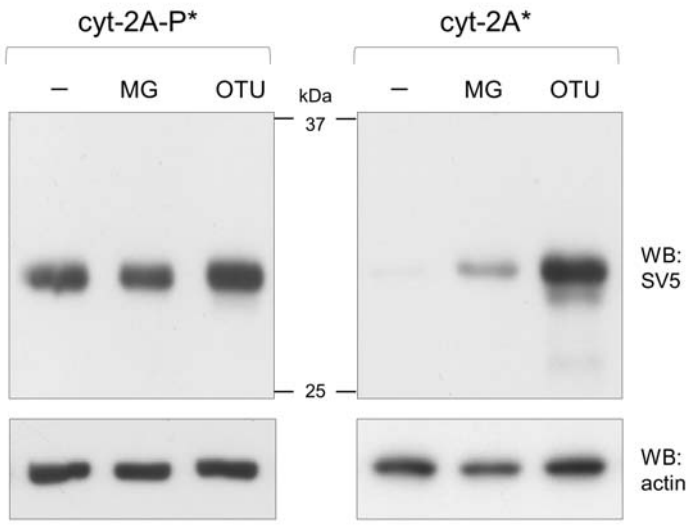

Figure 38. Degradation pathway of cytosolically expressed 2A proteins. HEK-293T lysates of cells expressing cyt-2A-P (on the left) or cyt-2A (on the right) reporter proteins and treated with proteasome inhibitor MG132 (MG) 20 µM or co-transfected with OTU, as indicated. Western blots are representative of n=3 independent experiments.

To investigate if Listerin was responsible of ubiquitination of cyt-2A, we reproduced the same experiment performed for secretory reporters. After transient transfection of Listerin-specific siRNA, HEK-293T were transiently transfected with cyt-2A and cyt-2A-P expressing plasmids.

The results shown in Figure 39 highlight an accumulation of cyt-2A in cell extracts when Listerin is not expressed, while cyt-2A-P is not affected, indicating that the involvement of the ubiquitin ligase is specifically required only in the case of cytosolically expressed scFv proteins that caused ribosome stalling because of the 2A sequence present at their C-terminus.

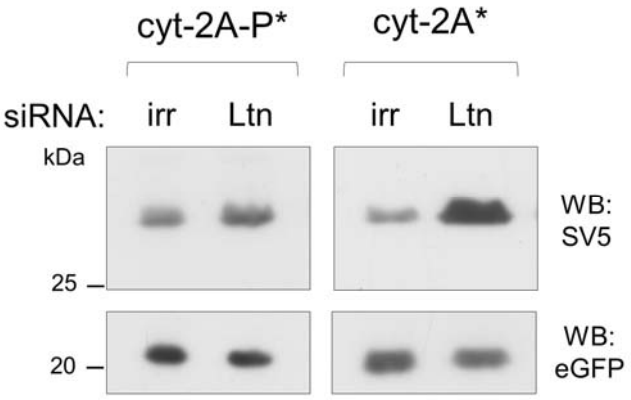

Figure 39. Western blots of extracts of HEK-293T cells transfected with Listerin (Ltn)-specific or irrelevant (irr) siRNA and followed by transient transfection of constructs cyt-2A* or cyt-2A-P* and pEGFP, as transfection control. Representative of n=2 independent experiments.

The following step was to confirm the involvement of the VCP/p97 ATPase. As already reported, this enzyme was associated to the degradation of peptides originated from stalled ribosomes.

Plasmids encoding cyt-2A and p97QQ were co-transfected. Analysis of cell extracts revealed that p97 is involved also for the degradation of cyt-2A polypeptides (Figure 40).

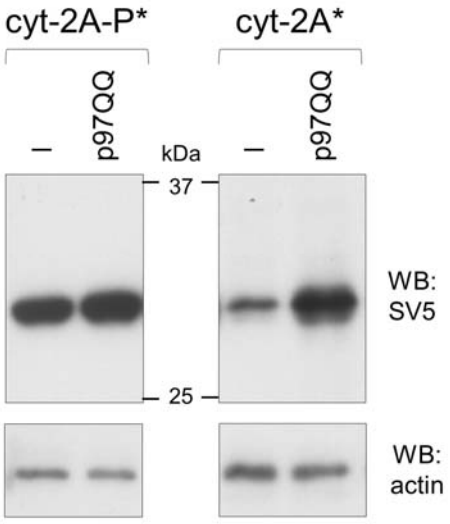

Figure 40. Lysates of cells HEK-293T expressing cyt-2A-P (on the left) or cyt-2A (on the right) reporter proteins and co-transfected with the dominant negative of VCP/p97 ATPase, p97QQ, as indicated. Representative of n=3 independent experiments.

In conclusion of this first part of the thesis, we demonstrated that tagging a reporter protein with 2A caused stalling of translation, with ribosomes stuck at the termination codon. This condition is induced by the amino acid sequence of the peptide 2A followed by a termination codon and triggers the degradation of the stalled protein, whether the ribosomes are ER-bound or free. Moreover, we found that degradation of polypeptides translated at the ER membrane required the intervention of catalytically active VCP/p97 ATPase and the ERAD deubiquitinase YOD1 to target 2A peptides to the proteasome, while ubiquitination depended in part on Listerin, but our data indicate the possible involvement of other ubiquitin ligases.

VCP/p97 and Listerin were important for degradation of 2A reporters produced by free ribosomes as well, as previously reported for other peptide sequences that induce translational stalling.

Noteworthy, the same reporter proteins produced instead by non-conventional termination of constructs 2A-P* were found translated in high amount both by free and cytosolic ribosomes and were not targeted to degradation.

2. ER-TARGETED 2A PROTEINS ARE SUBSTRATES OF THE ER-ASSOCIATED DEGRADATION

We demonstrated that proteins tagged with 2A induce stalling of both free and ER-associated ribosomes at the STOP-codon and that the newly synthetized polypeptides are specifically selected for proteasomal degradation and thus poly-ubiquitinated, at least in part by Listerin, in line with what described for proteins derived from mRNAs trunked or lacking a termination codon.

Moreover, we found that the two ERAD players p97 and YOD1 were also important for 2A proteins degradation, so we suspected that products of ER-stalled ribosomes are targeted to ERAD. This means that they must be inserted in the ER lumen and recognised for degradation. Common substrates of the ERAD pathway, however, are misfolded or totally unfolded proteins. In our case, we might consider that 2A-tagged proteins should not be misfolded, as they are identical to the control protein produced by non-conventional termination from construct 2A-P, which differs only for the presence of the latest Pro-codon.

We thought that the 2A-induced stalling at the STOP-codon could be used as a model to study the mechanism that target to degradation the products of ribosomes stalled at the ER membrane.

2.1 SECRETORY 2A PROTEINS DERIVED FROM RIBOSOME STALLING ARE NOT FULLY N-GLYCOSYLATED

First of all, we decided to study if the product of 2A-stalled ribosome is fully inserted in the ER lumen. A widely used system to prove if a protein of interest is in the ER, is the endogenous N-glycosylation. N-glycosylation is a co-translational modification that takes

place exclusively in the ER lumen by a cascade of enzymatic reactions upon recognition of the NXT/S amino acid sequence on nascent proteins, where X is any amino acid except Pro. To allow the co-translational enzymatic conjugation of the preformed oligosaccharides, it was calculated that the N-glycosylation site must be around 70 amino acids upstream the ribosomal peptidyl transferase centre (PTC) (Whitley et al., 1996).

We designed two different constructs, with the N-glycosylation site NGT inserted at the N-terminus (constructs N^N-2A* and N^N-2A-P*) or at the C-terminus (constructs N^C-2A* and N^C-2A-P*), 45 amino acids upstream termination codon of our reporters scFv 2A-P and 2A-tagged. A scheme of the new constructs is shown in Figure 41.

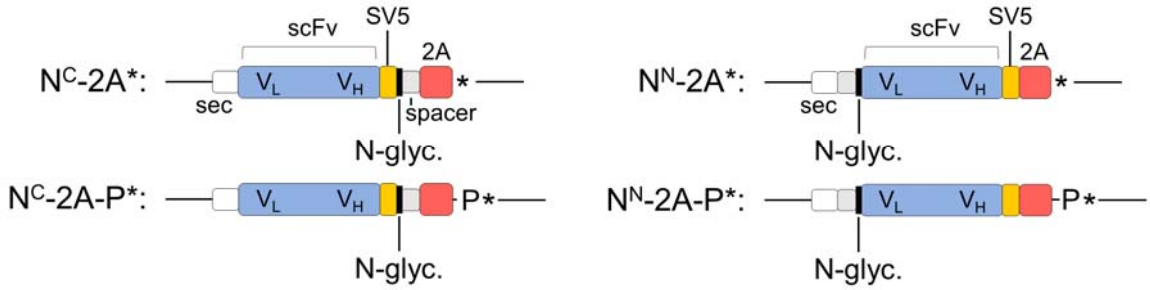

Figure 41. Scheme of the constructs bearing the N-glycosylation site NGT (indicated in black) at the N-terminus or at the C-terminus of the 2A- and 2A-P-tagged reporter proteins.

We reasoned that while N-terminal NGT site should be easily accessible at the ER environment for glycosylation, the C-terminal one will be glycosylated only if the 2A-tagged proteins are fully translated and inserted in the ER lumen.

Plasmids were independently transfected in HEK-293T cells and extracts were analysed by Western blot. We found that 2A-tagged proteins were only partially glycosylated, regardless whether the N-glycosylation site was at N- or at C-terminus of the reporters (Figure 42). The controls bearing C-tail 2A-P were instead fully glycosylated, indicating that the NGT sequences were engineered at accessible positions.

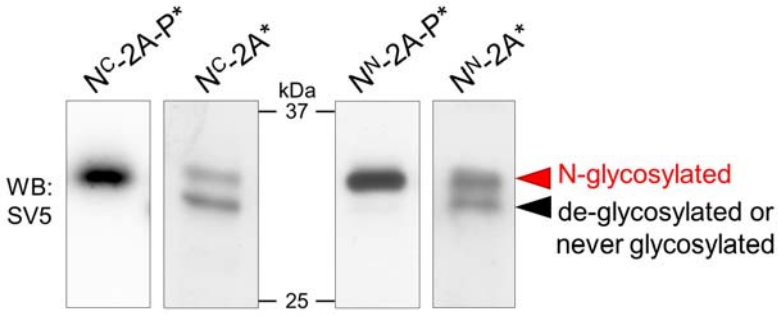

Figure 42. Western blots of HEK-293T transfected with the indicated plasmids. Red arrowhead indicates N-glycosylated proteins, while black arrowhead deglycosylated or never glycosylated proteins.

N-linked glycosylation of N^C-2A and N^C-2A-P was confirmed by *in vitro* deglycosylation assays. Extracts of cells transfected with constructs N^C-2A* or N^C-2A-P* were incubated with the enzyme PNGase F (Figure 43). Upon treatment with the glycosidase, the band corresponding to N-linked 2A-P and 2A proteins showed a faster electrophoretic migration, because of sugar removal.

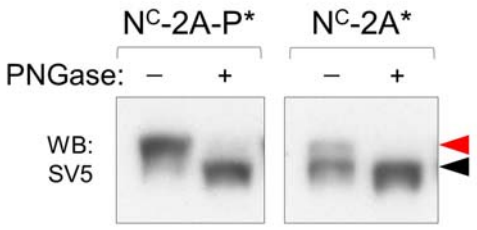

Figure 43. Western blots of HEK-293T cells transfected with plasmid encoding N^C-2A and N^C-2A-P, lysated in TNN buffer and incubated with glycosidase PNGase, as indicated. Red arrowhead indicates N-glycosylated proteins, black arrowhead the deglycosylated ones.

However, we were not able to say if the band corresponding to non-glycosylated 2A proteins was never glycosylated or the result of deglycosylation. N-linked oligosaccharides removal is a process described for ERAD glycosylated substrates that take places once they reach the cytosol and is catalysed by the enzyme N-glycanase 1 (NGLY1) (Enns et al., 2014; Huang et al., 2015; Suzuki et al., 2016). In fact, glycosylated ERAD substrates accumulate in their deglycosylated form upon proteasome inhibition (Petris et al., 2011).

We found that treatment of N^C-2A-trasfected cells with proteasome inhibitor MG132 stabilised mostly non-glycosylated proteins, confirming that N^C-2A proteins, like all 2A-tagged reporters, are targeted to degradation and suggesting that the non-glycosylated band derived by NGLY1 activity (Figure 44).

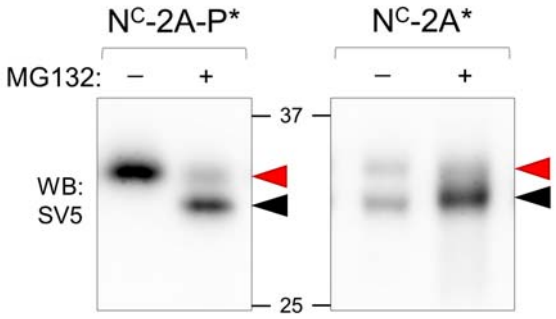

Figure 44. Extracts of cells transfected with NGT^C-2A* or NGT^C-2A-P* encoding plasmids and treated with MG132 as indicated. Red arrowhead indicates N-glycosylated proteins, while black arrowhead the non-glycosylated ones. Representative of n=3 experiments.

However, taken together these observations are not enough to understand if non-glycosylated proteins resulted from (i) retro-translocation, followed by NGLY1 deglycosylation of cytosolically exposed substrates; (ii) N-glycosylation impairment, as a consequence of the stalling, thus the proteins have never been glycosylated; (iii) impairment in 2A protein insertion in the ER lumen.

To understand which was the case, we created a stable HEK-293T cell line with non-functional NGLY1. NGLY1 is reported to be the only enzyme responsible for ERAD substrate deglycosylation. If deglycosylation is a consequence of ERAD, reporter constructs should be fully glycosylated in cells NGLY defective; otherwise, if non-glycosylated fraction persists, it is an indication that proteins are never glycosylated.

To create HEK cells without the endogenous NGLY1, we used the CRISPR-Cas9 nuclease previously described (Cong et al., 2013) to delete several exons from the gene encoding for NGLY. We tested several target RNA guides for Cas9 cloned into pX330 vector with puromycin resistance. Several combinations of two plasmids with different RNA guides were co-transfected in HEK-293T by calcium-phosphate transfection. After 4 days of

puromycin selection, surviving cells were diluted to isolate single clones. Clones were then analysed for exons deletion by RT-PCR and fragments obtained were sequenced. One clone was found positive for deletion of exons 3 to 6 (Figure 45).

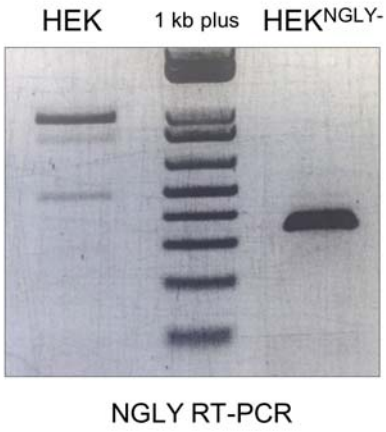

Figure 45. Agarose gel stained with ethidium bromide of NGLY PCR amplification after extraction and retro-transcription of total mRNA from HEK-293T and the clone HEK NGLY defective (HEK^{NGLY-}).

The positive clone (HEK^{NGLY-}) was expanded and transfected with plasmids encoding secretory proteins that have one or more sites for N-glycosylation, like a secretory non-active TEVp (with 4 sites for N-glycosylation) and Null Hong Kong mutant of α1 anti-trypsin (NHK-α1AT), to control if the NGLY1 activity was abrogated. To induce accumulation of deglycosylated material, cells were also treated with proteasome inhibitor MG132 as previously reported (Petris et al., 2011; Cesaratto et al., 2015).

As shown in Figure 46, no deglycosylated proteins were accumulated, indicating that HEK^{NGLY-} cell line didn't express an active NGLY1.

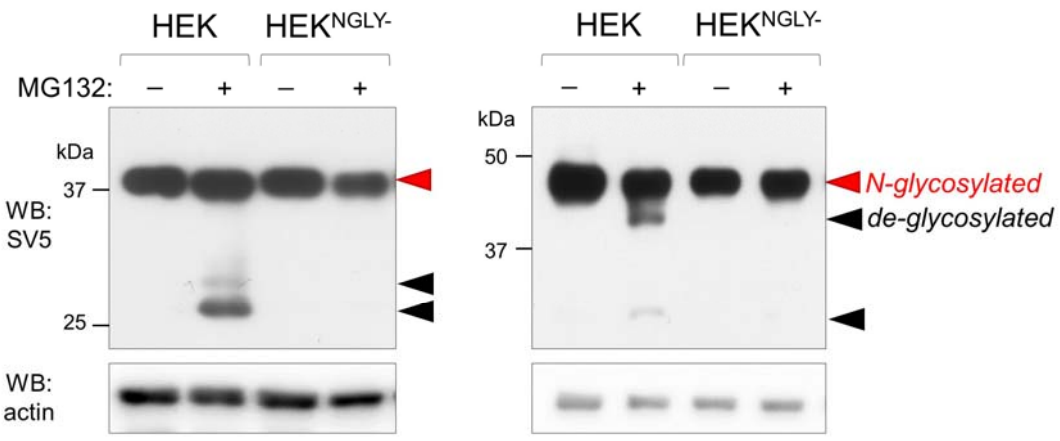

Figure 46. Western blots of secretory non-active TEVp (on the left) or NHK-α1AT (on the right) expressed in HEK-293T or HEK^{NGLY-} and treated or not with MG132, as indicated. Red arrowheads indicate N-glycosylated proteins, while black arrowheads the deglycosylated ones.

We then transfected HEK^{NGLY-} cells with constructs N^{C}-2A* and N^{C} -2A-P* and cell lysates where resolved by Western blotting. N^{C}-2A proteins were still represented by both a glycosylated fraction and what now we suspect to be a non-glycosylated fraction. We noticed an increase in the ratio between glycosylated and non-glycosylated fraction, due to retro-translocated proteins that are no more deglycosylated (Figure 47). However, the fraction of non-glycosylated protein remained represented. It is possible that, in the context of ribosomes stalling, N-glycosylation is partially compromised.

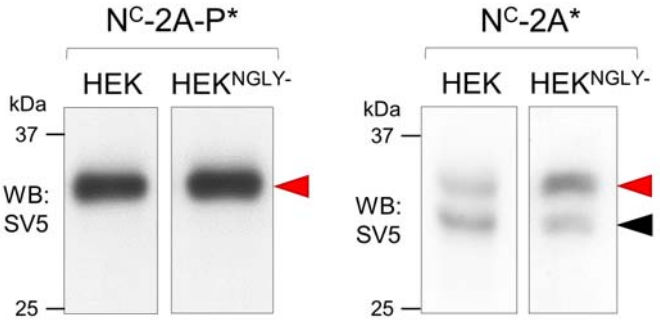

Figure 47. Western blots of cell extract of HEK-293T or HEK^{NGLY-} independently transfected with plasmids N^{C}-2A* and N^{C}-2A-P*. Red arrowheads indicate N-glycosylated proteins, while black arrowhead the deglycosylated ones.

2.2 LOCALIZATION OF 2A POLYPEPTIDES DERIVED FROM ER-STALLED RIBOSOMES

The use of HEK^{NGLY-} cell line was not sufficient to completely clarify the localisation of 2A proteins resulted from stalling at the ER membrane, so we decided to use some enzymatic tools: the *in vivo* biotinylation and *in vivo* proteolysis of luminal 2A-proteins.

In vivo biotinylation is a useful technique to study intracellular localisation of a protein of interest. The most widely used biotin ligase is the *E. coli* BirA, which conjugate one molecule of biotin to a Lysin located within the biotin acceptor peptide (BAP) sequence GLNDIFEAQ**K**IEWHE (Beckett et al., 2008; Chapman-Smith and Cronan, 1999; Schatz, 1993). If the protein of interest tagged with BAP is in the same subcellular compartment of BirA, it will get biotinylated. Furthermore, we can discriminate between proteins that are mono-biotinylated from those that are not simply by Western blot analysis, incubating the cellular extracts with Streptavidin (StrAv). The binding of StrAv to biotin is resistant to dissociation by SDS and adds an apparent mass of 30-40 kDa that delays protein migration (Western blot-retardation assay, WB-ra) (Petris et al., 2014b, 2011; Predonzani et al., 2008; Sasset et al., 2015). Secretory scFv reporter was engineered with the BAP-tag between the SV5-tag and the 2A* or the 2A-P* used as control (Figure 48), thus forming constructs sec-BAP-2A* and sec-BAP-2A-P*. The Lysine of the BAP-tag, which is the acceptor of biotinylation, is positioned 32-33 aa upstream the termination codon of 2A and 2A-P, respectively. This means that the BAP-tag is buried between the end of the RET and the translocon channel during translational stalling.

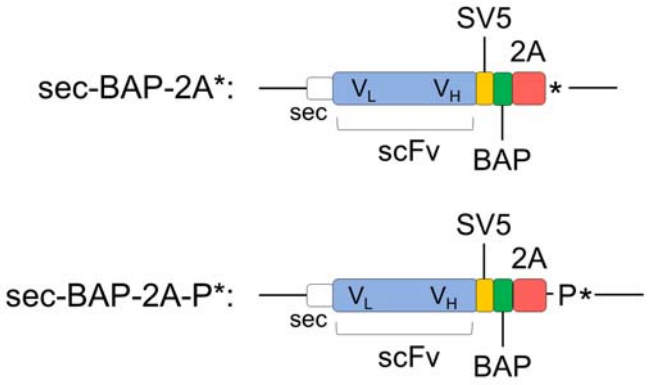

Figure 48. Scheme of constructs used for *in vivo* biotinylation experiments. The BAP-tag was engineered between the SV5-tag and the 2A* or 2A-P* sequence.

BAP-tagged 2A or 2A-P reporters were co-expressed in HEK-293T cells with a secretory active BirA (sec-BirA). Cells were incubated with a supplement of biotin for 4 hours before cellular lysis in SDS buffer in presence of the alkylating agent N-Ethylmaleimide (NEM) to abrogate post-lysis biotinylating activity. The BAP-tag should be biotinylated by sec-BirA only if it reaches the lumen environment and the amount of biotinylated proteins will be shifted in electrophoretic migration by addition of StrAv.

Figure 49 shows the Wb-ra assay results: all the proteins produced by both 2A and 2A-P reporters were fully biotinylated and retarded by StrAv binding, as we didn't detect any fraction of non-biotinylated proteins after StrAv incubation (lanes 2 and 4). These observations suggest they are fully inserted in the lumen.

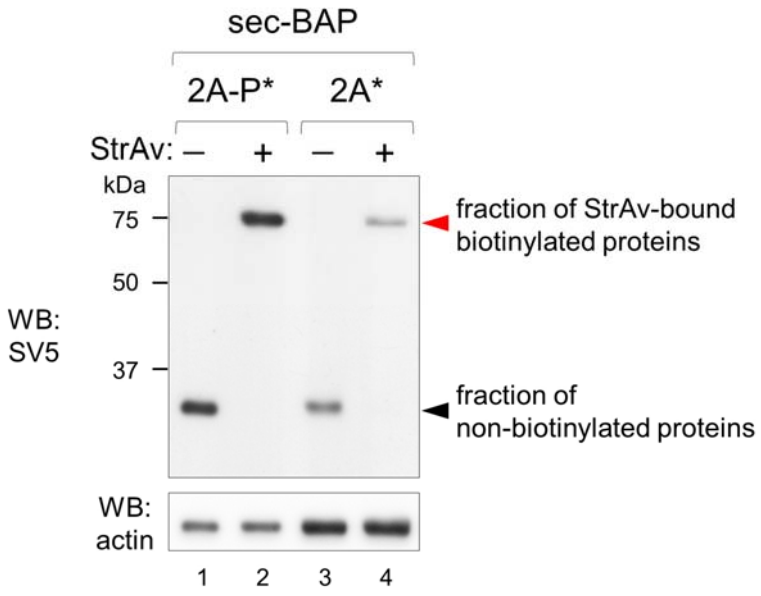

Figure 49. *In vivo* biotinylation of luminal proteins. Secretory BAP-tagged 2A* or 2A-P* constructs were co-expressed in HEK-293T with a secretory BirA and labelled with biotin. Western blot-retardation assay (Wb-ra) is performed without (-) or with (+) Streptavidin (StrAv) incubation of cell extracts. Red arrowhead indicates the fraction of biotinylated proteins that is bound to StrAv and has a retarded migration (lanes 2 and 4). Black arrowhead indicates the non-biotinylated fraction of proteins in lane 2 and 4, which is extremely low represented. Wb-ra is representative of n=3 independent experiments.

The second enzymatic tool we used is based on the Tobacco Etch Virus protease (TEVp) and on its proteolytic cleavage of the TEVp cleavage sequence (TS) ENLYFQ-G/S, which occurs between final Q and the following G or S (Dougherty et al., 1988; Dougherty and Parks, 1991; Kostallas et al., 2011).

A TEVp active in the ER lumen of mammalian cells was previously developed in our laboratory (Cesaratto et al., 2016, 2015), so we included a TS-tag in our reporter construct sec-BAP-2A*, thus generating construct sec-TS-2A* and the corresponding control sec-TS-2A-P* (Figure 50, left panel). In this way the cleavage occurs 64 amino acids upstream the termination codon, namely inside the ER lumen, and upstream the SV5-tag. If the 2A proteins are efficiently processed by TEVp, the SV5-tag is removed.

TS-tagged constructs were co-transfected with a plasmid expressing the ER-active TEVp (sec-TEVp) or, as controls, with a cytosolic (cyt-TEVp) or an enzymatically dead TEVp C151A (with C151 mutated into A (Parks et al., 1995)). Cell extracts were collected, load on SDS-PAGE and immunoblotted with anti-SV5 antibody.

From the results obtained, the SV5-tag was removed only when sec-TS-2A* was co-expressed together with sec-TEVp, in line with *in vivo* biotinylation experiments.

However, a reduction in SV5 signal was noticed also when 2A-tagged reporter was expressed with cytosolic TEVp, while TS-2A-P was not (Figure 50, right panel): even if the products of stalling are in the ER, a fraction is found also in the cytosol and is recognised and processed by cyt-TEVp. This is an additional indication that proteins derived from stalling at the STOP-codon are retro-translocated from the ER lumen to the cytosol.

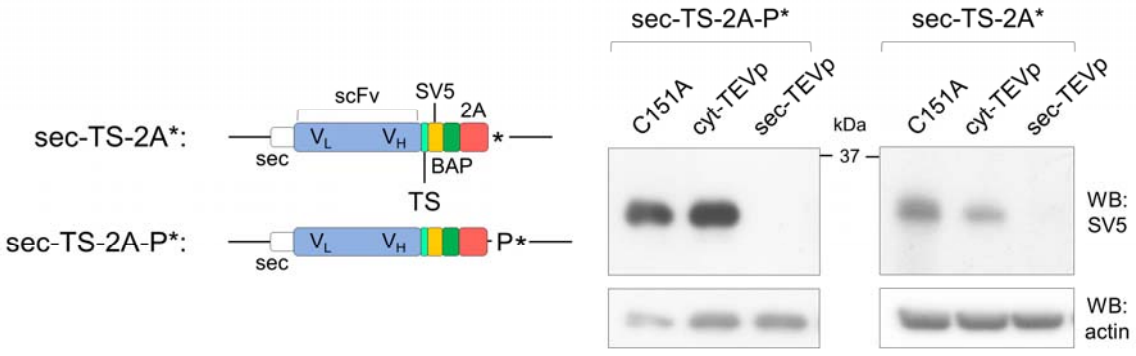

Figure 50. On the left, a scheme of sec-TS-2A* and sec-TS-2A-P* constructs. On the right, *in vivo* proteolysis of luminal proteins. Western blot of extracts of HEK-293T cells co-transfected with constructs sec-TS-2A* or sec-TS-2A-P* and dead TEVp (C151A), cytoplasmic (cyt-) or secretory (sec-) TEVp. Representative of n=2 independent experiments.

We then added a TS-tag in the construct N^N-2A* as well, named construct N^N-TS-2A*, to perform *in vivo* proteolysis by cyt- or sec-TEVp. We found that both N-glycosylated and non-glycosylated proteins were processed upon co-expression with secretory protease, indicating that both variants of 2A were inside the ER (Figure 51). cyt-TEVp processed almost all the non-glycosylated fraction and a bit of the N-glycosylated one, indicating that they became accessible to the cytosolic environment. This was another indication that 2A peptides are retro-translocated.

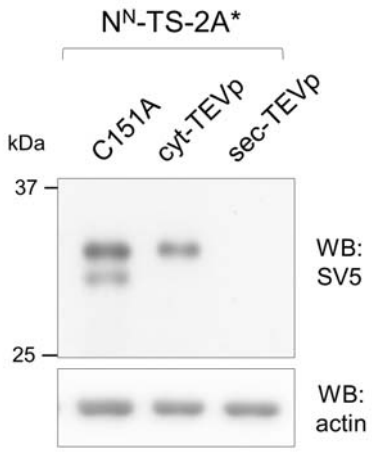

Figure 51. Western blot of cell extracts of HEK-293T co-transfected with N^N-TS-2A* and the indicated plasmids expressing dead, cyt- or sec-TEVp.

However, sec-TEVp was found to be active in part also in the cytosol (Figure 52): SV5-tag was partially cleaved also from a cytosolic TS-tagged 2A co-transfected with the secretory enzyme, indicating that its activity is not restricted to the ER lumen, because a fraction of sec-TEVp itself is retro-translocated and is temporarily active also on the cytosolic side before degradation. We observed a similar behaviour also for secretory BirA (data not show).

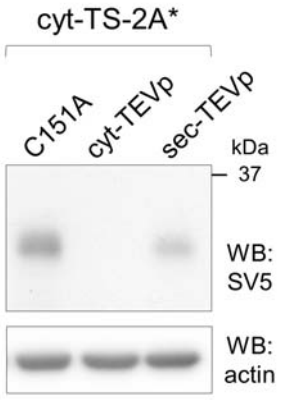

Figure 52. Extracts of HEK-293T cells transfected with constructs cyt-TS-2A* and dead (C151A), cytoplasmic (cyt-) or secretory (sec-) TEVp, as indicated. Representative of n=2 independent experiments.

The efficiency of retro-translocated sec-TEVp or sec-BirA, however, is not comparable to cytosolically expressed counterparts (here shown in Figure 52 only for sec-TEVp). For this reason, although we cannot conclude that all the secretory proteins derived from 2A-stalled ribosomes are fully release in the ER environment, both *in vivo* biotinylation and *in vivo* proteolysis indicate that most of the 2A molecules are in the ER lumen. Moreover, enzymatic cleavage of 2A reporters by a cytosolic TEVp indicate that these substrates are retro-translocated.

We next decided to express sec-BAP-2A in an appropriate *in vitro* system to prove that proteins are successfully translated and inserted in the ER, using *in vitro* biotinylation to see whether BAP-tagged 2A was protected by microsomes membranes or not. An important advantage of using *in vitro* systems, in this case, is that retro-translocation is not efficient as *in vivo*.

We used a transcription and translation system based on HeLa cell lysates that allows translation of secretory proteins in ER-derived microsomes. Reaction was then blocked with cycloheximide and incubated with a fresh cell lysate (obtained without the use of detergents) containing an active cytosolic BirA. Construct sec-BAP-2A-P* was used as a negative control of biotinylation, while a plasmid expressing a cytosolic BAP-tagged reporter was used as the positive one. Samples were resolved on SDS-PAGE, blotted and

reacted with anti-SV5 to reveal protein production and with StrAv-HRP to visualize only biotinylated proteins (Figure 53).

While the cytosolic BAP-tagged reporter was biotinylated, we found that neither sec-BAP-2A-P nor sec-BAP-2A proteins were detected with StrAv-HRP, suggesting they were both translated and translocated into the ER-derived microsomes. Considering that this system has not an active retro-translocation apparatus, these results are an indirect indication that the products we found *in vivo* in the cytosol are the result of retro-translocation rather than inefficient ER insertion.

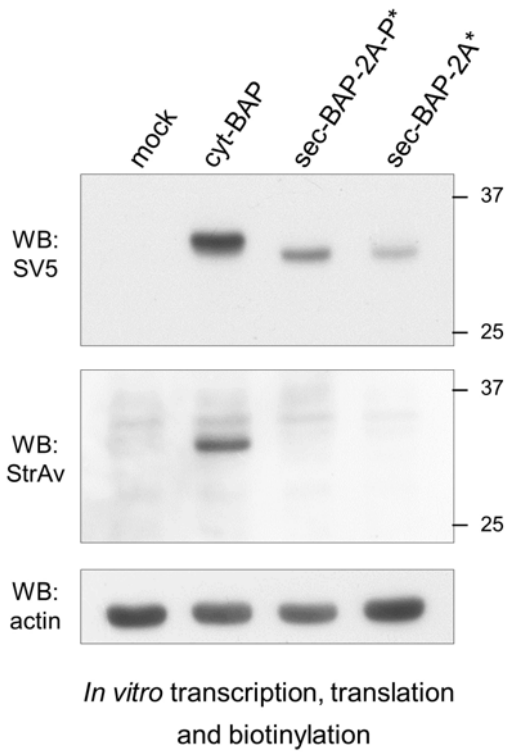

Figure 53. Plasmids coding for sec-BAP-2A and sec-BAP-2A-P were expressed i*n vitro* in a system based on HeLa cell lysate, followed by *in vitro* biotinylation. Construct expressing a cytosolic BAP-tagged reporter was used as a control for biotinylation. Representative of n=2 independent experiments.

Taken together, all these data indicate that the products of 2A-stalled ribosomes are translocated inside the ER lumen, both *in vitro* and *in vivo*, where they become accessible to co-localising enzymes.

Our results suggest that they are retro-translocated to the cytosol, as they are degraded by the proteasome. Since retro-translocation is a characteristic step of the ERAD pathway and,

taking into consideration also the involvement of p97 and YOD1, the data strongly suggest that 2A proteins derived from stalled ribosomes are substrates of the ERAD pathway.

2.3 ER-TARGETED 2A PROTEINS RETRO-TRANSLOCATE TO THE CYTOSOL INDEPENDENTLY OF P97, UBIQUITINATION AND PROTEASOME ACTIVITIES

In our laboratory, the *in vivo* biotinylation system was successfully adapted to specifically marked ERAD substrates when they reach the cytosol, engineering a BAP-tag in several ERAD substrates and co-expressing them with the cytosolic biotin ligase BirA (Petris et al., 2014b, 2011; Sasset et al., 2015). In this way, BAP-tag is accessible to BirA only when both co-localize in the cytosol, namely after ERAD substrates retro-translocation. This allows also to analyse the rate of protein dislocation, because of the possibility to discriminate between retro-translocated (and biotinylated) proteins from those that are in the ER lumen by Wb-ra.

We used the same secretory scFv reporter already described as constructs sec-BAP-2A* and sec-BAP-2A-P* (Figure 48). Constructs were co-transfected with a plasmid encoding cyt-BirA and cells were incubated with biotin for 4 hours. Cellular extracts were incubated with StrAv under denaturing condition before loading the acrylamide gel. As shown in Figure 54, most of the control proteins produced from construct sec-BAP-2A-P* are not biotinylated: only a small fraction is shifted by addition of StrAv. This is in line with our previous experiments that demonstrate that this protein produced from non-conventional termination is normally translated and secreted. On the contrary, the majority of sec-BAP-2A synthesised by stalled ribosomes was found biotinylated (and shifted), because targeted to degradation and retro-translocated, thus becoming cytosolically exposed to cyt-BirA.

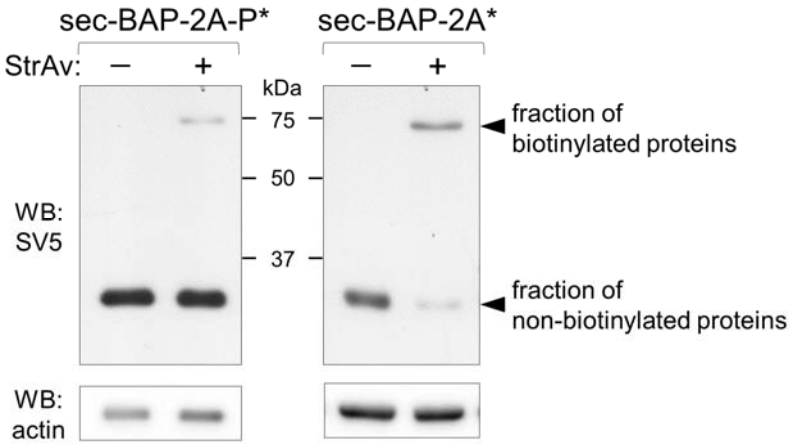

Figure 54. WB-ra of extracts of cells co-transfected with constructs sec-BAP-2A-P* (in the left) or sec-BAP-2A* (on the right) and a plasmid coding for the cytosolic biotin ligase BirA. Migration of *in vivo* biotinylated proteins is retarded when Streptavidin (StrAv) is added to the samples, as indicated. Figures are representative of n=3 independent experiments.

A similar result was observed for BAP-tagged N^C-2A reporter proteins. A BAP-tag was engineered in place of the spacer (see Figure 41) generating construct N^C-BAP-2A*, which was co-transfected with cyt-BirA in HEK-293T cells. Cells were then incubated for 15 min with [^{35}S]-Methionine and biotin. SV5-tagged proteins were purified from total cell extract by immunoprecipitation and incubated with or without StrAv. Samples were run in SDS-PAGE under reducing conditions and detected by autoradiography. From the retardation assay reported in Figure 55 (left panel), a pulse of biotin of 15 minute was enough for cyt-BirA to label both N-glycosylated and non-glycosylated N^C-BAP-2A proteins, indicating their cytosolic localisation. The same finding was confirmed by Wb-ra (Figure 55, right panel).

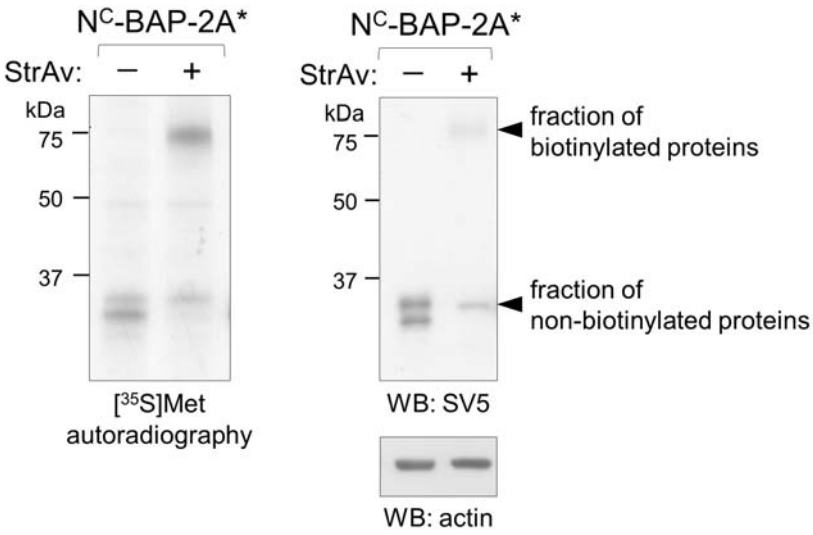

Figure 55. On the left, autoradiography of a retardation assay performed on N^C-2A reporters co-expressed with cyt-BirA and labelled for 15 min with biotin and [^{35}S]-Methionine. On the right panel, WB-ra of extracts of cells co-transfected as reported for the alongside experiment and treated with biotin for 4 hours. Migration of *in vivo* biotinylated proteins is retarded by StrAv addiction, as indicated. Figures are representative of n=2 and 3 independent experiments, respectively.

Another evidence that the 2A-derived peptides are retro-translocated to the cytosol is the analysis of the reducing state of the scFv reporters. Both the V_L and V_H have an intradomain disulphide bridge, meaning that when the scFv is in the oxidising environment of the ER lumen, the two bridges are formed. On the contrary, disulphide bonds are disrupted after retro-translocation to the cytosolic side. In non-reducing conditions, reduced proteins have a more extended conformation that retards their electrophoretic mobility in relation to oxidized ones.

We transfected HEK-293T cells with construct sec-2A* or 2A-P* and we collected cell extracts using SDS lysis buffer with NEM to prevent reformation of disulphide bridges. Samples where loaded in presence or absence of reducing agent β-mercaptoethanol. As reported in Figure 56, we found that in non-reducing conditions the majority of 2A-tagged proteins migrated with disulphide bridges already reduced, a result comparable to the fraction of molecules cytosolically biotinylated in figure 54, while a minor fraction was found oxidised, thus confirming protein insertion in the ER and retro-translocation.

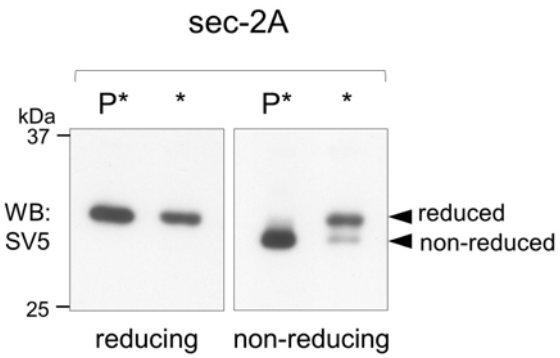

Figure 56. Cell extracts of HEK-293T transfected with construct sec-2A* or sec-2A-P*, as indicated, and loaded in reducing or non-reducing condition. Fractions of non-reduced and reduced proteins are indicated by arrowheads. Figure is representative of n=2 independent experiments.

We next decided to use the *in vivo* biotinylation to characterise the role of p97, proteasome and ubiquitination during 2A protein retro-translocation.

We performed the assay in condition of proteasome inhibition or upon co-expression of OTU or p97QQ (Figure 57). We observed that the accumulation of the reporter produced from construct 2A* construct occurred predominantly in the cytosol, and not inside the ER lumen, as most of the proteins are biotinylated by cyt-BirA and shifted with StrAv. As previously observed, the proteins produced from control construct were instead slightly affected, as only a small fraction of biotinylated proteins was found.

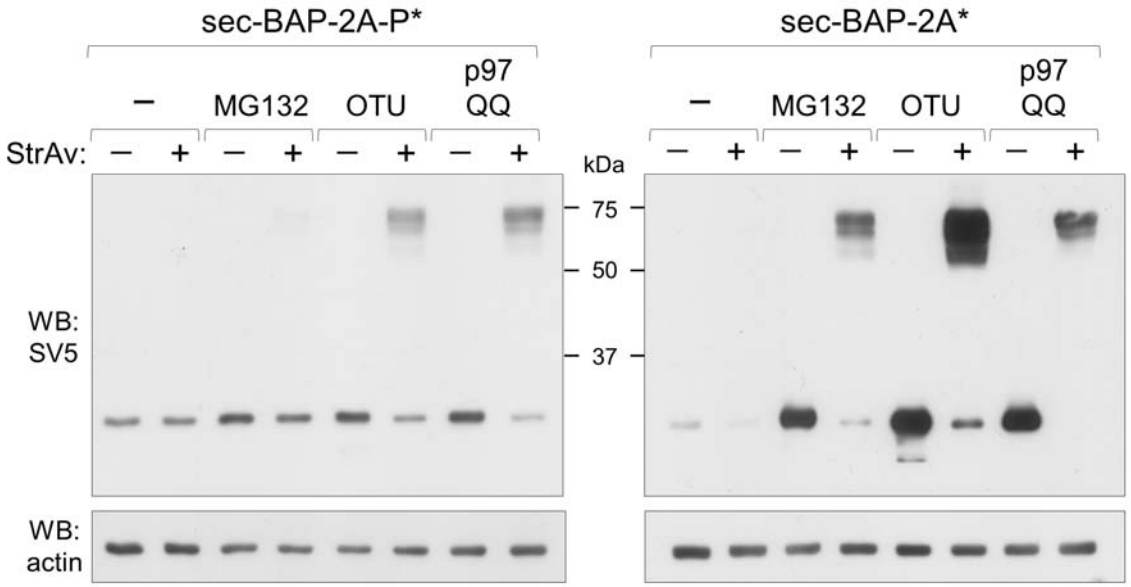

Figure 57. WB-ra of extracts of cells co-transfected with constructs sec-BAP- 2A-P* (on the left) or sec-BAP-2A* (on the right) and cytosolic BirA, with OTU or p97QQ or treated with MG132, as indicated. Figures are representative of n=3 independent experiments.

These findings demonstrated that, as expected, p97, poly-ubiquitination and proteasome degradation are essential for 2A-tagged proteins degradation, playing their roles once the substrates reach the cytosol, namely after retro-translocation. If p97 and poly-ubiquitin-proteasome steps were involved in protein extraction from the ER lumen, 2A polypeptides would have accumulated inside the ER lumen and biotinylation by cyt-BirA would have been prevented. However, with this experiment we can't exclude that first rounds of Ub conjugation can be necessary to stimulate retro-translocation.

To conclude the second part of this work, we demonstrated that ER-targeted 2A proteins synthetized by stalled ribosomes are translated in the ER lumen and engaged by ERAD. Therefore, we questioned what mechanism selected for retro-translocation these proteins, which are identical to those produced by constructs 2A-P* with the sole exception of the terminal Pro-codon. Canonical ERAD clients are misfolded or unfolded proteins, but in the case of 2A-tagged polypeptides, misfolding may not be the triggering factor.

3. IDENTIFICATION OF PROTEINS INVOLVED IN 2A POLYPEPTIDES DEGRADATION

We wanted to study 2A-tagged polypeptides interactions, to identify other proteins involved in degradation targeting. First, we tried the silver staining technique to detect interacting proteins after co-immunoprecipitation with anti-SV5 of the sec-BAP-2A reporter, with no clear results. We also tested *in vivo* chemical crosslinking of intracellular proteins, treating with DSP HEK-293T cells transfected with constructs sec-BAP-2A* or the control sec-BAP-2A-P*. Again, no encouraging results were obtained.

More recently, an enzymatic biotinylation methodology was developed to allow proximity labelling in living cells, the proximity-dependent Biotin Identification (BioID) method. It was reported that mutation R118G within the biotin catalytic domain of *E. coli* BirA abolished specificity for the BAP-tag, thus enabling the enzyme to biotinylate indiscriminately proteins that interact or are in proximity with the protein of interest, usually expressed as a fusion with the BirA mutant (Choi-Rhee et al., 2004; Roux et al., 2013). This technique was further improved using a similar enzyme from *Aquifex aeolicus*, which has no DNA binding domain (named BioID2). The biotin ligase of *A. aeolicus* was humanised and a conserved residue of the catalytic domain was mutated (R40G) to allow promiscuous biotinylation (Kim et al., 2016).

3.1 STUDY OF 2A PROTEINS INTERACTIONS

We then decided to adapt the *in vivo* promiscuous biotinylation system to our stalling model, so the synthetic sequence of BioID2 with mutation R40G was cloned with a C-tail 2A* and an upstream RoTag in the secretory format, thus generating construct BioID2-2A* and its control BioID2-2A-P* (Figure 58). We thought that in this way, if BioID2-2A proteins

are active in the ER lumen and in the cytosol, proteins involved in targeting them to degradation will be biotinylated.

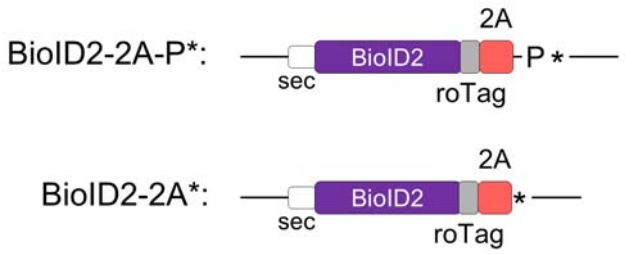

Figure 58. Scheme of constructs BioID2-2A-P* and BioID2-2A*. BioID2 R40 is mutated into G and cloned with a RoTag upstream the 2A sequence.

Plasmids expressing the BioID2 were transfected in HEK-293T cells, with media supplemented with biotin. After 24 hours, cell extracts were collected and analysed by Western blot using anti-RoTag antibody to see BioID2 expression and Streptavidin-HRP to visualise biotinylated proteins. As shown in figure 59, the BioID2 protein was able to biotinylate itself, as it was detectable by both anti-RoTag and StrAv-HRP.

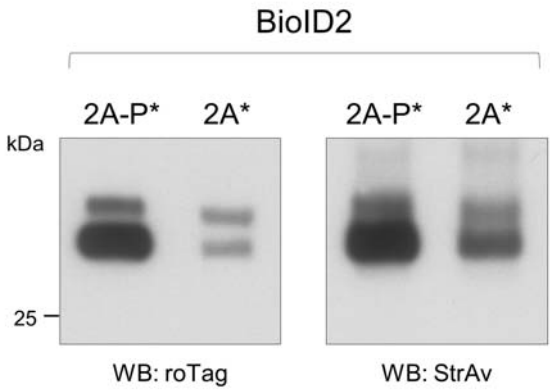

Figure 59. Western blots developed with anti-roTag antibody and StrAv-HRP of extracts of HEK-293T cells expressing construct BioID2-2A-P* or BioID2-2A*, as indicated. Representative of n=2 independent experiments.

The most interesting results are shown in figure 60. 2A-tagged BioID2 labelled with biotin two proteins of around 75 kDa and one of around 20 kDa that were not found in cells expressing BioID2-2A-P proteins. Of note, the band above 75 kDa was highly represented.

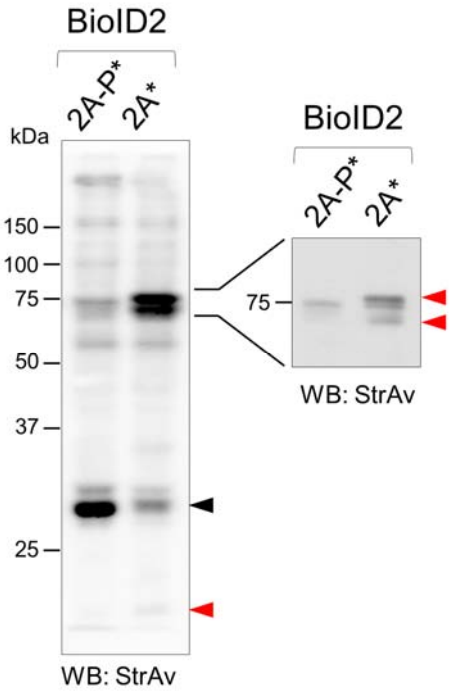

Figure 60. Streptavidin (StrAv) Western blot of extracts of HEK-293T transfected with plasmids expressing BioID2-2A-P and BioID2-2A and labelled with biotin for 24 h. The right panel shows the 75 kDa region of an SDS-PAGE 7% polyacrylamide developed with lower exposure. Black arrowhead indicates the self-biotinylated BioID2, while red arrowheads indicate biotinylated bands present only in extracts of cells transfected with BioID2-2A*. Representative of n=3 independent experiments.

To understand the nature of proteins identified by BioID, we pulled-down with StrAv-bound magnetic beads all the biotinylated proteins from extracts of cells independently transfected with construct BioID2-2A* or BioID2-2A-P* and samples were subjected to semi-quantitative mass spectrometry analysis.

Mass spectrometry of proteins biotinylated by BioID2-2A detected the 78 kDa Glucose Regulated Protein GRP78 (the ER chaperone BiP), the 71 kDa cytosolic chaperone HSPA8 and the 23 kDa nascent polypeptide-associated complex α-subunit (NACA). The mass of these proteins matched those previously observed in Western blot and they were not identified by mass spectrometry of proteins biotinylated by BioID2-2A-P.

The complete list of polypeptides found with both proteins is reported in a table annexed to the Results.

3.2 2A POLYPEPTIDES DERIVED FROM RIBOSOME STALLING AT THE ER MEMBRANE ARE SUBSTRATES OF BiP/GRP78

To confirm that the band of around 78 kDa biotinylated in cells expressing BioID2-2A* was BiP/GRP78, we looked for it with a specific antibody on StrAv pulled-down extracts of cells expressing constructs BioID2-2A* or BioID2-2A-P*. In parallel, we performed as well BiP immunoprecipitation followed by detection with StrAv-HRP.

As represented in Figure 61, BiP was found biotinylated only upon expression of BioID2-2A, in fact it is present among the biotinylated proteins purified with StrAv (upper panel) and a fraction of immunoprecipitated BiP was found biotinylated (middle panel).

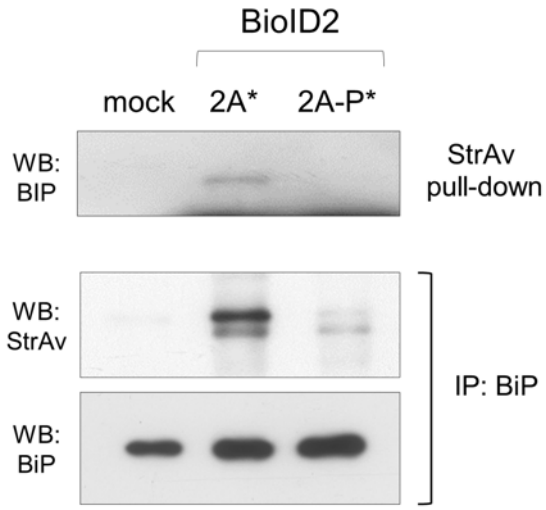

Figure 61. Western blots of extracts of HEK-293T cells mock-transfected or transfected with the indicated BioID2 constructs. In the upper panel, anti-BiP immunoblotting of proteins pulled-down with StrAv beads; middle and lower panels StrAv-HRP or anti-BiP blots of proteins immunoprecipited (IP) with anti-BiP. Data are representative of n=2 independent experiments.

It was also found that overexpression of wild type BiP increased the amount of secreted sec-2A reporters and the expression of both N-glycosylated and non-glycosylated variants of NGT^{C}-2A (Figure 62), suggesting that BiP stabilised 2A proteins. Increase in secretion, however, can be the consequence of a general increase in the intracellular amount of sec-2A. These results confirm that BiP is involved in 2A-tagged proteins management.

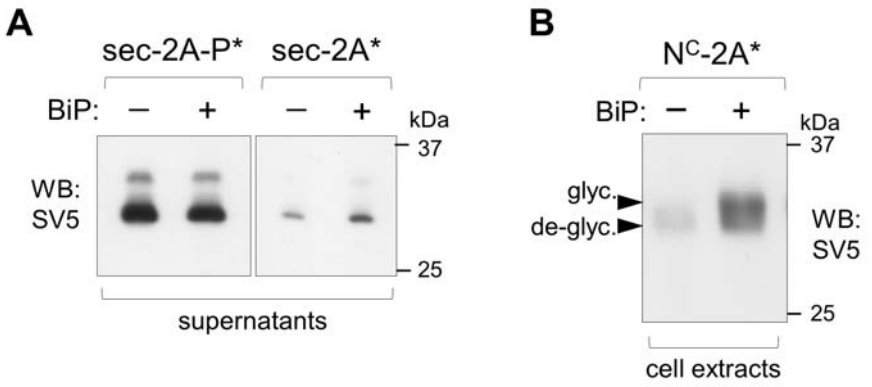

Figure 62. Overexpression of wild type BiP. **A:** Western blots of supernatants from HEK-293T cells expressing plasmids sec-2A-P* or sec-2A* co-transfected with BiP, as indicated. Representative of n=2 independent experiments. **B:** Western blot of cell extracts of HEK-293T plasmids NGT^{C}-2A-P* or NGT^{C}-2A* co-transfected with BiP, as indicated. Representative of n=2 independent experiments.

We also tested the effect of a BiP mutated with a G in place of a T at position 37, which is reported to abolish endogenous BiP activity in a dominant negative manner and to retain BiP substrates within the lumen (Wei et al., 1995).

We co-expressed BiP (T37G) with constructs sec-BAP-2A* or NGLY^{C}-2A* and we found that it induced accumulation of both reporters. Moreover, *in vivo* biotinylation with citosolic BirA allowed us to demonstrate that sec-BAP-2A accumulated inside the ER lumen, as no biotinilated protein was detected upon BiP (T37G) expression (figure 63A). Furthermore, NGLY^{C}-2A was found fully glycosylated, because BiP (T37G) retention in the lumen blocked substrate retro-translocation thus allowing stabilisation of the complete N-glycosylated protein NGLY^{C}-2A (figure 63B).

Collectively, the data from mass spectrometry and from interactome study with BioID2 confirm that 2A-tagged proteins produced by membrane-bound stalled ribosome are handled by BiP.

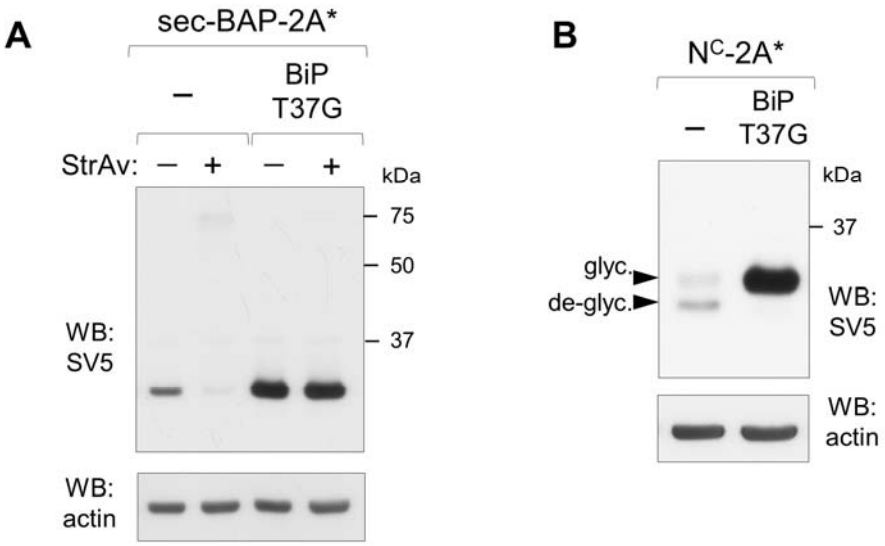

Figure 63. A: Western blots of lysates of HEK-293T cells expressing plasmids sec-2A-P* or sec-2A* co-transfected with cyt-BirA and with the dominant negative BiP (T37G) where indicated. Representative of n=3 independent experiments. **B:** Western blot of cell extracts of HEK-293T transfected with constructs NGT^{C}-2A-P* or NGT^{C}-2A* and with BiP (T37G), as indicated. Representative of n=3 independent experiments.

Considering that scFv reporters, when tagged with C-terminal 2A-P, are regularly translated and secreted while those with 2A are not, and that the only difference is the presence of the terminal Pro-codon, we hypothesised that 2A-tagged scFv are not misfolded. The fact that BioID2-2A was enzymatically active within the ER lumen enforced this hypothesis. As a consequence, we speculated that 2A-tagged proteins are targeted to ERAD not because they are mis/unfolded, but because they are recognised as peptides derived from stalled ribosomes.

3.3 ROLE OF THE RIBOSOME QUALITY CONTROL COMPLEX IN THE DEGRADATION OF RIBOSOME-STALLED 2A POLYPEPTIDES

Of note, BioID2 did not label any of the proteins we previously identified, like Listerin or p97 and YOD1, and not even other proteins previously reported to be involved in the RQC pathway. We decided to look if 2A-induced stalling required some of the players described

in literature for the clearance of polypeptides derived from other types of stalling, like its association to RQC components. We did some driving experiments, expressing in HEK-293T cells our constructs sec-2A* and sec-2A-P* and after 48 hours we blocked translation incubating the cells with cycloheximide. Cell lysates were collected and separated by ultracentrifugation on a sucrose gradient (15% on the top and 40% on the bottom of the gradient). The gradient was collected from the bottom in 12-15 fractions, which were analysed by Western blotting. Most of the 2A proteins were found in the top fractions, as the control 2A-P (Figure 64). This observation suggests that they are predominantly soluble.

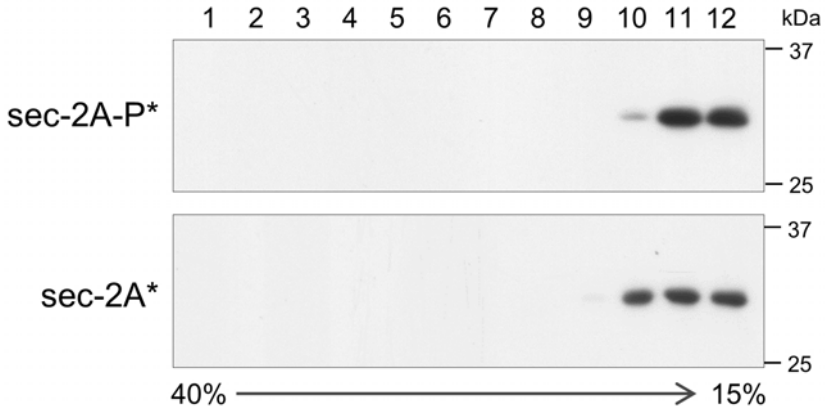

Figure 64. Western blot of 40-15% sucrose gradient of cell extracts of HEK-293T independently transfected with constructs sec-2A* or sec-2A-P*.

A similar experiment was carried treating cells with proteasome inhibitors (MG132 and bortezomib). In this case, we noticed accumulation of 2A proteins not only on the top of the gradient, but also in different fractions, thus suggesting that a small portion of the 2A reporters aggregated with other proteins (Figure 65). However, this type of experiments is not highly reproducible, and we still haven't performed poly-ribosome analysis, which is required for example to understand if 2A reporters associates with 80S ribosomes or with 60S split subunits, and we didn't look yet for other proteins sedimented in the same fractions with 2A.

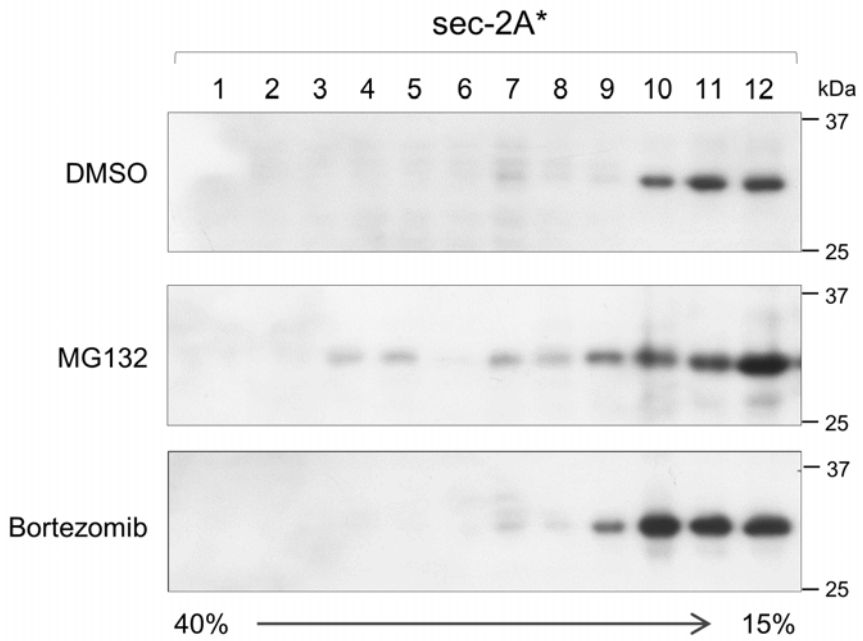

Figure 65. Western blot of 40-15% sucrose gradient fractions derived from cell extracts of HEK-293T transfected with construct sec-2A* and treated with MG132 and Bortezomib, as indicated.

4. EFFECT OF NON-VIRAL C-TERMINAL SEQUENCES ON PROTEIN EXPRESSION

4.1 IDENTIFICATION OF HUMAN SEQUENCES TERMINATING IN NPG

One of the most challenging issue in this field is the identification of other sequences capable of inducing ribosome stalling. Our model based on peptide 2A has the advantage of being highly conserved at the last three C-terminal amino acids (NPG). For this reason, we thought to search for human proteins terminating with the same NPG sequence, or NPGP, in the Ensembl data bank. The results and specifications of the bioinformatic analysis are listed in Table 1 and highlighted the existence of only six proteins ending with NPG and one with NPGP, in most cases described as the result of alternative splicing. The proteins belonging the first category are isoforms of the CD99 molecule like 2 (CD99L2), the POTE (prostate, ovary, testis and placenta) ankyrin domain family members E and I (POTEE and POTEI, which share the same C-terminal amino acidic sequence), the tubulin folding co-factor A (TBCA), the spire-type actin nucleating factor 2 (SPIRE2) and the reticulophagy regulator family member 3 (RETREG3 or FAM134C). The only protein ending with NPGP is the Fc fragment of the IgA and IgM receptor (FCAMR).

The corresponding full-length sequences of the identified proteins are shown in Table 2. For the next experiments, we decided to test only the C-terminal sequences of the identified proteins (Table 2, indicated in red). So far, we tested the sequences corresponding to CD99L2, SPIRE2, TBCA2, POTEE and POTEI (that share identical C-termini) and FCAMR, but we still need to study FAM134C.

Ensembl Protein ID	Transcript Support Level (TSL)	GENCODE basic annotation	APPRIS annotation	Associated Gene Name	Associated Transcript Name	Associated Transcript Source	Transcript type	Source (gene)	Source (transcript)	Status (gene)	Status (transcript)	Version (gene)	Version (transcript)
ENSP00000316491	tsl2	GENCODE basic	alternative2	FCAMR	FCAMR-002	HGNC transcript name	protein_coding	ensembl_havana	ensembl_havana	KNOWN	KNOWN	14	8
ENSP00000429046	tsl3	GENCODE basic		TBCA	TBCA-007	HGNC transcript name	protein_coding	ensembl_havana	havana	KNOWN	KNOWN	13	1
ENSP00000457981	tsl5			SPIRE2	SPIRE2-005	HGNC transcript name	nonsense_mediated_decay	ensembl_havana	havana	KNOWN	KNOWN	10	5
ENSP00000467332	tsl4			FAM134C	FAM134C-005	HGNC transcript name	protein_coding	ensembl_havana	havana	KNOWN	KNOWN	10	1
ENSP00000477649	tsl2			POTEE	POTEE-002	HGNC transcript name	nonsense_mediated_decay	ensembl_havana	havana	KNOWN	KNOWN	14	5
ENSP00000485683	tsl2	GENCODE basic		POTEE	POTEE-202	HGNC transcript name	protein_coding	ensembl_havana	ensembl	KNOWN	KNOWN	14	1
ENSP00000486532	tsl2	GENCODE basic		POTEI	POTEI-202	HGNC transcript name	protein_coding	ensembl_havana	ensembl	KNOWN	KNOWN	11	1
ENSP00000489222	tsl1			CD99L2	CD99L2-002	HGNC transcript name	nonsense_mediated_decay	ensembl_havana	havana	KNOWN	KNOWN	20	8

Table 1. The results of the bioinformatic analysis performed in Ensembl, with the indicated proteins IDs, names and annotations.

Protein	Amino acid sequence
SPIRE2	GLRGSPGRRLRDTGDLLLRGDGSVGAREPEAAVEEVR**NPG**
POTEE	MVVEVDSMPAASSVKKPFGLRSKMGKWCCRCFPCYRESGKSNVGTSGDHDDSAMKTLRSKMGKW CHHCFPCCRGSGKSNVGASGDHDDSAMKTLRNKMGKWCCHCFPCCRGSGKSKVGAWGDYDDSAF MEPRYHVRGEDLDKLHRAAWWGKVPRKDLIVMLRDTDVNKKDKQKRTALHLASANGNSEVVKLL LDRRCQLNVLDNKKRTALIKAVQCQEDECALMLLEHGTDPNIPDEYGNTTLHYAIYNEDKLMAK ALLLYGADIESKNKHGLTPLLLGVHEQKQQVVKFLIKKKANLNALDRYGRTALILAVCCGSASI VSLLLEQNIDVSSQDLSGQTAREYAVSSHHHVICQLLSDYKEKQMLKISSENS**NPG**
POTEI	MVAEVDSMPAASSVKKPFVLRSKMGKWCRHCFPCCRGSGKSNVGTSGDQDDSTMKTLRSKMGKW CCHCFPCCRGSGKSNVGTSGDHDDSAMKTLRSKMGKWCCHCFPCCRGSGKSNVGAWGDYDDSAF VEPRYHVRREDLDKLHRAAWWGKVARKDLIVMLRDTDVNKQDKQKRTALHLASANGNSGVVKLL LDRRCQLNVLDNKKRTALTKAVQCQEDECALMLLEHGTDPNIPDEYGNTTLHYAIYNEDKLMAK ALLLYGADIESKNKHGLTPLLLGVHEQKQQVVKFLIKKKANLNALDRYGRTALILAVCCGSASI VSLLLEQNIDVSSQDLSGQTAREYAVSSHHHVICQLLSDYKEKQMLKISSENS**NPG**
CD99L2	MVAWRSAFLVCLAFSLATLVQRGSGDFDDFNLEDAVKETSSVKPALGMYHKLDGLKQQNFILSL FWMLEVLYQGVGWATFSLKALGKNLSLTFPTSGGSRCSLVCGCITPISASVVTWCSPFCVSLLS LTKMLVSGFKAHLD**NPG**
TBCA	MADPRVRQIKIKTGVVKRQRSYK**NPG**
FAM134C	MQIARARLRMRLGASGSGSAPQFFALTSLRLVFLLAFGLMIIVCIDQWKNKIWPEIKVPRPDAL DNESWGFVHPRLLSVPELCHHVAEVWVSGTIFIRNVLLFKKQ**NPG**
FCAMR	MDGEATVKPGEQKEVVRRGREVDYSRLIAGTLPQSHVTSRRAGWKMPLFLILCLLQGSSFALPQ KRPHPRWLWEGSLPSRTHLRAMGTLRPSSPLCWREESSFAAPNSLKGSRLVSGEPGGAVTIQCH YAPSSVNRHQRKYWCRLGPPRWICQTIVSTNQYTHHRYRDRVALTDFPQRGLFVVRLSQLSPDD IGCYLCGIGSENNMLFLSMNLTISAGPASTLPTATPAAGELTMRSYGTASPVANRWTPGTTQTL GQGTAWDTVASTPGTSKTTASAEGRRTPGATRPAAPGTGSWAEGSVKAPAPIPESPPSKSRSMS NTTEGVWEGTRSSVTNRARASKDRREMTTTKADRPREDIEGVRIALDAAKKVLGTIGPPALVSE TLAWEILPQATPVSKQQSQGSIGETTPAAGMWTLGTPAADVWILGTPAADVWTSMEAASGEGSA AGDLDAATGDRGPQATLSQTPAVGPWGPPGKESSVKRTFPEDESSSRTLAPVSTMLALFMLMAL VLLQRKLWRRRTSQEAERVTLIQMTHFLEVNPQADQLPHVERKMLQDDSLPAGASLTAPER**NPG** **P**

Table 2. Full sequences of the proteins identified in the Ensembl data bank. In red are indicated the C-terminus sequences used for cloning and in bold the termination in NPG or NPGP. POTEE and POTEI share the same C-terminal sequence.

4.2 EFFECT OF NON-VIRAL C-TERMINAL PEPTIDES ON PROTEIN EXPRESSION BY FREE RIBOSOMES

We tested if the C-terminal sequences could influence expression of the upstream protein using the same cytosolic scFv reporter used for 2A (cyt-2A*). Starting from construct cyt-2A, we cloned in place of the 2A* nucleotide sequence the C-termini of CD99L2, POTEE/POTEI, SPIRE and TBCA without or with the addition of a Pro-codon before the

termination codon, thus generating construct listed in Figure 66. Regarding the NPGP C-terminal sequence of FCAMR, it was cloned downstream the same scFv reporter without or with the deletion of its own terminal Pro-codon (Figure 66).

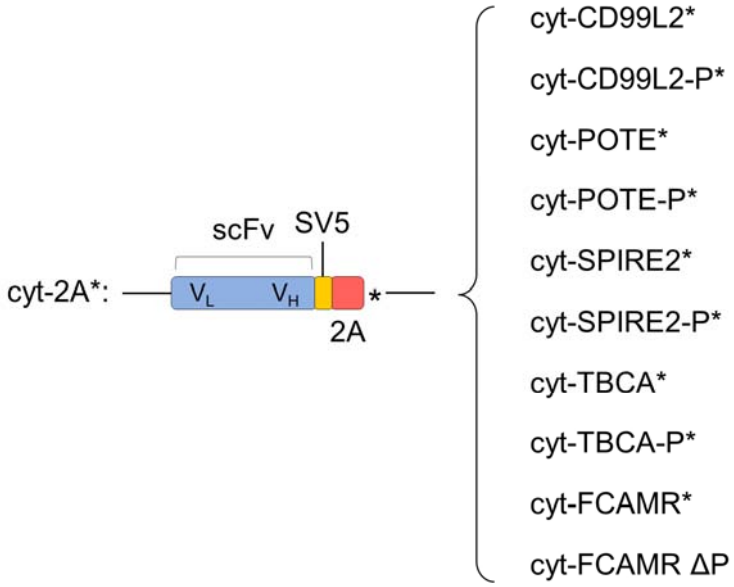

Figure 66. Scheme of the cytosolic scFv reporter construct used as a base to clone in place of 2A sequence, the C-terminal sequences of CD99L2, POTEI/POTEE, TBCA and SPIRE2 identified by bioinformatic analysis. All the sequences have been cloned without or with the addition of a Proline before the termination codon. C-terminal NPGP sequence of FCAMR was cloned in the same position with or without the terminal Proline.

Constructs were transfected in HEK-293T and cyt-2A*, cyt-2A-P* and the untagged cyt-scFv (no 2A) were used as controls.

SDS-PAGE of cellular extracts and immunoblotting with anti-SV5 antibody revealed that the C-termini from CD99L2 and POTE caused a strong reduction in the expression of the scFv reporter protein in comparison to the same scFv without terminal sequences (Figure 67A). Moreover, the addition of the C-terminal Pro partially rescued the expression of proteins terminating with CD99L2 or POTE, in a similar way to peptide 2A. However, proteins tagged with TBCA, SPIRE2 (Figure 67A) or FCAMR (Figure 67B) did not have any effect on protein translation, nor the removal of the terminal Pro from the FCAMR sequence to resemble the NPG C-terminus (Figure 67).

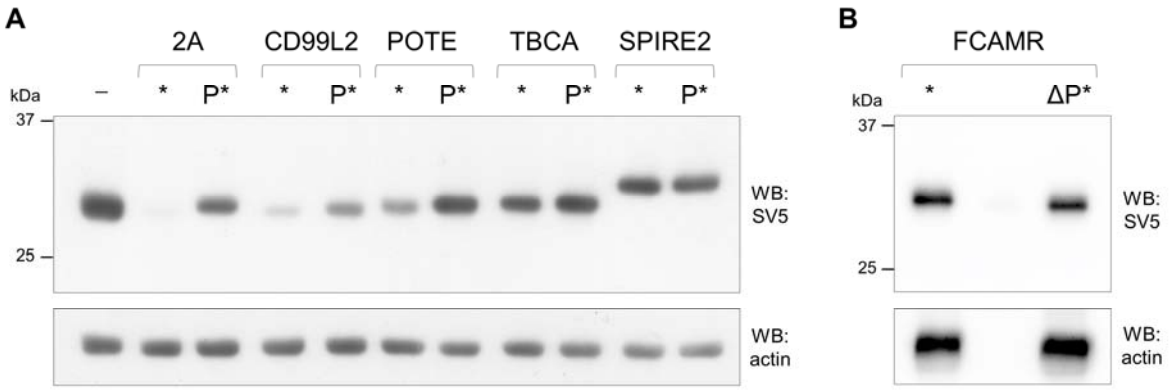

Figure 67. A: Western blots of extracts form HEK-293T cells expressing the cytosolic scFv reporter represented in the previous figure, without or with the C-terminal Proline, as indicated. Figure is representative of n=3 independent experiments. **B:** Western blots of extracts form HEK-293T cells expressing the cytosolic scFv reporter including or not the FCAMR C-terminal Proline as indicated. Figure is representative of n=2 independent experiments.

We then observed that upon *in vitro* translation, plasmids encoding cyt-CD99L2 or cyt-POTE did not display the same effect as in living cells or as 2A (Figure 68), which was used as control, and the addition of the terminal Pro did not rescue proteins expression. However, we already noticed that *in vitro* the difference in expression between cyt-2A and cyt-2A-P was 10-fold less than *in vivo*, probably due to the absence of an efficient degradation apparatus and to the reduce formation of translating poly-ribosomes. In addition, we should also consider that the reduction of scFv expression induced in living cells by POTE and CD99L2 is lower than the one induced by 2A.

These differences can explain why we don't see the same effect *in vitro* and *in vivo*.

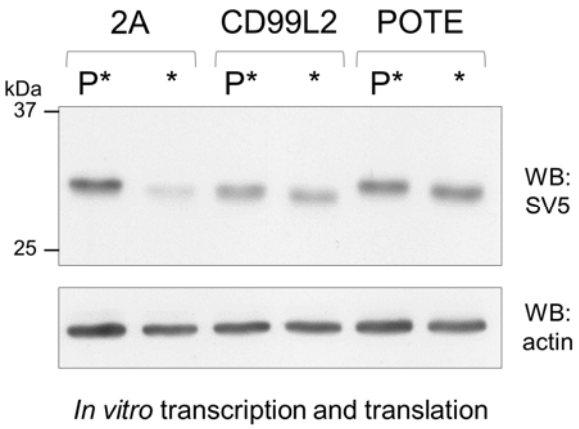

Figure 68. Expression in *in vitro* reticulocytes lysate system of constructs encoding cyt-2A, cyt-CD99L2 or cyt-POTE with or without the C-terminal Proline.

4.3 EFFECT OF NON-VIRAL C-TERMINAL PEPTIDES ON PROTEIN EXPRESSION BY ER-BOUND RIBOSOMES

The following step was to test if CD99L2 and POTE reduce translation also of secretory proteins. A signal for secretion was added at the N-terminus of the scFv reporter, as schematised in Figure 69 (left panel).

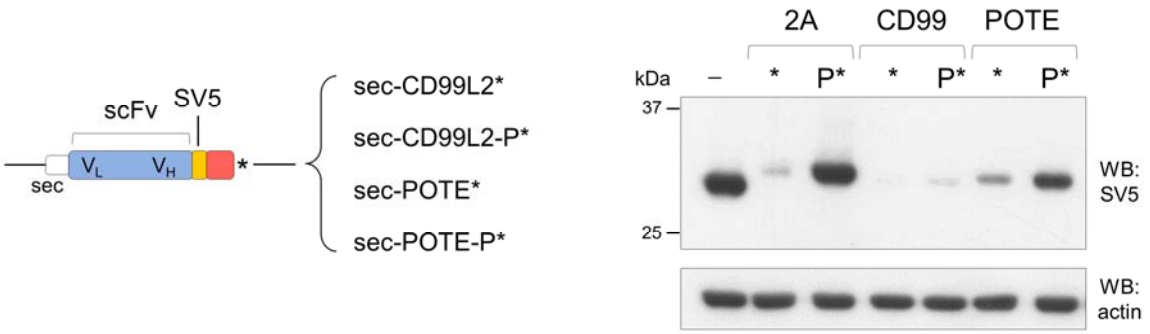

Figure 69. On the left, the scheme of scFv reporter with the secretion signal (sec) and the C-terminal sequences of 2A substituted by CD99L2 or POTE engineered without or with C-terminal Proline. On the right panel, Western blot of extracts of HEK-293T transfected as indicated with constructs shown on the left panel. Representative of n=3 independent experiments.

The results obtained by transient transfection confirmed what observed for cytoplasmic reporters: translation of the upstream protein was impaired when compared to the construct with a Proline.

Considering the similarities with 2A, we hypothesised that also proteins produced with CD99L2 or POTE C-termini were object of proteasomal degradation. Secretory reporters were then expressed in HEK-293T cells and treated with the proteasome inhibitor MG132 or co-transfected with deubiquitinase OTU or p97 dominant negative p97QQ. Both products were stabilised by MG132 treatment as well as co-expression with OTU and p97QQ (Figure 70), indicating that C-terminal sequences of CD99L2 and POTE induce degradation of nascent chains through the ubiquitin-proteasome pathway, in a similar way as 2A.

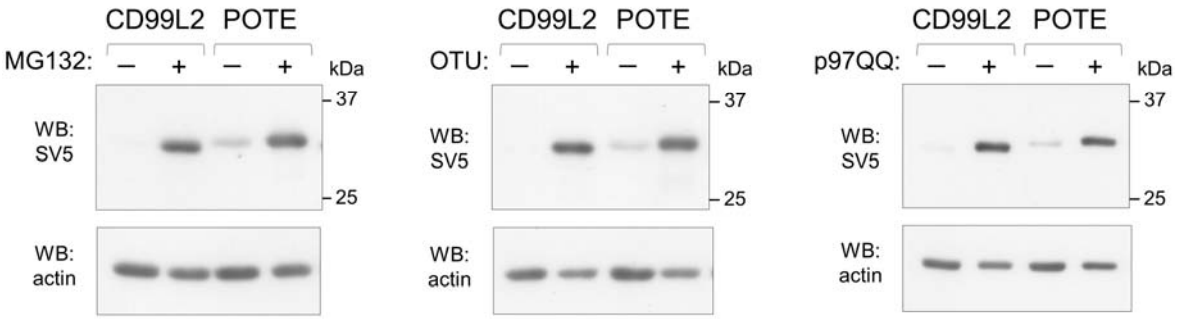

Figure 70. SDS-PAGE of sec-scFv tagged with CD99L2 or POTE C-termini expressed in HEK-293T and treated with MG132 (left panel) or co-expressed with OTU (middle panel) or p97QQ (right panel), as indicated. Figure is representative on n=2 independent experiments.

Collectively, these data suggest that other sequences rather than 2A can cause ribosome stalling at the STOP-codon, thus indicating a new mechanism to control gene expression at the translational level. Moreover, it is possible that other sequences can induce a similar cellular response, also not ending as NPG, because also other amino acid residues within the RET can influence translational stalling at the termination codon.

4.4 ANALYSIS OF A C-TERMINAL PEPTIDE NOT ENDING IN NPG

Recently, a short sequence capable of inducing ribosome stalling was described in an ORF located at the 3'UTR of human AMD1 mRNA, which encodes AdoMetDC (Yordanova et al., 2018). Curiously, ribosomes footprint analysis highlighted that ribosomes were stalled on the 63 nucleotides downstream the STOP-codon. As shown in Figure 70A, this sequence encodes for a 21 amino acids-long peptide that does not terminate in NPG. We tested this C-tail in our reporter construct for cytosolically or ER-targeted expression and found that in both cases, the C-tail strongly affected expression of the reporter protein to a level comparable to that of 2A (Figure 70B and 70C). In this case, however, addition of a Proline upstream of the STOP-codon did not rescue expression.

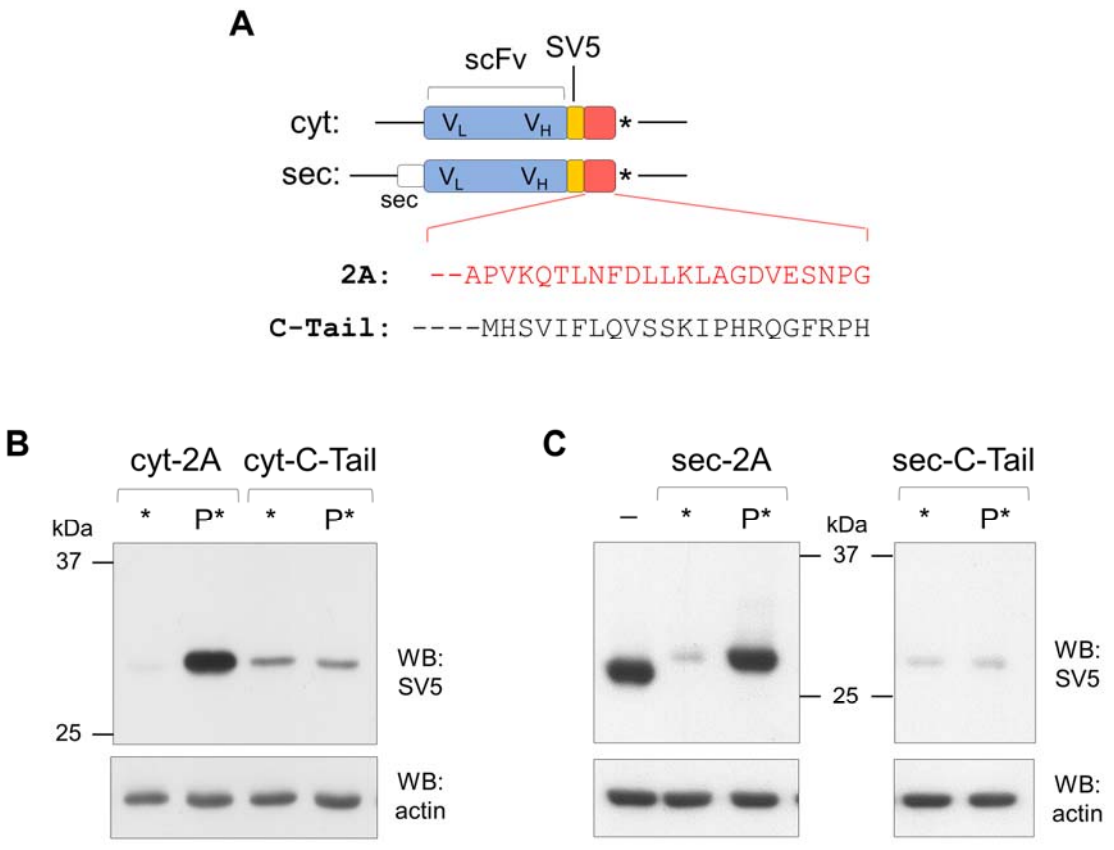

Figure 71. A: scheme of the scFv constructs engineered with the C-terminal AMD1 3' tail (C-tail) and its corresponding sequence. Western blots of cytosolic (**B**) and ER (**C**) reporters without or with C-terminal Proline, as indicated. N=2 independent experiments.

Deletion of the two terminal amino acids Proline and Histidine partially rescued the expression of the upstream reporter protein (Figure 72), indicating that they are important to induce the ribosome stalling.

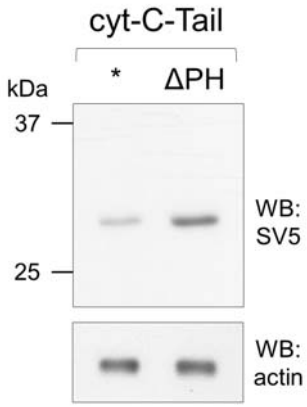

Figure 72. Extracts of HEK-293T cells transfected with constructs encoding the cytosolic reporter bearing at the C-terminus the C-tail or C-tail with deletion of the last Pro and His (ΔPH). Representative of n=2 independent experiments.

Interestingly, even if protein expression is strongly abrogated by the presence of the C-tail, it induced a modest protein degradation by the ubiquitin-proteasome pathway, as the reporter protein is slightly sensitive to impairment of the proteasome, poly-ubiquitination or p97 ATPase activity (Figure 73).

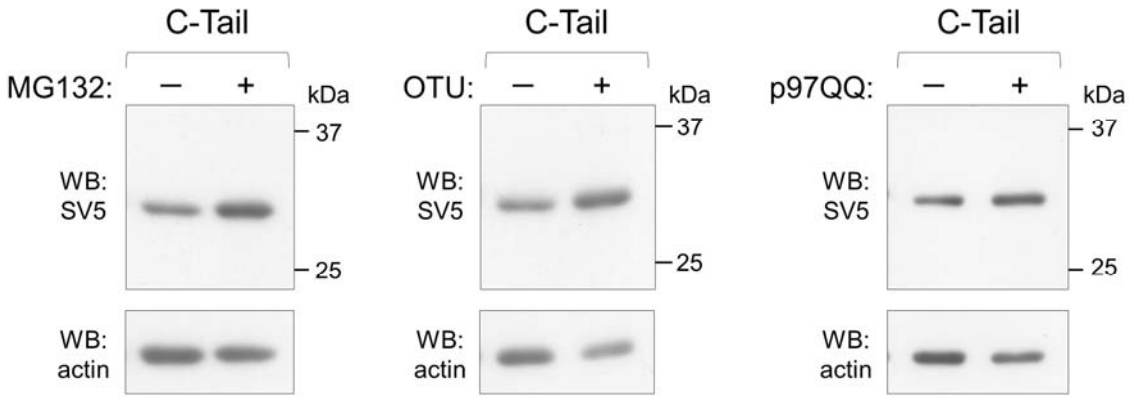

Figure 73. Treatment with proteasome inhibitor MG132 (left panel) or co-expression with OTU (middle panel) or p97QQ (right panel) of HEK-293T cells transfected with the reporter proteins engineered with C-tail. Representative of n=2 independent experiments.

Taking together, these findings suggest that stalling induced by C-tail of AMD1 occurs with a mechanism different from 2A, as it is not dependent on the presence of a termination codon.

4.5 NON-CONVENTIONAL TERMINATION

The sequence formed by amino acids NPGP is reported to be essential for peptide 2A non-conventional termination and, in fact, it is highly conserved (Sharma et al., 2012). We were curious to see if the peptides we identified with the NPG terminal sequence could have a similar activity when the Proline is added immediately downstream, thus resembling the NPGP sequence of viral peptide 2A. For this reason, a short tag of 11 amino acid (roTag) was engineered downstream the NPGP sequence of POTE- and C-tail-tagged reporter proteins (constructs POTE-P-roTag* and C-tail-P-roTag*, schematically represented in Figure 74, left panel). If these peptides can catalyse non-conventional termination downstream the Gly, the proteins should have an electrophoretic migration comparable to proteins terminating in NPG (pr1) and we should not detect the protein with the roTag in the Western blot analysis, because it will not be translated as the same protein. On the contrary, if non-conventional termination does not occur, ribosomes will translate regularly until the STOP-codon after the roTag (pr2), and so the reporter proteins will migrate slower and the included roTag will be recognised by its specific antibody. Plasmids coding for these new constructs were transfected in HEK-293T cells and the same constructs without roTag were expressed as controls (POTE-P* and C-tail-P*). Of note, if POTE-P or C-tail-P acquired non-conventional termination activity, the C-terminal Pro will be also cleaved. However, considering the difficult in discriminating such a small difference by Western blot, we will refer to these proteins as pr1 as well (schematised in Figure 74, left panel).

Neither POTE nor C-tail sequences displayed non-conventional translation termination, as both of them were translated with roTag included, as shown in Figure 74 (right panel).

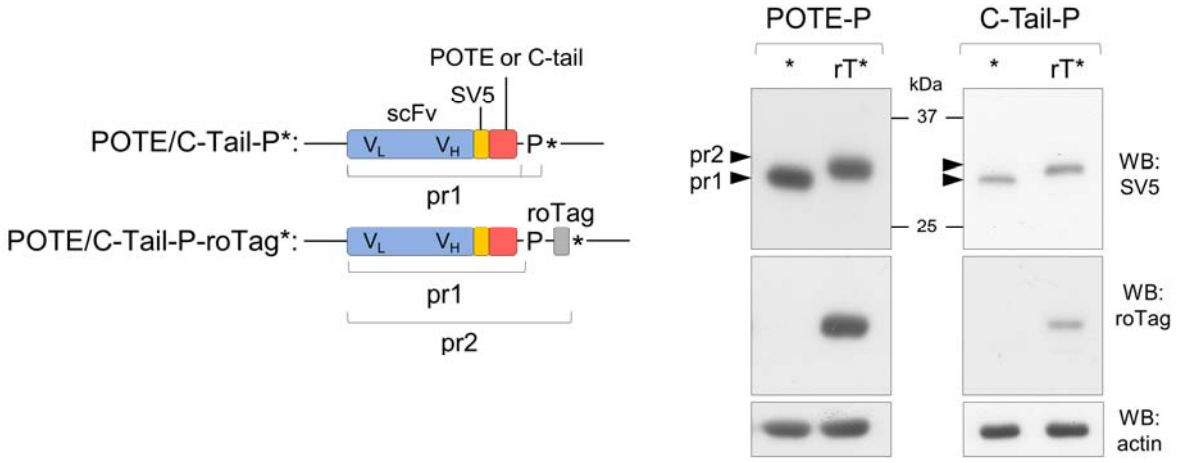

Figure 74. On the left panel, a scheme of POTE-P* or C-tail-P* control constructs, expressing protein 1 (pr1). The terminal Proline is translated within pr1 in case of conventional termination or is not included if non-conventional termination occurs. Proteins resulting from non- conventional (pr1) or conventional (pr2) translation termination of constructs POTE-P-roTag* and C-Tail-P-roTag* are also shown. On the right panel, Western blots of extracts of HEK-293T cells transfected with the reported constructs, as indicated. rT is an abbreviation for roTag. Representative of n=2 independent experiments.

Mass Spectrometry Analysis of BioID-2A

rank	log(e)	log(I)	% measured	% corrected	unique	total	Mr	Accession	Description
1	-125.6	8.00	23	41	10	79	46.5	ENSP00000347005	LUC7L2:p , LUC7 like 2, pre-mRNA splicing factor [Source:HGNC Symbol;Acc: HGNC:21608]
2	-110.4	7.23	19	25	13	28	77.5	ENSP00000325376	HNRNPM:p , heterogeneous nuclear ribonucleoprotein M [Source:HGNC Symbol;Acc: HGNC:5046]
3	-105.6	7.36	28	42	11	32	49.6	ENSP00000339001	TUBB:p , tubulin beta class I [Source:HGNC Symbol;Acc: HGNC:20778]
4	-91.0	7.23	17	32	9	23	59.3	ENSP00000253363	RBM39:p , RNA binding motif protein 39 [Source:HGNC Symbol;Acc: HGNC:15923]
5	-88.3	6.74	5.2	7	11	12	269.8	ENSP00000344789	ACACA:p , no protein text annotation available
6	-86.4	7.43	33	52	9	25	27.7	ENSP00000258962	SRSF1:p , serine and arginine rich splicing factor 1 [Source:HGNC Symbol;Acc: HGNC:10780]
7	-83.4	7.53	7.4	12	2	6	38.4	ENSP00000337507	LUC7L:p , LUC7 like [Source:HGNC Symbol;Acc: HGNC:6723]
8	-75.9	7.87	37	71	8	26	19.3	ENSP00000362820	SRSF3:p , serine and arginine rich splicing factor 3 [Source:HGNC Symbol;Acc: HGNC:10785]
9	-75.2	7.23	43	65	9	20	17.7	ENSP00000393241	RPS18:p , ribosomal protein S18 [Source:HGNC Symbol;Acc: HGNC:10401]
10	-71.2	7.16	3.2	5	1	1	49.6	ENSP00000264071	TUBB4:p , tubulin beta 4A class Iva [Source:HGNC Symbol;Acc: HGNC:20774]
11	-48.1	7.17	20	37	4	6	27.4	ENSP00000325905	SRSF7:p , serine and arginine rich splicing factor 7 [Source:HGNC Symbol;Acc: HGNC:10789]
12	-47.3	7.01	16	24	6	14	50.1	ENSP00000336799	TUBA1B:p , tubulin alpha 1b [Source:HGNC Symbol;Acc: HGNC:18809]
13	-45.9	6.57	23	41	6	8	21.4	ENSP00000339566	HIST1H1C:p , histone cluster 1 H1 family member c [Source:HGNC Symbol;Acc: HGNC:4716]
14	-45.4	6.64	18	32	5	10	23.7	ENSP00000441406	ADP ribosylation factor like GTPase 6 interacting protein 4 [Source:HGNC Symbol;Acc: HGNC:18076]
15	-35.8	6.51	8.7	16	1	1	21.9	ENSP00000307705	HIST1H1E:p , histone cluster 1 H1 family member e [Source:HGNC Symbol;Acc: HGNC:4718]
16	-31.4	7.20	20	42	4	17	25.5	ENSP00000376276	SRSF2:p , serine and arginine rich splicing factor 2 [Source:HGNC Symbol;Acc: HGNC:10783]
17	-29.9	6.57	7.3	11	4	9	72.3	ENSP00000324173	HSPA5:p , heat shock 70kDa protein 5 glucose-regulated protein, 78kDa [Source:HGNC Symbol;Acc: HGNC:5238]
18	-27.5	6.73	17	26	4	6	29.4	ENSP00000272139	C1orf35:p , chromosome 1 open reading frame 35 [Source:HGNC Symbol;Acc: HGNC:19032]
19	-25.1	6.58	16	50	3	5	18.8	ENSP00000244227	SNRNP27:p , small nuclear ribonucleoprotein U4/U6.U5 subunit 27 [Source:HGNC Symbol;Acc: HGNC:30240]
20	-24.7	7.01	14	22	3	9	27.6	ENSP00000343557	ZCCHC17:p , zinc finger CCHC-type containing 17 [Source:HGNC Symbol;Acc: HGNC:30246]
21	-24.6	7.04	24	30	3	9	14.4	ENSP00000422078	SUB1:p , SUB1 homolog, transcriptional regulator [Source:HGNC Symbol;Acc: HGNC:19985]
22	-24.0	6.54	23	31	4	6	16.4	ENSP00000251453	RPS16:p , ribosomal protein S16 [Source:HGNC Symbol;Acc: HGNC:10396]
23	-22.8	6.62	17	35	3	7	22.9	ENSP00000448039	nascent polypeptide-associated complex alpha subunit [Source:HGNC Symbol;Acc: HGNC:7629]
24	-21.5	6.53	9.9	19	4	4	33.2	ENSP00000383059	ARGLU1:p , arginine and glutamate rich 1 [Source:HGNC Symbol;Acc: HGNC:25482]
25	-18.6	6.21	9.3	11	2	2	53.5	ENSP00000404372	HSPA8:p
26	-17.4	6.61	14	25	2	5	15.8	ENSP00000296674	RPS23:p , ribosomal protein S23 [Source:HGNC Symbol;Acc: HGNC:10410]
27	-10.6	5.89	1.8	3	2	2	117.4	ENSP00000416534	DDX46:p
28	-9.6	6.00	5.6	8	2	2	49.2	ENSP00000377082	HNRNPH1:p , heterogeneous nuclear ribonucleoprotein H1 [Source:HGNC Symbol;Acc: HGNC:5041]
29	-9.6	5.94	8.1	13	2	2	26.1	ENSP00000297157	RP9:p , RP9, pre-mRNA splicing factor [Source:HGNC Symbol;Acc: HGNC:10288]
30	-9.6	5.82	7.0	8	2	2	32.7	ENSP00000435905	PC:p
31	-9.2	5.62	20	34	2	2	14.8	ENSP00000346088	RPL22:p , ribosomal protein L22 [Source:HGNC Symbol;Acc: HGNC:10315]
32	-8.6	5.79	3.0	4	2	2	80.4	ENSP00000265594	MCCC1:p , methylcrotonoyl-CoA carboxylase 1 (alpha) [Source: HGNC 6936]
33	-8.6	5.76	8.7	14	2	2	37.5	ENSP00000305556	PCBP1:p , poly(rC) binding protein 1 [Source: HGNC 8647]
34	-8.6	6.25	2.4	3	2	2	163.0	ENSP00000397570	MAPKBP1:p
35	-7.9	6.34	6.4	17	2	3	28.7	ENSP00000369757	RPS6:p , ribosomal protein S6 [Source:HGNC Symbol;Acc: HGNC:10429]
36	-7.1	5.96	12	29	2	2	13.7	ENSP00000435096	RPS25:p , ribosomal protein S25 [Source:HGNC Symbol;Acc: HGNC:10413]
37	-6.7	6.06	5.0	8	1	2	27.9	ENSP00000291552	U2AF1:p , U2 small nuclear RNA auxiliary factor 1 [Source:HGNC Symbol;Acc: HGNC:12453]

38	-5.4	5.91	14	18	1	2	9.5	ENSP00000357555	RPS27:p , ribosomal protein S27 [Source:HGNC Symbol;Acc: HGNC:10416]
39	-4.9	6.53	9.4	21	1	3	10.6	ENSP00000362671	RPL35:p , ribosomal protein L35 [Source:HGNC Symbol;Acc: HGNC:10344]
40	-4.6	5.60	2.3	4	1	1	47.7	ENSP00000311430	RPL4:p , ribosomal protein L4 [Source:HGNC Symbol;Acc: HGNC:10353]
41	-4.0	6.26	6.3	10	1	2	16.4	ENSP00000404375	RPL36A:p , ribosomal protein L36a [Source:HGNC Symbol;Acc: HGNC:10359]
42	-3.8	5.60	0.6	1	1	1	269.3	ENSP00000354085	ANKHD1:p , ankyrin repeat and KH domain containing 1 [Source:HGNC Symbol;Acc: HGNC:24714]
43	-3.7	5.47	5.2	11	1	2	33.6	ENSP00000416959	TRA2B:p , transformer 2 beta homolog [Source:HGNC Symbol;Acc: HGNC:10781]
44	-3.6	5.51	12	22	1	1	13.0	ENSP00000348849	RPS26:p , ribosomal protein S26 [Source:HGNC Symbol;Acc: HGNC:10414]
45	-3.5	6.58	6.8	14	1	3	16.6	ENSP00000346015	RPL27A:p , ribosomal protein L27a [Source:HGNC Symbol;Acc: HGNC:10329]
46	-3.5	5.51	6.6	22	1	1	16.3	ENSP00000385958	RPS14:p , ribosomal protein S14 [Source:HGNC Symbol;Acc: HGNC:10387]
47	-3.1	6.83	2.6	3	1	4	74.8	ENSP00000305107	GIMAP8:p , GTPase, IMAP family member 8 [Source:HGNC Symbol;Acc: HGNC:21792]
48	-3.1	6.02	6.4	8	1	1	14.9	ENSP00000420311	RPL23:p , ribosomal protein L23 [Source:HGNC Symbol;Acc: HGNC:10316]
49	-2.9	5.72	6.6	12	1	1	12.5	ENSP00000346012	RPL36AL:p , ribosomal protein L36a like [Source:HGNC Symbol;Acc: HGNC:10346]
50	-2.7	5.32	3.9	8	1	2	51.4	ENSP00000425092	LUC7L3:p , LUC7 like 3 pre-mRNA splicing factor [Source:HGNC Symbol;Acc: HGNC:24309]
51	-2.5	6.00	33	44	1	1	2.2	ENSP00000451870	T-cell receptor alpha joining 56 [Source:HGNC Symbol;Acc: HGNC:12088]
52	-2.5	6.22	5.5	10	1	3	22.2	ENSP00000342913	SRSF10:p
53	-2.4	7.05	3.0	4	1	6	24.4	sp|TRYP_PIG|	Trypsin; EC 3.4.21.4; Flags: Precursor
54	-2.3	5.06	7.1	15	1	1	18.2	ENSP00000427401	SREK1IP1:p
55	-2.2	5.52	14	17	1	1	10.5	ENSP00000215570	TIMM13:p
56	-2.1	5.54	0.8	3	1	1	161.0	ENSP00000420477	NACAD:p
57	-2.1	5.89	4.5	9	1	1	17.8	ENSP00000377640	RPL24:p , ribosomal protein L24 [Source:HGNC Symbol;Acc: HGNC:10325]
58	-1.9	5.52	2.7	5	1	1	72.9	ENSP00000356311	C1orf106:p
59	-1.9	5.39	1.4	4	1	1	103.9	ENSP00000345308	UBAP2L:p , ubiquitin associated protein 2 like [Source:HGNC Symbol;Acc: HGNC:29877]
60	-1.8	5.36	0.8	1	1	1	160.5	ENSP00000364979	COL4A1:p
61	-1.7	5.65	3.8	7	1	1	27.2	ENSP00000389783	FAM133B:p
62	-1.7	5.60	4.1	6	1	1	33.0	ENSP00000393746	FYTTD1:p
63	-1.6	5.61	12	21	1	1	6.7	ENSP00000245458	RPS29:p , ribosomal protein S29 [Source:HGNC Symbol;Acc: HGNC:10419]
64	-1.6	4.64	0.8	1	1	1	141.3	ENSP00000347730	ZNF536:p
65	-1.5	5.38	0.5	1	1	1	170.8	ENSP00000342434	BAZ1B:p
66	-1.5	5.45	6.5	13	1	1	17.7	ENSP00000366061	NMS:p
67	-1.5	6.01	0.5	1	1	1	150.7	ENSP00000303427	PDS5A:p
68	-1.5	5.52	1.8	3	1	1	116.6	ENSP00000382356	COL28A1:p
69	-1.4	5.31	1.1	2	1	1	110.6	ENSP00000353854	C15orf39:p
70	-1.4	5.54	1.5	3	1	2	53.5	ENSP00000307863	U2AF2:p , U2 small nuclear RNA auxiliary factor 2 [Source:HGNC Symbol;Acc: HGNC:23156]
71	-1.4	5.60	4.8	7	1	1	54.2	ENSP00000359160	CCDC76:p
72	-1.4	5.74	0.2	0	1	1	383.6	ENSP00000334714	IGFN1:p
73	-1.4	5.38	4.1	11	1	1	23.5	ENSP00000225430	RPL19:p , ribosomal protein L19 [Source:HGNC Symbol;Acc: HGNC:10312]
74	-1.4	5.40	9.5	15	1	1	11.8	ENSP00000447415	no protein information available
75	-1.3	6.12	0.3	0	1	1	348.2	ENSP00000424243	EYS:p
76	-1.3	5.74	4.2	7	1	1	25.5	ENSP00000385298	MEI1:p
77	-1.3	5.34	1.8	2	1	1	163.9	ENSP00000379866	COL4A4:p , collagen, type IV, alpha 4 [Source: HGNC 2206]
78	-1.3	5.58	2.2	3	1	1	101.9	ENSP00000432728	TYK2:p
79	-1.3	5.55	3.5	5	1	1	54.4	ENSP00000260228	MMP20:p
80	-1.3	5.67	1.1	1	1	1	112.8	ENSP00000367787	LIG3:p
81	-1.3	5.45	12	31	1	1	23.6	ENSP00000242284	CLTA:p
82	-1.2	5.27	1.9	4	1	1	69.8	ENSP00000347451	LINGO1:p
83	-1.2	5.90	1.3	2	1	1	157.0	ENSP00000270238	LMTK3:p
84	-1.2	5.53	3.2	5	1	1	24.4	ENSP00000446215	RAN, member RAS oncogene family [Source:HGNC Symbol;Acc: HGNC:9846]
85	-1.2	5.58	18	90	1	1	6.4	ENSP00000355315	RPL39:p
86	-1.2	5.76	0.8	1	1	1	119.5	ENSP00000317614	ZNF518B:p
87	-1.2	5.32	1.9	3	1	1	67.8	ENSP00000359916	FRMD7:p
88	-1.2	6.00	0.4	1	1	1	237.9	ENSP00000276204	DOCK11:p
89	-1.2	5.89	4.6	6	1	1	45.1	ENSP00000384848	PRR5:p
90	-1.2	5.70	5.1	7	1	1	18.0	ENSP00000383981	RPS27A:p , ribosomal protein S27a [Source:HGNC Symbol;Acc: HGNC:10417]

91	-1.1	4.84	12	15	1	1	16.1	ENSP00000454239	no protein information available
92	-1.1	5.35	0.2	0	1	1	256.1	ENSP00000418510	FLNB:p
93	-1.1	5.16	17	20	1	1	9.7	ENSP00000334644	LCE3C:p
94	-1.1	5.35	2.3	4	1	1	67.6	ENSP00000217429	FAM83D:p
95	-1.1	5.27	2.4	5	1	1	27.0	ENSP00000456266	no protein information available
96	-1.1	5.59	1.1	2	1	1	96.6	ENSP00000413812	ERN2:p
97	-1.1	5.50	2.7	4	1	1	34.6	ENSP00000354822	XAF1:p
98	-1.1	5.70	1.3	2	1	1	138.0	ENSP00000364798	ZBTB40:p
99	-1.1	5.86	0.9	1	1	1	161.0	ENSP00000303153	COL22A1:p , collagen type XXII alpha 1 chain [Source:HGNC Symbol;Acc: HGNC:22989]
100	-1.0	5.59	2.7	4	1	1	46.9	ENSP00000272224	GDF7:p
101	-1.0	6.23	1.2	2	1	1	89.7	ENSP00000206765	TGM1:p
102	-1.0	5.59	0.9	1	1	1	127.7	ENSP00000268296	ITGAX:p
103	-1.0	5.17	0.6	1	1	1	222.9	ENSP00000262450	CHD5:p

Mass Spectrometry Analysis of BioID-2A-P

rank	log(e)	log(I)	% measured	% corrected	unique	total	Mr	Accession	Description
1	-129.6	8.02	23	41	10	63	46.5	ENSP00000347005	LUC7L2:p , LUC7 like 2, pre-mRNA splicing factor [Source:HGNC Symbol;Acc: HGNC:21608]
2	-111.9	7.19	18	23	12	19	77.5	ENSP00000325376	HNRNPM:p , heterogeneous nuclear ribonucleoprotein M [Source:HGNC Symbol;Acc: HGNC:5046]
3	-88.0	7.62	7.4	12	2	5	38.4	ENSP00000337507	LUC7L:p , LUC7 like [Source:HGNC Symbol;Acc: HGNC:6723]
4	-83.6	7.30	23	35	9	24	49.6	ENSP00000339001	TUBB:p , tubulin beta class I [Source:HGNC Symbol;Acc: HGNC:20778]
5	-82.6	7.64	36	57	9	30	27.7	ENSP00000258962	SRSF1:p , serine and arginine rich splicing factor 1 [Source:HGNC Symbol;Acc: HGNC:10780]
6	-74.8	7.15	9.9	15	3	7	49.6	ENSP00000264071	TUBB4:p , tubulin beta 4A class IVa [Source:HGNC Symbol;Acc: HGNC:20774]
7	-74.0	7.19	2.5	4	1	1	49.8	ENSP00000341289	TUBB2C:p , tubulin beta 4B class Ivb [Source:HGNC Symbol;Acc: HGNC:20771]
8	-73.5	7.31	14	26	6	15	59.3	ENSP00000253363	RBM39:p , RNA binding motif protein 39 [Source:HGNC Symbol;Acc: HGNC:15923]
9	-60.3	8.11	34	65	6	34	19.3	ENSP00000362820	SRSF3:p , serine and arginine rich splicing factor 3 [Source:HGNC Symbol;Acc: HGNC:10785]
10	-56.2	6.67	3.6	5	8	9	269.8	ENSP00000344789	ACACA:p , no protein text annotation available
11	-52.0	7.14	30	46	6	13	17.7	ENSP00000393241	RPS18:p , ribosomal protein S18 [Source:HGNC Symbol;Acc: HGNC:10401]
12	-49.7	7.20	16	24	6	14	50.1	ENSP00000336799	TUBA1B:p , tubulin alpha 1b [Source:HGNC Symbol;Acc: HGNC:18809]
13	-36.3	7.47	11	21	3	4	27.4	ENSP00000325905	SRSF7:p , serine and arginine rich splicing factor 7 [Source:HGNC Symbol;Acc: HGNC:10789]
14	-32.2	7.11	14	22	3	10	27.6	ENSP00000343557	ZCCHC17:p , zinc finger CCHC-type containing 17 [Source:HGNC Symbol;Acc: HGNC:30246]
15	-31.8	6.56	19	28	4	5	29.4	ENSP00000272139	C1orf35:p , chromosome 1 open reading frame 35 [Source:HGNC Symbol;Acc: HGNC:19032]
16	-29.9	6.80	22	40	4	7	21.9	ENSP00000307705	HIST1H1E:p , histone cluster 1 H1 family member e [Source:HGNC Symbol;Acc: HGNC:4718]
17	-29.1	7.39	17	36	3	22	25.5	ENSP00000376276	SRSF2:p , serine and arginine rich splicing factor 2 [Source:HGNC Symbol;Acc: HGNC:10783]
18	-28.9	6.79	7.0	12	1	2	21.4	ENSP00000339566	HIST1H1C:p , histone cluster 1 H1 family member c [Source:HGNC Symbol;Acc: HGNC:4716]
19	-27.9	6.49	21	38	4	5	12.5	ENSP00000346012	RPL36AL:p , ribosomal protein L36a like [Source:HGNC Symbol;Acc: HGNC:10346]
20	-27.1	6.81	6.3	10	2	5	16.4	ENSP00000404375	RPL36A:p , ribosomal protein L36a [Source:HGNC Symbol;Acc: HGNC:10359]
21	-26.6	6.27	9.0	10	3	3	42.0	ENSP00000355645	ACTA1:p , actin, alpha 1, skeletal muscle [Source:HGNC Symbol;Acc: HGNC:129]
22	-26.1	6.44	16	28	3	4	23.7	ENSP00000441406	ADP ribosylation factor like GTPase 6 interacting protein 4 [Source:HGNC Symbol;Acc: HGNC:18076]
23	-26.1	7.00	16	50	3	7	18.8	ENSP00000244227	SNRNP27:p , small nuclear ribonucleoprotein U4/U6.U5 subunit 27 [Source:HGNC Symbol;Acc: HGNC:30240]
24	-23.8	6.73	16	45	4	6	28.7	ENSP00000369757	RPS6:p , ribosomal protein S6 [Source:HGNC Symbol;Acc: HGNC:10429]
25	-23.4	6.58	21	38	3	4	15.8	ENSP00000296674	RPS23:p , ribosomal protein S23 [Source:HGNC Symbol;Acc: HGNC:10410]
26	-22.8	6.23	7.3	11	3	3	49.2	ENSP00000377082	HNRNPH1:p , heterogeneous nuclear ribonucleoprotein H1 [Source:HGNC Symbol;Acc: HGNC:5041]
27	-22.5	7.02	24	30	3	8	14.4	ENSP00000422078	SUB1:p , SUB1 homolog, transcriptional regulator [Source:HGNC Symbol;Acc: HGNC:19985]
28	-15.8	6.08	3.0	4	3	3	163.7	ENSP00000361290	COL4A6:p , collagen type IV alpha 6 chain [Source:HGNC Symbol;Acc: HGNC:2208]
29	-15.3	6.65	7.3	14	3	3	33.2	ENSP00000383059	ARGLU1:p , arginine and glutamate rich 1 [Source:HGNC Symbol;Acc: HGNC:25482]

30	-15.3	6.04	11	19	3	3	34.9	ENSP00000352228	PCBP2:p , poly(rC) binding protein 2 [Source:HGNC Symbol;Acc: HGNC:8648]
31	-13.4	6.46	13	27	2	2	16.6	ENSP00000346015	RPL27A:p , ribosomal protein L27a [Source:HGNC Symbol;Acc: HGNC:10329]
32	-10.9	6.50	12	16	2	3	16.4	ENSP00000251453	RPS16:p , ribosomal protein S16 [Source:HGNC Symbol;Acc: HGNC:10396]
33	-10.7	5.90	8.5	14	2	2	24.2	ENSP00000307889	RPL13:p , ribosomal protein L13 [Source:HGNC Symbol;Acc: HGNC:10303]
34	-10.1	5.99	8.0	17	2	3	33.6	ENSP00000416959	TRA2B:p , transformer 2 beta homolog [Source:HGNC Symbol;Acc: HGNC:10781]
35	-9.7	6.00	7.7	14	2	2	28.4	ENSP00000398401	FAM133B:p , family with sequence similarity 133 member B [Source:HGNC Symbol;Acc: HGNC:28629]
36	-9.1	6.16	19	34	2	2	13.0	ENSP00000348849	RPS26:p , ribosomal protein S26 [Source:HGNC Symbol;Acc: HGNC:10414]
37	-8.9	6.40	12	25	2	3	17.8	ENSP00000377640	RPL24:p , ribosomal protein L24 [Source:HGNC Symbol;Acc: HGNC:10325]
38	-8.7	6.12	4.5	7	2	2	26.1	ENSP00000297157	RP9:p , RP9, pre-mRNA splicing factor [Source:HGNC Symbol;Acc: HGNC:10288]
39	-8.5	7.09	4.4	6	2	2	70.0	ENSP00000364802	HSPA1A:p , heat shock protein family A (Hsp70) member 1A [Source:HGNC Symbol;Acc: HGNC:5232]
40	-8.2	6.10	3.6	5	2	2	61.3	ENSP00000343657	MCCC2:p , methylcrotonoyl-CoA carboxylase 2 [Source:HGNC Symbol;Acc: HGNC:6937]
41	-5.5	5.81	2.3	4	1	1	47.7	ENSP00000311430	RPL4:p , ribosomal protein L4 [Source:HGNC Symbol;Acc: HGNC:10353]
42	-5.2	5.88	9.6	11	1	1	12.3	ENSP00000451080	ERH, mRNA splicing and mitosis factor [Source:HGNC Symbol;Acc: HGNC:3447]
43	-4.8	5.68	4.1	11	1	1	23.5	ENSP00000225430	RPL19:p , ribosomal protein L19 [Source:HGNC Symbol;Acc: HGNC:10312]
44	-4.6	5.80	1.5	2	1	2	83.2	ENSP00000360709	HSP90AB1:p , heat shock protein 90 alpha family class B member 1 [Source:HGNC Symbol;Acc: HGNC:5258]
45	-4.5	4.96	3.9	8	1	1	51.4	ENSP00000425092	LUC7L3:p , LUC7 like 3 pre-mRNA splicing factor [Source:HGNC Symbol;Acc: HGNC:24309]
46	-4.4	4.99	3.9	6	1	1	42.4	ENSP00000360033	SERBP1:p , SERPINE1 mRNA binding protein 1 [Source:HGNC Symbol;Acc: HGNC:17860]
47	-4.4	5.79	4.6	8	1	2	34.2	ENSP00000380275	RNPS1:p , RNA binding protein with serine rich domain 1 [Source:HGNC Symbol;Acc: HGNC:10080]
48	-3.6	5.94	5.1	7	1	2	18.0	ENSP00000383981	RPS27A:p , ribosomal protein S27a [Source:HGNC Symbol;Acc: HGNC:10417]
49	-3.5	5.95	1.8	3	1	1	69.1	ENSP00000440276	DEAD-box helicase 5 [Source:HGNC Symbol;Acc: HGNC:2746]
50	-3.3	5.72	12	21	1	1	6.7	ENSP00000245458	RPS29:p , ribosomal protein S29 [Source:HGNC Symbol;Acc: HGNC:10419]
51	-3.2	6.21	14	18	1	3	9.5	ENSP00000357555	RPS27:p , ribosomal protein S27 [Source:HGNC Symbol;Acc: HGNC:10416]
52	-3.1	6.76	9.4	21	1	4	10.6	ENSP00000362671	RPL35:p , ribosomal protein L35 [Source:HGNC Symbol;Acc: HGNC:10344]
53	-2.8	5.27	5.0	8	1	1	27.9	ENSP00000291552	U2AF1:p , U2 small nuclear RNA auxiliary factor 1 [Source:HGNC Symbol;Acc: HGNC:12453]
54	-2.7	5.92	5.4	7	1	1	16.7	ENSP00000228140	RPS13:p , ribosomal protein S13 [Source:HGNC Symbol;Acc: HGNC:10386]
55	-2.5	7.12	3.0	4	1	6	24.4	sp|TRYP_PIG|	Trypsin; EC 3.4.21.4; Flags: Precursor
56	-2.3	5.51	1.8	2	1	1	80.0	ENSP00000365462	PCCA:p , propionyl-CoA carboxylase alpha subunit [Source:HGNC Symbol;Acc: HGNC:8653]
57	-2.3	5.52	1.4	4	1	1	103.9	ENSP00000345308	UBAP2L:p , ubiquitin associated protein 2 like [Source:HGNC Symbol;Acc: HGNC:29877]
58	-2.2	6.23	6.4	8	1	1	14.9	ENSP00000420311	RPL23:p , ribosomal protein L23 [Source:HGNC Symbol;Acc: HGNC:10316]
59	-2.1	6.05	33	44	1	1	2.2	ENSP00000451870	T-cell receptor alpha joining 56 [Source:HGNC Symbol;Acc: HGNC:12088]
60	-2.1	5.47	2.2	3	1	1	80.6	ENSP00000362929	GSN:p , gelsolin [Source:HGNC Symbol;Acc: HGNC:4620]
61	-2.0	5.45	0.7	1	1	1	211.0	ENSP00000356000	PLXNA2:p , plexin A2 [Source:HGNC Symbol;Acc: HGNC:9100]
62	-1.9	5.46	9.4	16	1	1	14.8	ENSP00000346088	RPL22:p , ribosomal protein L22 [Source:HGNC Symbol;Acc: HGNC:10315]
63	-1.9	5.64	5.5	10	1	1	22.2	ENSP00000342913	SRSF10:p
64	-1.9	6.07	1.7	3	1	1	50.1	ENSP00000339063	EEF1A1:p , eukaryotic translation elongation factor 1 alpha 1 [Source:HGNC Symbol;Acc: HGNC:3189]
65	-1.9	5.91	1.5	2	1	1	99.5	ENSP00000393313	EPS15L1:p
66	-1.9	5.57	1.9	2	1	1	58.9	ENSP00000263284	CCDC61:p
67	-1.9	6.29	6.8	18	1	1	14.4	ENSP00000435370	FAU:p , FAU, ubiquitin like and ribosomal protein S30 fusion [Source:HGNC Symbol;Acc: HGNC:3597]
68	-1.8	5.06	14	24	1	1	13.7	ENSP00000437206	ST3GAL3:p
69	-1.8	5.84	7.5	12	1	1	16.3	ENSP00000271843	JTB:p
70	-1.7	6.16	3.2	5	1	1	68.8	ENSP00000263663	TAF1B:p
71	-1.7	6.16	0.3	0	1	1	293.3	ENSP00000222270	Histone-lysine N-methyltransferase 2B
72	-1.7	5.64	1.1	2	1	1	131.8	ENSP00000384169	FBLN2:p
73	-1.7	5.73	5.3	10	1	1	30.3	ENSP00000358731	ADORA3:p

74	-1.6	5.38	0.7	1	1	1	242.8	ENSP00000363215	MED12:p
75	-1.5	5.39	1.4	2	1	1	127.9	ENSP00000364973	COL4A1:p
76	-1.5	5.29	0.6	1	1	1	269.3	ENSP00000354085	ANKHD1:p , ankyrin repeat and KH domain containing 1 [Source:HGNC Symbol;Acc: HGNC:24714]
77	-1.5	5.51	4.8	12	1	1	13.7	ENSP00000435096	RPS25:p , ribosomal protein S25 [Source:HGNC Symbol;Acc: HGNC:10413]
78	-1.4	5.39	22	29	1	1	14.6	ENSP00000414803	LASP1:p
79	-1.4	5.74	6.0	11	1	1	17.0	ENSP00000268483	TXNL4B:p
80	-1.4	6.41	3.1	4	1	1	61.6	ENSP00000276211	ARHGAP36:p
81	-1.4	5.59	1.0	1	1	1	136.7	ENSP00000264229	KIAA1211:p
82	-1.4	5.82	6.5	12	1	1	21.6	ENSP00000342156	NCR3:p
83	-1.4	5.84	6.1	10	1	1	31.9	ENSP00000397385	DALRD3:p
84	-1.4	5.85	3.7	6	1	1	75.0	ENSP00000318429	CCDC114:p
85	-1.4	5.28	2.8	4	1	1	58.2	ENSP00000251654	PCCB:p , propionyl CoA carboxylase, beta polypeptide [Source: HGNC 8654]
86	-1.3	5.46	1.9	3	1	1	71.6	ENSP00000380557	AKAP8L:p
87	-1.3	5.48	0.9	1	1	1	295.0	ENSP00000332371	COL7A1:p , collagen type VII alpha 1 chain [Source:HGNC Symbol;Acc: HGNC:2214]
88	-1.3	5.51	0.7	1	1	1	222.1	ENSP00000383303	DSCAM:p
89	-1.3	4.25	2.2	4	1	1	73.0	ENSP00000348959	MAN1A2:p
90	-1.3	5.51	2.4	4	1	1	62.0	ENSP00000246662	KRT9:p , keratin 9 [Source:HGNC Symbol;Acc: HGNC:6447]
91	-1.3	5.33	0.9	2	1	1	116.9	ENSP00000265069	ZFR:p
92	-1.2	5.63	1.0	2	1	1	160.5	ENSP00000323720	MED14:p
93	-1.2	5.97	2.4	4	1	1	82.8	ENSP00000410846	XPO5:p
94	-1.2	5.48	5.1	6	1	1	40.5	ENSP00000393189	EFCAB8:p
95	-1.2	5.48	4.1	6	1	1	33.0	ENSP00000393746	FYTTD1:p
96	-1.2	5.91	1.5	2	1	1	56.6	ENSP00000358417	PHGDH:p , phosphoglycerate dehydrogenase [Source:HGNC Symbol;Acc: HGNC:8923]
97	-1.2	5.57	1.1	2	1	1	83.1	ENSP00000435557	KIF21B:p
98	-1.2	5.62	0.4	1	1	1	213.5	ENSP00000352400	NUP214:p
99	-1.1	5.59	0.2	0	1	1	301.5	ENSP00000402033	PDZD2:p , PDZ domain containing 2 [Source: HGNC 18486]
100	-1.1	5.75	23	28	1	1	9.2	ENSP00000430824	CDK16:p
101	-1.1	5.50	20	21	1	1	9.5	ENSP00000436333	PARP10:p
102	-1.1	5.51	4.0	10	1	1	38.1	ENSP00000364265	FOXE1:p
103	-1.1	5.72	4.3	13	1	1	55.0	ENSP00000261622	SLC7A5:p
104	-1.1	5.28	1.9	3	1	1	42.2	ENSP00000298317	RPUSD4:p
105	-1.1	5.76	1.7	3	1	1	44.1	ENSP00000404464	CCBE1:p
106	-1.1	5.54	1.7	3	1	1	53.9	ENSP00000321835	ETV4:p
107	-1.1	5.44	3.7	4	1	1	26.7	ENSP00000413999	CKMT1B:p
108	-1.1	6.06	0.5	1	1	1	208.2	ENSP00000371994	NYNRIN:p
109	-1.1	5.55	1.2	2	1	1	111.5	ENSP00000435421	C11orf82:p
110	-1.1	5.79	1.2	2	1	1	102.4	ENSP00000453574	no protein information available
111	-1.1	5.70	1.1	1	1	1	112.8	ENSP00000367787	LIG3:p

DISCUSSION

2A-induced ribosome stalling at the STOP-codon triggers degradation of the nascent protein

In the first part of this work, we studied in human cells the effect of tagging a protein with a FMDV-derived 2A peptide with a conventional termination codon downstream the C-terminal Gly, instead of the Pro-codon that is instead required for the non-conventional termination. This mutation was previously described to cause ribosome stalling *in vitro*, because the 2A peptide was found mostly as peptidyl-tRNA, but there are no further investigations to understand the mechanism beyond.

For the first time, we demonstrate in living human cells that 2A reduces the amount of the upstream protein produced, regardless of the reporter used, and both on free and membrane-bound ribosomes. The effect relays on a restricted amino acid sequence, LLKLAGDVESNPG, followed by the termination codon (Sasset, 2013). In particular, C-terminal amino acids NPG were indispensable to abolish translation. We also found that substitution of the STOP-codon with one or more amino acids different from Pro rescued protein expression, thus indicating that translation impairment depends on the presence of the STOP-codon after amino acids NPG. Moreover, the presence of 2A reduced the rate of protein synthesis and, in the case of cytosolic reporters, it induced a modest degradation of the mRNA. These observations indicate translational stalling of the ribosomes. A reduction in the amount of cytosolic proteins with C-tail 2A in comparison to control 2A-P was found also after *in vitro* translation, even if it was less dramatic. In fact, it was calculated to be around 3.5-fold *in vitro*, against a reduction of 33-fold *in vivo*. However it was already observed that *in vitro* systems can have a reduced translational efficiency (Cao and Geballe, 1996b) and the reduced or absence of translating poly-ribosomes and of proteins degradation can explain such a difference of 10-fold we saw.

Because of all these findings, we referred to 2A-induced translational stalling as “stalling at the STOP-codon”. However, the mechanism that caused the translating ribosome to stall instead of terminating translation is not intuitive.

Picornaviral 2A peptide was described to require the same sequence for its activity of self-termination, probably because is related to the structure acquired by the peptide within the RET that favour termination by causing a transient ribosome stalling when the A site of the ribosome in occupied by the $tRNA^{Pro}$. In fact, it was reported that 2A forms an amphipathic α-helix, with a reverse turn at the C-terminus. Based on this model, when the 2A peptide Gly-codon and the following Pro are in the ribosome P and A sites, respectively, the re-orientation of the peptidyl-$tRNA^{Gly}$ abolishes peptide bond formation with the prolyl-$tRNA^{Pro}$, promoting instead hydrolysis and release of the upstream polypeptide (Donnelly et al., 2001a, 2001b; Ryan et al., 1999; Sharma et al., 2012).

In the 2A stalling model, the amino acid sequence is exactly the same, but a STOP-codon instead of the Pro-codon is found in the ribosomal A site. Reasonably, the conformation of 2A within the RET causes transient stalling, but the absence of a $tRNA^{Pro}$ (or any other tRNA) enforces the stalling and impedes the release of the upstream protein.

Another explanation is that the presence of 2A blocked in the RET can disfavour the activity of release factors, in particular eRF1. In fact, there are evidences of eRF1 involvement in the case of stalling mediated by the hCMV uORF2 of the UL4 gene, where eRF1 is thought to interact with peptidyl-tRNA causing ribosome stalling (Janzen et al., 2002; Matheisl et al., 2015). The mechanism and the biological significance of uORF-induced stalling are clearly different than our model, however this is the only example of ribosome stalling STOP-codon-dependent described until now that doesn’t require *trans*-acting factors (Cao and Geballe, 1996b). In a high resolution structural study, a human 80S ribosome is purified as stalled on mRNA of the CMV uORF2, with the translated peptide in the RET, the tRNA in the ribosome P site and eRF1 already in the A site (Matheisl et al., 2015). Notably, the CMV stalling peptide induces stalling of the ribosome contacting ribosomal proteins at the level of the L4-L22 tunnel restriction and with the penultimate Pro, which caused a rotation of the rRNA nucleotide U4493 that disfavour eRF1-mediated tRNA hydrolysis and the consequent release of the peptide. Curiously, the FMDV peptide 2A used in this study was found partially as peptidyl-tRNA and has a Pro in the same position of CMV uORF2 peptide,

that we found to be important to induce ribosome stalling at the termination codon (Sasset, 2013).

Therefore, the 2A structure acquired within the RET and the position of the penultimate Proline may contribute to the mechanism of stalling.

However, a significant fraction of polypeptides found in our experiments were hydrolysed from tRNA. This observation indicates that, even if the ribosome is stalled and its activity is slow, most of the proteins are fully terminated. It remains to be determined whether this is eRF1-dependent. Even if a previous work found peptide 2A mostly as peptidyl-tRNA *in vitro*, our observations are in line with another work, performed in yeast cells, where the majority of ubiquitinated products derived from stalled ribosomes and substrates of the ribosome quality control (RQC) pathway, were found already hydrolysed from the tRNA, because of the activities of the yeast Release Factors Sup45-Sup35 (mammalian eRF1-3 homologues) instead of their paralogues Dom3-Hbs1, which lack of the tRNA hydrolysis activity and are considered until now the major actors of the RQC pathway involved in the clearance of stalled products (Chen et al., 2010; Izawa et al., 2012; Pisareva et al., 2011; Shcherbik et al., 2016; Tsuboi et al., 2012).

As a consequence of the stalling at the STOP-codon, polypeptides derived from ER membrane-bound or free stalled ribosomes are targeted to degradation through the ubiquitin-proteasome pathway: experiments with the proteasome inhibitor MG132 prevented degradation of poly-ubiquitinated 2A proteins resulting from stalled ribosomes and similar observation were obtained using the deubiquitinase protein OTU. The identical protein, which differs only for the C-terminal Pro-codon (2A-P) was instead regularly translated and secreted, indicating that degradation is activated specifically by the 2A-mediated stalling. These experiments are in line with what previously described predominantly for peptides derived from stalling on free ribosomes, but also in a few works regarding membrane-bound stalled ribosomes (Crowder et al., 2015; Malsburg et al., 2015), in which stalled peptides with poly-lysine extension or trunked are also found poly-ubiquitinated and degraded by the proteasome.

Interestingly, we found the requirement also of the E3 ubiquitin-ligase Listerin, involved in the degradation of polypeptides from free or membrane-bound ribosomes stalled at the STOP-codon. Consistently, Listerin has been previously described to specifically

ubiquitinylate polypeptides originating from both free and membrane-bound stalled ribosomes, which induced NMD or NGD (Bengtson and Joazeiro, 2010; Brandman et al., 2012; Crowder et al., 2015; Malsburg et al., 2015; Shao et al., 2013). However, in experiments of Listerin silencing, the accumulation observed for 2A reporters, in particular the secretory one, was not so large as in the case of proteasome inhibition. We investigated if the ERAD-associated ubiquitin ligase Hrd1 was involved in ubiquitination of sec-2A. A previous work in yeast concluded it was not (Crowder et al., 2015). Our results, however, suggest that Hrd1 may be implicated in 2A poly-ubiquitination. We can't even exclude the enrolment of other E3 ligases of the ERAD pathway because, particularly in mammals, several ubiquitin ligases have been identified and they can display interconnected or even overlapping activities (Yoshida and Tanaka, 2010).

We also found that the AAA ATPase VCP/p97 and its associated deubiquitinase YOD1 were important for degradation of polypeptides generated from ribosomes stalled at the ER-membrane. They are well-known players of ERAD, in particular during the retro-translocation step of the luminal misfolded/unfolded substrates. However, while p97 was already described to be involved also in degradation of peptides stalled on free ribosomes (Defenouillère et al., 2013; Verma et al., 2013), this is the first time that it is reported to play a fundamental role in degradation of polypeptides generated by ER-bound stalled ribosomes. Moreover, we also found engagement of the ERAD-specific deubiquitinase YOD1 in the case of stalling at the STOP-codon. These results also suggested that 2A-tagged proteins are ERAD clients.

2A-tagged polypeptides translated by free ribosomes share a degradation pathway similar to that described for other proteins generated by ribosomes stalled because of poly(A) translation or from trunked mRNAs, namely involving the E3 ubiquitin ligase Listerin, the ATPase VCP/p97 and the proteasome. This indicates that the stalling at the STOP-codon induces a clearance mechanism similar to other types of ribosomal stalling described in eukaryotes.

ER-targeted 2A proteins are substrates of the ER-associated degradation

Because of the similarities between the 2A-induce stalling at the STOP-codon and other models of stalling, in the second part of our research we focused on the study of the degradation pathway of 2A products derived from ribosomes stalled at the ER membrane, a mechanism still poorly investigated.

To understand if they are targeted to ERAD, we first wanted to prove that 2A peptides were fully inserted in the ER and then retro-translocated, which was hardworking, because it implied that we should mark reporters strictly inside the ER to distinguish them from those in the cytosol that are targeted to the proteasome. We tried several approaches: the *in vivo* biotinylation, TEVp cleavage and N-glycosylation of 2A reporter proteins specifically engineered with the appropriate tag (BAP for *in vivo* biotinylation, TS for TEVp cleavage and NGT as a N-glycosylation site). Most of the 2A reporters were efficiently labelled with biotin by a secretory active BirA or cleaved by a TEV protease active in the ER lumen. These assays gave us strong indications that 2A proteins derived from stalling at the STOP-codon were in fact inside the lumen. Unfortunately, their enzymatic activity was not completely ER-restricted, and they were slightly active also on cytosolic side.

N-glycosylation, which is a widely used system to prove ER localization of the protein of interest, in the case of 2A-tagged proteins was not completely helpful, because reporters were glycosylated only partially, independently of the N-glycosylation site position. 2A-P controls were instead fully glycosylated, indicating that the sites used were accessible to glycosylating enzymes. However, previous works reported that products of ER-stalled ribosomes were efficiently N-glycosylated in yeast (Crowder et al., 2015; Izawa et al., 2012). Both the glycosylated and non-glycosylated variants were efficiently cleaved by ER-active TEVp, indicating they are both in the ER lumen and suggesting an impairment of N-glycosylation for 2A substrates. We also found in following experiments that almost all the non-glycosylated fraction and part of the glycosylated one were also biotinylated by cytosolic BirA and processed by cytosolic TEVp, indicating their exposure to the cytosolic side and therefore to the ERAD N-glycanase NGLY1. This theory was consistent also with accumulation of the non-glycosylated products under proteasome inhibition. Hence, it wasn't clear if non-glycosylated bands were represented by proteins deglycosylated or

never glycosylated. For this reason, we create a HEK-293T stable cell line defective of NGLY1. This cell line was mutated in the genomic DNA with the CRISPR-Cas9 technology (Cong et al., 2013), to deplete the region that transcribes for exon 3 to 6 of NGLY1. Deletion was verified by RT-PCR and sequencing of the fragments obtained. The loss of function was tested indirectly by expression of some glycosylated ERAD substrates, which were no more deglycosylated. However, we didn't check directly for NGLY1 expression.

By the use of this cell line with non-functional NGLY1, we found that a significative fraction of 2A non-glycosylated proteins resulted from retro-translocation, while a minor part of them seems to be never glycosylated. We reasoned that the possible explanations can be (i) inefficient N-glycosylation or (ii) inefficient insertion of 2A proteins in the ER. However, *in vitro* expression of ER-targeted 2A reporters revealed that all the proteins were inside the microsomes and protected from a biotinylation assay, and this observation is enforced also by the TEVp cleavage assay, thus suggesting that products resulted from stalling at the ER are not efficiently N-glycosylated. However, further experiments should be done, with different reporter glycoproteins, to confirm this hypothesis.

An interesting advantage of using an *in vitro* system of translation of ER proteins is that ERAD is not active. Thus, the complete absence of 2A proteins in the cytosolic fraction of HeLa cell lysates was an indirect indication that the amount of 2A proteins found in the cytosol of living cells derived from retro-translocation. In fact, ER-targeted 2A proteins were accessible *in vivo* to both cyt-BirA and cyt-TEVp and the two disulphide bridges of the scFv reporter were mostly reduced, meaning they are dislocated from the ER lumen to the cytosolic side. This was restricted to 2A-tagged proteins, as 2A-P were predominantly found in the lumen, with folded disulphide bridges and barely biotinylated or processed by cytosolic enzymes, in line with our previous data that demonstrated that its rate of degradation is extremely low, because is normally translated and secreted.

Moreover, the *in vivo* biotinylation technique and the reducing state of the scFv allowed us to determine the fraction of 2A reporters that was retro-translocated, which was the major part, indicating that these products of stalled ribosome are efficiently engaged into the retro-translocation pathway.

Our next step was to analyse the involvement of poly-ubiquitination, p97 and proteasome in 2A protein extraction from the ER membrane. In fact, they have been described to play different roles, depending on the type of ERAD substrate (Sasset et al., 2015). For example, p97 was essential for retro-translocation of MHC class-Iα and CD4, but not of immunoglobulin κ light chain NS1, Null Hong Kong mutant of the α1 anti-trypsin or BST-2/Tetherin. We used the *in vivo* biotinylation to see whether their impairment induced accumulation of 2A in the ER lumen or in the cytosol and we found that neither poly-ubiquitination nor p97 or proteasome were involved in protein exposure from the ER, because 2A proteins accumulated in the cytosol and were biotinylated. These findings indicate that in this case, they participate downstream of the retro-translocation step. However, initial steps of ubiquitination may be required to initiate substrates retro-translocation and experiments with OTU are not enough to understand this point.

Collectively, our results support the hypothesis that polypeptides derived from ER-bound ribosomes stalled at the STOP-codon are disposed of by ERAD. Moreover, they are well-discriminated from the identical reporters produced by non-conventional termination, thus suggesting that ERAD targeting has a broader activity of substrates that does not depend only on misfolded proteins but could include also folded clients recruited because originating from stalled ribosomes.

Identification of proteins involved in 2A polypeptides degradation

In the following part of the thesis, we looked for identification of other proteins possibly involved in 2A-tagged protein degradation. The most successful approach was the proximity-dependent Biotin Identification (BioID) method, which consisted in the *in vivo* expression of the biotin ligase from *A. aeolicus* (BioID2) bearing mutation R40G to abrogate its specificity and allow biotin labelling of interacting proteins (Kim et al., 2016). We expressed this promiscuous biotin ligase tailed with 2A at its C-terminus and it labelled three different proteins, which were not detected by the same ligase tagged with 2A-P. Mass spectrometry of the whole biotinylated pulled-down proteins identified three proteins as well, with molecular masses comparable to what observed by western blotting: the 78 kDa ER chaperone BiP/GRP78, the 71 kDa cytosolic chaperone HSPA8 and the 23

kDa nascent polypeptide-associated complex α-subunit (NACA). We confirmed that the band observed in western blot was BiP/GRP78 by immunoprecipitation of endogenous BiP, a fraction of which was biotinylated in presence on 2A-tagged biotin ligase and not in controls, and by BiP identification in pull-down of biotinylated proteins.

Overexpression of wild type BiP induced an increment in scFv 2A reporter expression, probably because it favoured its stability or helped in the Sec61 translocon clearance. A BiP dominant negative mutant fully retained 2A proteins within the ER lumen and favoured also their N-glycosylation. We reasoned that BiP/GRP78 can be recruited (i) by the prolonged occupation of the translocon by the 2A polypeptides stalled with the ribosome on the cytosolic side and/or (ii) because stalled polypeptides are not able to complete folding. However, BioID2 was functional inside the ER lumen, as it labelled with biotin BiP/GRP78 and itself, suggesting that it was properly folded. Furthermore, secretory scFv bearing C-terminal 2A-P are secreted: considering that they differ from 2A reporters only for the terminal Pro-codon that allows non-conventional termination, we can reasonably think that also 2A-tagged proteins are able to acquire the proper folding. Moreover, in previous works non-stop stalled proteins are reported to remain blocked in the translocon in yeast (Izawa et al., 2012) and to precipitate with the Sec61 translocon in mammals (Malsburg et al., 2015). Consequently, BiP/GRP78 is probably recruited by translocon occupancy of 2A products rather than by their misfolding.

Being BiP/GRP78 one of the major interactors of 2A proteins resulted from stalling, we hypothesise that it can be involved in their targeting to ERAD. One previous work suggested, instead of ERAD, a back-sliding movement through the translocon of stalled proteins to extract them and allow their ubiquitination (Malsburg et al., 2015). However, our findings strongly suggest that ERAD is activated for 2A peptides and extraction from the translocon from the cytosolic side is unlikely, in particular for glycosylated substrates, because the translocon channel width will not allow the passage of a glycosylated protein. In addition, it was also demonstrated for other ERAD substrates that they can retro-translocate in a rather folded structure (Fiebiger et al., 2002; Petris et al., 2014b; Rapoport, 2007; Tirosh et al., 2003).

Interestingly, BioID2 labelled with biotin also NACA, which is part of the co-translational quality control machinery associated to ribosomes. NACA is described to participate in

translational targeting to the ER and protects nascent proteins from the cytosolic environment during translation in the translocon (Beatrix et al., 2000; Wiedmann et al., 1994; Zhang et al., 2012). These observations suggest that this complex may be also involved in interactions with the polypeptide during translation or during or after retro-translocation. However, this must be confirmed with more targeted experiments.
The third protein identified by mass spectrometry is the cytosolic HSPA8, a member of the HSC70 chaperone family, that is reported to have multiple functions important for cell survival, including protein folding and post-translational import to the ER (Stricher et al., 2013). However, its role in ribosome stalling must be further investigated.

We noticed that BioID2 did not label cytosolic proteins like p97, YOD1 or Listerin that we know to be involved in 2A protein degradation. A possible explanation is that ERAD substrates can be partially misfolded during or after retro-translocation, also because of poly-ubiquitination, so BioID2 may have lost its activity. This indicate that the proximity labelling cannot be the proper method to identified other cytosolic players of the 2A degradation pathway. For this reason, we also performed proteins separation by ultracentrifugation on sucrose gradients, to try to identify other proteins that can form a complex with 2A polypeptides, like the components of the Ribosome Quality Control pathway. We found that secretory 2A reporter was mostly in fractions corresponding to the top of the gradient, compatible with soluble proteins, and coherent with our previous observations that the 2A proteins are hydrolysed and probably released from the ribosome. However, upon treatment with proteasome inhibitors, some 2A proteins were found also in other fractions closer to the bottom of the gradient, indicating they are aggregated or in complex with other proteins. Although these fractions are not the most represented, it would be interesting to analyse them to see if some 2A proteins remain associated to the 80S ribosome or to the split 60S subunit and to look for the presence of proteins of the RQC or eRF1, which we already hypothesised to be involved.

Effect of non-viral C-terminal sequences on protein expression

Over the past years, the idea that ribosome translational stalling represents a mechanism to control protein expression at the translation level has become more widespread. In fact,

there are several examples of small coding sequences, the upstream ORFs (uORF), present in the 5' untranslated regions of mRNAs, that can regulate translation initiation of the downstream principal ORF inducing stalling of the ribosomes, probably because of amino acid interactions with the RET (Re et al., 2016; Wilson et al., 2016; Yan et al., 2010). Some of them, like hCMV uORF2 of the UL4 gene, have been reported to occur also on a termination codon (Cao and Geballe, 1996a; Yamashita et al., 2017). Moreover, a recent work demonstrated that an independent ORF located in the 3' UTR of mRNA coding for protein AMD1/AdoMetDC, namely downstream the principal ORF, was able to regulate AMD1 translation because ribosomes readthrough the canonical STOP-codon of AMD1 and then form a queue on the following stalling sequence (Yordanova et al., 2018).

Our model based on peptide 2A, however, differs from the previous ones because it regulates expression of an entire protein translated upstream and in the same ORF, indicating that some C-terminal sequences can also work as translational regulatory motifs. To investigate this hypothesis, we reasoned that being the NPG sequence of 2A so well-conserved in viruses, we could find other peptides terminating similarly in NPG that could induce translational stalling at the STOP-codon in humans. Bioinformatic analysis performed against the human protein database Ensembl identified as ending in NPG the products of alternatively spliced FAM134C, CD99L2, POTE family members E and I, SPIRE2 and TBCA, and FCAMR as ending with NPGP. We tested the effect on protein expression in living cells engineering only the C-termini of the proteins identified and two of them, POTE and CD99L2, showed stalling activity on both free and ER-bound ribosomes. Translation of the reporter proteins was partially rescued when a Proline was introduced before the STOP-codon, in a similar way to 2A, confirming that also CD99L2 and POTE C-termini cause stalling of ribosomes at the STOP-codon. However, when the cytosolic constructs were expressed in *in vitro* system, they didn't show the same effect on translation as 2A and the presence of the terminal Proline didn't have any influence. Nevertheless, we must consider that the reduction in protein expression induced in living cells by POTE or CD99L2 is not of the same extent as 2A. Moreover, the difference in reporter proteins expression between 2A and 2A-P is reduced of 10-fold *in vitro* than in living cells. Consequently, the differences observed *in vivo* can be not evident in the *in vitro* system used.

More important, both POTE and CD99L2 sequences induced degradation of the secretory reporter through the proteasome pathway, as the reporter proteins accumulated upon

proteasome inhibition or p97 and ubiquitination impairment. This similarity to the 2A model indicates that they also activate degradation of the associated proteins through the ERAD pathway.

Based on our observations, we propose that stalling events on STOP-codon could represent a regulatory mechanism for protein expression in mammalian cells, even though they are difficult to detect, and they can depend on sequences completely different in their amino acid compositions. In fact, 2A, CD99L2 and POTE share only the last 3 amino acids, but those translated immediately upstream, which are still inside the RET, can be influent as well.

On the contrary, the analysis of the activity of the polypeptide derived from the 3' UTR of AMD1 (C-tail), which terminates in RPH and not NPG, showed a mechanism of ribosome stalling different from 2A, with no dependence on the termination codon and no rescue of expression by adding a terminal Pro. We observed a partial reduction of C-tail effect by removing the last two amino acids (PH), suggesting they role in causing ribosome stalling. However, in this case the reduction in protein expression did not result in a high rate of targeting to proteasome degradation, as the polypeptide chain was less sensitive to impairment of proteasome, poly-ubiquitination or p97 than 2A-, CD99L2- or POTE-tagged reporters. A possible explanation is that this sequence induces instead mRNA decay, strongly reducing the amount of protein synthesised; or these data may suggest a mechanism of protein co-translation quality control different also from what commonly described for peptides derived from ribosome stalled on mRNAs lacking a termination codon, whose proteasome degradation require poly-ubiquitination and p97 ATPase activity (Bengtson and Joazeiro, 2010; Brandman et al., 2012). This is a very interesting hypothesis and require further investigations.

We also analysed whether POTE or C-tail gain the non-conventional termination activity as peptide 2A, when the Proline is inserted immediately after NPG or RPH, respectively. The results obtained, however, showed that both of them terminate by conventional translation termination. This is not surprising, because peptides 2A are highly conserved and mutations occurring within their sequences completely abrogate the self-termination activity (Sharma et al., 2012).

Conclusions

We demonstrated that imposing conventional termination after peptide 2A induces ribosome stalling in a STOP-codon-dependent manner in mammals and nascent chains originating from these ribosomes are degraded. We investigated particularly the mechanism of degradation of those proteins that are targeted for translation in the secretory pathway. We found that they are fully translated inside the ER lumen, but they are not secreted. They are instead engaged by the ER chaperone BiP/GRP78 that is candidate to trigger their ER-associated degradation. We have indications that 2A-derived proteins are not misfolded, so we speculate that ERAD has the ability to eliminate a wider range of proteins than what previously thought. How 2A proteins, as other ERAD substrates, retro-translocate to the cytosolic side remains still unclear. Once 2A proteins reach the cytosol, they are poly-ubiquitinated and the E3 ubiquitin ligase Listerin takes part to this process, but we do not exclude the involvement of other ubiquitin ligases of the ERAD pathway. Poly-ubiquitination, the ATPasic activity of p97 and its deubiquitinase YOD1 are then fundamental to promote 2A substrates degradation *via* the proteasome.
The model we proposed for degradation of peptide chains originated by ER stalled ribosome is represented in Figure 75, but it requires more experiments to answer all the open questions previously discussed.

Based on the C-terminal sequence of 2A, we also identified two human proteins, resulting from alternative splicing, terminating with same NPG amino acids that cause stalling at the STOP-codon. This suggests that ribosome stalling at the termination codon could affect a broad number of translational products, also terminating with amino acidic sequences diverse from NPG, thus representing a mechanism of post-translational control of the proteome.

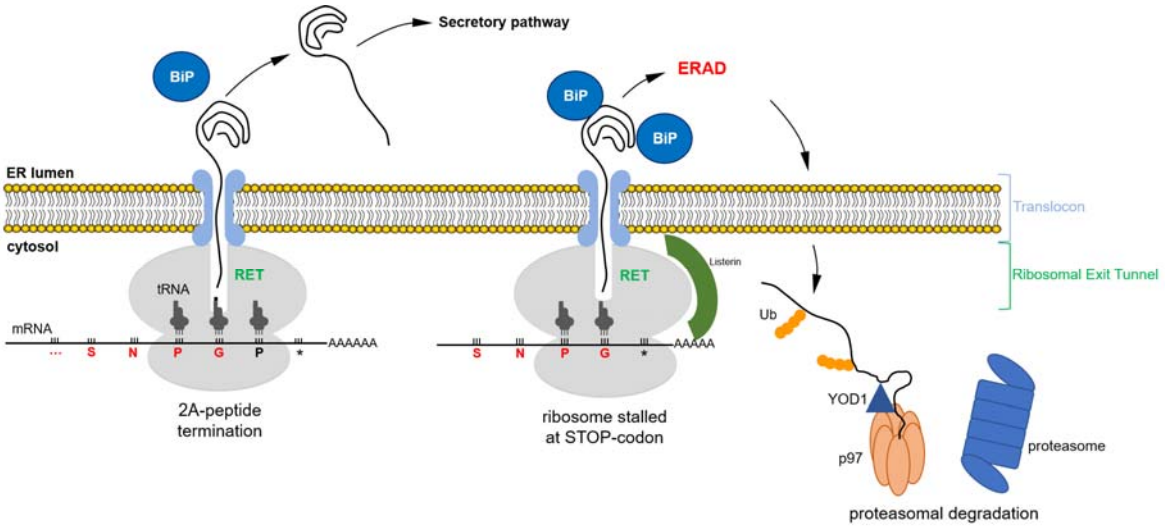

Figure 75. 2A-tagged proteins resulted from ribosomes stalled at the ER membrane are recognised by BiP/GRP78 and targeted for ERAD retro-translocation, while the same reporter tagged instead with 2A-P follows the secretory pathway. When 2A are exposed to the cytosolic side, poly-ubiquitination, p97 and YOD1 promote proteasomal degradation.

ACKNOWLEDGEMENTS

Experiments on characterisation of STOP-codon-dependant stalling and degradation pathway of the associated polypeptides were performed by collaboration with Dr Linda Sasset. Dr Gianluca Petris (CIBIO, University of Trento) contributed in the validation of TEVp system and with suggestions for the 2A project. Dr Michael P. Myers (ICGEB) performed Mass spectrometry and Dr Angela Re (CIBIO, University of Trento) the bioinformatic analysis.

CCHFV-L OTU plasmid was kindly provided by Adolfo García-Sastre, the N-terminal FLAG-tagged human and YOD-C160S plasmids by Christian Schlieker, the His6-tagged rat p97QQ and Myc-tagged Hrd1 C291S plasmids by Linda Hendershot.

BIBLIOGRAPHY

Aebi, M., Bernasconi, R., Clerc, S., Molinari, M., 2010. N-glycan structures: recognition and processing in the ER. Trends Biochem. Sci. 35, 74–82. doi:10.1016/j.tibs.2009.10.001

Alkalaeva, E.Z., Pisarev, A. V., Frolova, L.Y., Kisselev, L.L., Pestova, T. V., 2006. In Vitro Reconstitution of Eukaryotic Translation Reveals Cooperativity between Release Factors eRF1 and eRF3. Cell 125, 1125–1136. doi:10.1016/j.cell.2006.04.035

Aly, H.H., Suzuki, J., Watashi, K., Chayama, K., Hoshino, S.-I., Hijikata, M., Kato, T., Wakita, T., 2016. RNA Exosome Complex Regulates Stability of the Hepatitis B Virus X-mRNA Transcript in a Non-stop-mediated (NSD) RNA Quality Control Mechanism. J. Biol. Chem. 291, 15958–74. doi:10.1074/jbc.M116.724641

Amrani, N., Ganesan, R., Kervestin, S., Mangus, D.A., Ghosh, S., Jacobson, A., 2004. A faux 3'-UTR promotes aberrant termination and triggers nonsense-mediated mRNA decay. Nature 432, 112–8. doi:10.1038/nature03060

Arakawa, S., Yunoki, K., Izawa, T., Tamura, Y., Nishikawa, S.I., Endo, T., 2016. Quality control of nonstop membrane proteins at the ER membrane and in the cytosol. Sci. Rep. 6. doi:10.1038/srep30795

Aridor, M., 2007. Visiting the ER: The endoplasmic reticulum as a target for therapeutics in traffic related diseases. Adv. Drug Deliv. Rev. 59, 759–781. doi:10.1016/j.addr.2007.06.002

Awad, W., Estrada, I., Shen, Y., Hendershot, L.M., 2008. BiP mutants that are unable to interact with endoplasmic reticulum DnaJ proteins provide insights into interdomain interactions in BiP. Proc. Natl. Acad. Sci. U. S. A. 105, 1164–1169. doi:10.1073/pnas.0702132105

Baboshina, O. V, Haas, A.L., 1996. Novel multiubiquitin chain linkages catalyzed by the conjugating enzymes E2EPF and RAD6 are recognized by 26 S proteasome subunit 5. J. Biol. Chem. 271, 2823–31.

Bagola, K., Mehnert, M., Jarosch, E., Sommer, T., 2011. Protein dislocation from the ER. Biochim. Biophys. Acta - Biomembr. 1808, 925–936. doi:10.1016/j.bbamem.2010.06.025

Baldridge, R.D., Rapoport, T.A., 2016. Autoubiquitination of the Hrd1 Ligase Triggers Protein Retrotranslocation in ERAD. Cell 166, 1–14. doi:10.1016/j.cell.2016.05.048

Ballar, P., Shen, Y., Yang, H., Fang, S., 2006. The role of a novel p97/valosin-containing protein-interacting motif of gp78 in endoplasmic reticulum-associated degradation. J. Biol. Chem. 281, 35359–68. doi:10.1074/jbc.M603355200

Beatrix, B., Sakai, H., Wiedmann, M., 2000. The alpha and beta subunit of the nascent polypeptide-associated complex have distinct functions. J. Biol. Chem. 275, 37838–45. doi:10.1074/jbc.M006368200

Beckett, D., Kovaleva, E., Schatz, P.J., 2008. A minimal peptide substrate in biotin holoenzyme synthetase-catalyzed biotinylation. Protein Sci. 8, 921–929. doi:10.1110/ps.8.4.921

Bengtson, M.H., Joazeiro, C.A.P., 2010. Role of a ribosome-associated E3 ubiquitin ligase in protein quality control. Nature 467, 470–473. doi:10.1038/nature09371

Berg, B. van den, Clemons, W.M., Collinson, I., Modis, Y., Hartmann, E., Harrison, S.C., Rapoport, T.A., 2004. X-ray structure of a protein-conducting channel. Nature 427, 36–44. doi:10.1038/nature02218

Bernardi, K.M., Forster, M.L., Lencer, W.I., Tsai, B., 2008. Derlin-1 facilitates the retro-translocation of cholera toxin. Mol. Biol. Cell 19, 877–84. doi:10.1091/mbc.E07-08-0755

Bernardi, K.M., Williams, J.M., Inoue, T., Schultz, A., Tsai, B., 2013. A deubiquitinase negatively regulates retro-translocation of nonubiquitinated substrates. Mol. Biol. Cell 24, 3545–3556. doi:10.1091/mbc.E13-06-0332

Bestagno, M., Sola, I., Dallegno, E., Sabella, P., Poggianella, M., Plana-Duran, J., Enjuanes, L., Burrone, O.R., 2007. Recombinant dimeric small immunoproteins neutralize transmissible gastroenteritis virus infectivity efficiently in vitro and confer passive immunity in vivo. J. Gen. Virol. 88, 187–195. doi:10.1099/vir.0.82192-0

Bhushan, S., Meyer, H., Starosta, A.L., Becker, T., Mielke, T., Berninghausen, O., Sattler, M., Wilson, D.N., Beckmann, R., 2010. Structural basis for translational stalling by human cytomegalovirus and fungal arginine attenuator peptide. Mol. Cell 40, 138–46. doi:10.1016/j.molcel.2010.09.009

Borissenko, L., Groll, M., 2007. 20S proteasome and its inhibitors: crystallographic knowledge for drug development. Chem. Rev. 107, 687–717. doi:10.1021/cr0502504

Brandman, O., Hegde, R.S., 2016. Ribosome-associated protein quality control. Nat. Struct. Mol. Biol. 23, 7–15. doi:10.1038/nsmb.3147

Brandman, O., Stewart-Ornstein, J., Wong, D., Larson, A., Williams, C.C., Li, G.-W., Zhou, S., King, D., Shen, P.S., Weibezahn, J., Dunn, J.G., Rouskin, S., Inada, T., Frost, A., Weissman, J.S., 2012. A ribosome-bound quality control complex triggers degradation of nascent peptides and signals translation stress. Cell 151, 1042–54. doi:10.1016/j.cell.2012.10.044

Cao, J., Geballe, A.P., 1996a. Inhibition of nascent-peptide release at translation termination. Mol. Cell. Biol. 16, 7109–14.

Cao, J., Geballe, A.P., 1996b. Coding sequence-dependent ribosomal arrest at termination of translation. Mol. Cell. Biol. 16, 603–608. doi:10.1128/MCB.16.2.603

Capodagli, G.C., Mckercher, M.A., Baker, E.A., Masters, E.M., Brunzelle, J.S., Pegan, S.D., 2011. Structural Analysis of a Viral Ovarian Tumor Domain Protease from the Crimean-Congo Hemorrhagic Fever Virus in Complex with Covalently Bonded Ubiquitin 85, 3621–3630. doi:10.1128/JVI.02496-10

Carvalho, P., Goder, V., Rapoport, T.A., 2006. Distinct Ubiquitin-Ligase Complexes Define Convergent Pathways for the Degradation of ER Proteins. Cell 126, 361–373. doi:10.1016/j.cell.2006.05.043

Cesaratto, F., Burrone, O.R., Petris, G., 2016. Tobacco Etch Virus protease: a shortcut across biotechnologies. J. Biotechnol. doi:10.1016/j.jbiotec.2016.06.012

Cesaratto, F., López-Requena, A., Burrone, O.R., Petris, G., 2015. Engineered tobacco etch virus (TEV) protease active in the secretory pathway of mammalian cells. J. Biotechnol. 212, 159–66. doi:10.1016/j.jbiotec.2015.08.026

Chang, Y.-F., Imam, J.S., Wilkinson, M.F., 2007. The nonsense-mediated decay RNA surveillance pathway. Annu. Rev. Biochem. 76, 51–74. doi:10.1146/annurev.biochem.76.050106.093909

Chapman-Smith, A., Cronan, J.E., 1999. In vivo enzymatic protein biotinylation. Biomol. Eng. 16, 119–125. doi:10.1016/S1050-3862(99)00046-7

Chau, V., Tobias, J.W., Bachmair, A., Marriott, D., Ecker, D.J., Gonda, D.K., Varshavsky, A., 1989. A multiubiquitin chain is confined to specific lysine in a targeted short-lived protein. Science 243, 1576–83.

Chen, L., Muhlrad, D., Hauryliuk, V., Cheng, Z., Lim, M.K., Shyp, V., Parker, R., Song, H., 2010. Structure of the Dom34-Hbs1 complex and implications for no-go decay. Nat. Struct. Mol. Biol. 17, 1233–40. doi:10.1038/nsmb.1922

Cheng, Z., Saito, K., Pisarev, A. V., Wada, M., Pisareva, V.P., Pestova, T. V., Gajda, M., Round, A., Kong, C., Lim, M., Nakamura, Y., Svergun, D.I., Ito, K., Song, H., 2009. Structural insights into eRF3 and stop codon recognition by eRF1. Genes Dev. 23, 1106–1118. doi:10.1101/gad.1770109

Choi-Rhee, E., Schulman, H., Cronan, J.E., 2004. Promiscuous protein biotinylation by Escherichia coli biotin protein ligase. Protein Sci. doi:10.1110/ps.04911804

Christianson, J.C., Shaler, T.A., Tyler, R.E., Kopito, R.R., 2008. OS-9 and GRP94 deliver mutant alpha1-antitrypsin to the Hrd1-SEL1L ubiquitin ligase complex for ERAD. Nat. Cell Biol. 10, 272–82. doi:10.1038/ncb1689

Chu, J., Hong, N.A., Masuda, C.A., Jenkins, B. V, Nelms, K.A., Goodnow, C.C., Glynne, R.J., Wu, H., Masliah, E., Joazeiro, C.A.P., Kay, S.A., 2009. A mouse forward genetics screen identifies LISTERIN as an E3 ubiquitin ligase involved in neurodegeneration. Proc. Natl. Acad. Sci. U. S. A. 106, 2097–2103. doi:10.1073/pnas.0812819106

Cong, L., Ran, F.A., Cox, D., Lin, S., Barretto, R., Habib, N., Hsu, P.D., Wu, X., Jiang, W., Marraffini, L.A., Zhang, F., 2013. Multiplex Genome Engineering Using CRISPR/Cas Systems. Science (80-.). 339, 819–823. doi:10.1126/science.1231143

Cronan Jr., J.E., 1990. Biotination of Proteins in Vivo. J. Biol. Chem. 265, 10327–10333.

Crowder, J.J., Geigges, M., Gibson, R.T., Fults, E.S., Buchanan, B.W., Sachs, N., Schink, A., Kreft, S.G., Rubenstein, E.M., 2015. Rkr1/Ltn1 ubiquitin ligase-mediated degradation of translationally stalled endoplasmic reticulum proteins. J. Biol. Chem. 290, 18454–18466. doi:10.1074/jbc.M115.663559

de Virgilio, M., Weninger, H., Ivessa, N.E., 1998. Ubiquitination is required for the retro-translocation of a short-lived luminal endoplasmic reticulum glycoprotein to the cytosol for degradation by the proteasome. J. Biol. Chem. 273, 9734–43.

Defenouillère, Q., Yao, Y., Mouaikel, J., Namane, A., Galopier, A., Decourty, L., Doyen, A., Malabat, C., Saveanu, C., Jacquier, A., Fromont-Racine, M., 2013. Cdc48-associated complex bound to 60S particles is required for the clearance of aberrant translation products. Proc. Natl. Acad. Sci. U. S. A. 110 VN-, 5046–5051. doi:10.1073/pnas.1221724110

Dever, T.E., Green, R., 2012. The Elongation, Termination, and Recycling Phases of Translation in Eukaryotes. Cold Spring Harb. Perspect. Biol. 4(7), 1–16.

Díaz-Villanueva, J., Díaz-Molina, R., García-González, V., 2015. Protein Folding and Mechanisms of Proteostasis. Int. J. Mol. Sci. 16, 17193–17230. doi:10.3390/ijms160817193

Dimitrova, L.N., Kuroha, K., Tatematsu, T., Inada, T., 2009. Nascent peptide-dependent translation arrest leads to Not4p-mediated protein degradation by the proteasome. J. Biol. Chem. 284, 10343–10352. doi:10.1074/jbc.M808840200

Doma, M.K., Parker, R., 2006. Endonucleolytic cleavage of eukaryotic mRNAs with stalls in translation elongation. Nature 440, 561–4. doi:10.1038/nature04530

Donnelly, M.L., Gani, D., Flint, M., Monaghan, S., Ryan, M.D., 1997. The cleavage activities of aphthovirus and cardiovirus 2A proteins. J. Gen. Virol. 78 (Pt 1), 13–21. doi:10.1099/0022-1317-78-1-13

Donnelly, M.L., Hughes, L.E., Luke, G., Mendoza, H., ten Dam, E., Gani, D., Ryan, M.D., 2001a. The "cleavage" activities of foot-and-mouth disease virus 2A site-directed mutants and naturally occurring "2A-like" sequences. J. Gen. Virol. 82, 1027–41. doi:10.1099/0022-1317-82-5-1027

Donnelly, M.L., Luke, G., Mehrotra, A., Li, X., Hughes, L.E., Gani, D., Ryan, M.D., 2001b. Analysis of the aphthovirus 2A/2B polyprotein "cleavage" mechanism indicates not a proteolytic reaction, but a novel translational effect: a putative ribosomal "skip". J. Gen. Virol. 82, 1013–25. doi:10.1099/0022-1317-82-5-1013

Doronina, V.A., de Felipe, P., Wu, C., Sharma, P., Sachs, M.S., Ryan, M.D., Brown, J.D., 2008a. Dissection of a co-translational nascent chain separation event. Biochem. Soc. Trans. 36, 712–716. doi:10.1042/BST0360712

Doronina, V.A., Wu, C., de Felipe, P., Sachs, M.S., Ryan, M.D., Brown, J.D., 2008b. Site-specific release of nascent chains from ribosomes at a sense codon. Mol. Cell. Biol. 28 VN-r, 4227–4239. doi:10.1128/MCB.00421-08

Dougherty, W.G., Carrington, J.C., Cary, S.M., Parks, T.D., 1988. Biochemical and mutational analysis of a plant virus polyprotein cleavage site. EMBO J. 7, 1281–1287.

Dougherty, W.G., Parks, T.D., 1991. Post-translational processing of the tobacco etch virus 49-kDa small nuclear inclusion polyprotein: identification of an internal cleavage site and delimitation of VPg and proteinase domains. Virology 183, 449–56.

Ellgaard, L., Helenius, A., 2003. Quality control in the endoplasmic reticulum. Nat. Rev. Mol. Cell Biol. 4, 181–91. doi:10.1038/nrm1052

Enns, G.M., Shashi, V., Bainbridge, M., Gambello, M.J., Zahir, F.R., Bast, T., Crimian, R., Schoch, K., Platt, J., Cox, R., Bernstein, J. a, Scavina, M., Walter, R.S., Bibb, A., Jones, M., Hegde, M., Graham, B.H., Need, A.C., Oviedo, A., Schaaf, C.P., Boyle, S., Butte, A.J., Chen, R., Clark, M.J., Haraksingh, R., Cowan, T.M., He, P., Langlois, S., Zoghbi, H.Y., Snyder, M., Gibbs, R. a, Freeze, H.H., Goldstein, D.B., 2014. Mutations in NGLY1 cause an inherited disorder of the endoplasmic reticulum-associated degradation pathway. Genet. Med. 16, 1–8. doi:10.1038/gim.2014.22

Ernst, R., Mueller, B., Ploegh, H.L., Schlieker, C., 2009. The Otubain YOD1 Is a Deubiquitinating Enzyme that Associates with p97 to Facilitate Protein Dislocation from the ER. Mol. Cell 36, 28–38. doi:10.1016/j.molcel.2009.09.016

Ewart, G.D., Sutherland, T., Gage, P.W., Cox, G.B., 1996. The Vpu protein of human immunodeficiency virus type 1 forms cation-selective ion channels. J. Virol. 70, 7108–15.

Fei, W., Wang, H., Fu, X., Bielby, C., Yang, H., 2009. Conditions of endoplasmic reticulum stress stimulate lipid droplet formation in Saccharomyces cerevisiae. Biochem. J. 424, 61–7. doi:10.1042/BJ20090785

Fiebiger, E., Story, C., Ploegh, H.L., Tortorella, D., 2002. Visualization of the ER-to-cytosol dislocation reaction of a type I membrane protein. EMBO J. 21, 1041–1053. doi:10.1093/emboj/21.5.1041

Finley, D., 2009. Recognition and processing of ubiquitin-protein conjugates by the proteasome. Annu. Rev. Biochem. 78, 477–513. doi:10.1146/annurev.biochem.78.081507.101607

Fisher, E.A., Ginsberg, H.N., 2002. Complexity in the secretory pathway: the assembly and secretion of apolipoprotein B-containing lipoproteins. J. Biol. Chem. 277, 17377–80. doi:10.1074/jbc.R100068200

Flierman, D., Ye, Y., Dai, M., Chau, V., Rapoport, T.A., 2003. Polyubiquitin serves as a recognition signal, rather than a ratcheting molecule, during retrotranslocation of proteins across the endoplasmic reticulum membrane. J. Biol. Chem. 278, 34774–82. doi:10.1074/jbc.M303360200

Frias-staheli, N., Giannakopoulos, N. V, Kikkert, M., Shannon, L., Bridgen, A., Paragas, J.J., Richt, J.A., Rowland, R.R., Schmaljohn, C.S., Lenschow, D.J., Snijder, E.J., García-, A., 2007. Ovarian Tumor (OTU)-domain Containing Viral Proteases Evade Ubiquitin- and ISG15-dependent Innate Immune Responses 2, 404–416.

Gebauer, F., Hentze, M.W., 2004. Molecular mechanisms of translational control. Nat. Rev. Mol. Cell Biol. 5, 827–835. doi:10.1038/nrm1488

Glickman, M.H., Rubin, D.M., Fried, V.A., Finley, D., 1998. The regulatory particle of the Saccharomyces cerevisiae proteasome. Mol. Cell. Biol. 18, 3149–62.

Goder, V., Carvalho, P., Rapoport, T.A., 2008. The ER-associated degradation component Der1p and its homolog Dfm1p are contained in complexes with distinct cofactors of the ATPase Cdc48p. FEBS Lett. 582, 1575–1580. doi:10.1016/j.febslet.2008.03.056

Graille, M., Chaillet, M., van Tilbeurgh, H., 2008. Structure of Yeast Dom34: a Protein related to Translation Termination Factor eRF1 and involved in No-Go Decay. J. Biol. Chem. 283, 7145–7154. doi:10.1074/jbc.M708224200

Graille, M., Séraphin, B., 2012. Surveillance pathways rescuing eukaryotic ribosomes lost in translation. Nat. Rev. Mol. Cell Biol. 13, 727–35. doi:10.1038/nrm3457

Greenblatt, E.J., Olzmann, J.A., Kopito, R.R., 2011. Derlin-1 is a rhomboid pseudoprotease required for the dislocation of mutant α-1 antitrypsin from the endoplasmic reticulum., Nature structural & molecular biology. doi:10.1038/nsmb.2111

Groll, M., Bajorek, M., Köhler, A., Moroder, L., Rubin, D.M., Huber, R., Glickman, M.H., Finley, D., 2000. A gated channel into the proteasome core particle. Nat. Struct. Biol. 7, 1062–7. doi:10.1038/80992

Halawani, D., Latterich, M., 2006. p97: The Cell's Molecular Purgatory? Mol. Cell 22, 713–717. doi:10.1016/j.molcel.2006.06.003

Harding, H.P., Zhang, Y., Bertolotti, A., Zeng, H., Ron, D., 2000. Perk is essential for translational regulation and cell survival during the unfolded protein response. Mol. Cell. doi:10.1016/S1097-2765(00)80330-5

Hirao, K., Natsuka, Y., Tamura, T., Wada, I., Morito, D., Natsuka, S., Romero, P., Sleno, B., Tremblay, L.O., Herscovics, A., Nagata, K., Hosokawa, N., 2006. EDEM3, a soluble EDEM homolog, enhances glycoprotein endoplasmic reticulum-associated degradation and mannose trimming. J. Biol. Chem. 281, 9650–8. doi:10.1074/jbc.M512191200

Hollien, J., Weissman, J.S., 2006. Decay of endoplasmic reticulum-localized mRNAs during the unfolded protein response. Science (80-.). doi:10.1126/science.1129631

Horn, S.C., Hanna, J., Hirsch, C., Volkwein, C., Schütz, A., Heinemann, U., Sommer, T., Jarosch, E., 2009. Usa1 Functions as a Scaffold of the HRD-Ubiquitin Ligase. Mol. Cell 36, 782–793. doi:10.1016/j.molcel.2009.10.015

Hosokawa, N., Kamiya, Y., Kamiya, D., Kato, K., Nagata, K., 2009. Human OS-9, a lectin required for glycoprotein endoplasmic reticulum-associated degradation, recognizes mannose-trimmed N-glycans. J. Biol. Chem. 284, 17061–8. doi:10.1074/jbc.M809725200

Hosokawa, N., Tremblay, L.O., You, Z., Herscovics, A., Wada, I., Nagata, K., 2003. Enhancement of endoplasmic reticulum (ER) degradation of misfolded Null Hong Kong alpha1-antitrypsin by human ER mannosidase I. J. Biol. Chem. 278, 26287–94. doi:10.1074/jbc.M303395200

Hosokawa, N., Wada, I., Natsuka, Y., Nagata, K., 2006. EDEM accelerates ERAD by preventing aberrant dimer formation of misfolded alpha1-antitrypsin. Genes Cells 11, 465–76. doi:10.1111/j.1365-2443.2006.00957.x

Huang, C., Harada, Y., Hosomi, A., Masahara-Negishi, Y., Seino, J., Fujihira, H., Funakoshi, Y., Suzuki, T., Dohmae, N., Suzuki, T., 2015. Endo-β-N-acetylglucosaminidase forms N-GlcNAc protein aggregates during ER-associated degradation in Ngly1-defective cells. Proc. Natl. Acad. Sci. 201414593. doi:10.1073/pnas.1414593112

Huang, C.H., Hsiao, H.T., Chu, Y.R., Ye, Y., Chen, X., 2013. Derlin2 protein facilitates HRD1-mediated retro-translocation of sonic hedgehog at the endoplasmic reticulum. J. Biol. Chem. 288, 25330–25339. doi:10.1074/jbc.M113.455212

Ikeuchi, K., Inada, T., 2016. Ribosome-associated Asc1/RACK1 is required for endonucleolytic cleavage induced by stalled ribosome at the 3’ end of nonstop mRNA. Sci. Rep. 6, 28234. doi:10.1038/srep28234

Ishimura, R., Nagy, G., Dotu, I., Zhou, H., Yang, X.-L., Schimmel, P., Senju, S., Nishimura, Y., Chuang, J.H., Ackerman, S.L., 2014. RNA function. Ribosome stalling induced by mutation of a CNS-specific tRNA causes neurodegeneration. Science 345, 455–9. doi:10.1126/science.1249749

Izawa, T., Tsuboi, T., Kuroha, K., Inada, T., Nishikawa, S. ichi, Endo, T., 2012. Roles of Dom34:Hbs1 in Nonstop Protein Clearance from Translocators for Normal Organelle Protein Influx. Cell Rep. 2, 447–453. doi:10.1016/j.celrep.2012.08.010

Jaiswal, H., Conz, C., Otto, H., Wölfle, T., Fitzke, E., Mayer, M.P., Rospert, S., 2011. The chaperone network connected to human ribosome-associated complex. Mol. Cell. Biol. 31, 1160–73. doi:10.1128/MCB.00986-10

Janzen, D.M., Frolova, L., Geballe, A.P., 2002. Inhibition of translation termination mediated by an interaction of eukaryotic release factor 1 with a nascent peptidyl-tRNA. Mol. Cell. Biol. 22,

8562–70.

Jarosch, E., Taxis, C., Volkwein, C., Bordallo, J., Finley, D., Wolf, D.H., Sommer, T., 2002. Protein dislocation from the ER requires polyubiquitination and the AAA-ATPase Cdc48. Nat. Cell Biol. 4, 134–9. doi:10.1038/ncb746

Johnson, A.E., van Waes, M.A., 1999. The translocon: a dynamic gateway at the ER membrane. Annu. Rev. Cell Dev. Biol. 15, 799–842. doi:10.1146/annurev.cellbio.15.1.799

Johnston, J.A., Ward, C.L., Kopito, R.R., 1998. Aggresomes: a cellular response to misfolded proteins. J. Cell Biol. 143, 1883–98.

Kalies, K.-U., Allan, S., Sergeyenko, T., Kröger, H., Römisch, K., 2005. The protein translocation channel binds proteasomes to the endoplasmic reticulum membrane. EMBO J. 24, 2284–93. doi:10.1038/sj.emboj.7600731

Kapp, L.D., Lorsch, J.R., 2004. The molecular mechanics of eukaryotic translation. Annu. Rev. Biochem. 73, 657–704. doi:10.1146/annurev.biochem.73.030403.080419

Kario, E., Tirosh, B., Ploegh, H.L., Navon, A., 2008. N-linked glycosylation does not impair proteasomal degradation but affects class I major histocompatibility complex presentation. J. Biol. Chem. 283, 244–254. doi:10.1074/jbc.M706237200

Khatter, H., Myasnikov, A.G., Natchiar, S.K., Klaholz, B.P., 2015. Structure of the human 80S ribosome. Nature 520, 640–645. doi:10.1038/nature14427

Kikkert, M., Hassink, G., Barel, M., Hirsch, C., van der Wal, F.J., Wiertz, E., 2001. Ubiquitination is essential for human cytomegalovirus US11-mediated dislocation of MHC class I molecules from the endoplasmic reticulum to the cytosol. Biochem. J. 358, 369–77.

Kim, D.I., Jensen, S.C., Noble, K.A., KC, B., Roux, K.H., Motamedchaboki, K., Roux, K.J., 2016. An improved smaller biotin ligase for BioID proximity labeling. Mol. Biol. Cell 27, 1188–1196. doi:10.1091/mbc.E15-12-0844

Kim, W., Spear, E.D., Ng, D.T.W., 2005. Yos9p Detects and Targets Misfolded Glycoproteins for ER-Associated Degradation. Mol. Cell 19, 753–764. doi:10.1016/j.molcel.2005.08.010

Klauer, A.A., van Hoof, A., 2012. Degradation of mRNAs that lack a stop codon: a decade of nonstop progress. Wiley Interdiscip. Rev. RNA 3, 649–60. doi:10.1002/wrna.1124

Klinge, S., Voigts-Hoffmann, F., Leibundgut, M., Arpagaus, S., Ban, N., 2011. Crystal structure of the eukaryotic 60S ribosomal subunit in complex with initiation factor 6. Science 334, 941–8. doi:10.1126/science.1211204

Koegl, M., Hoppe, T., Schlenker, S., Ulrich, H.D., Mayer, T.U., Jentsch, S., 1999. A novel ubiquitination factor, E4, is involved in multiubiquitin chain assembly. Cell. doi:10.1016/S0092-8674(00)80574-7

Komander, D., Rape, M., 2012. The Ubiquitin Code. http://dx.doi.org/10.1146/annurev-biochem-060310-170328.

Kononenko, A. V, Mitkevich, V.A., Dubovaya, V.I., Kolosov, P.M., Makarov, A.A., Kisselev, L.L., 2008. Role of the individual domains of translation termination factor eRF1 in GTP binding to eRF3. Proteins 70, 388–93. doi:10.1002/prot.21544

Korostelev, A.A., 2011. Structural aspects of translation termination on the ribosome. RNA 17,

1409–1421. doi:10.1261/rna.2733411

Kostallas, G., Löfdahl, P.A., Samuelson, P., 2011. Substrate profiling of tobacco Etch virus protease using a novel Fluorescence-Assisted whole-cell assay. PLoS One 6. doi:10.1371/journal.pone.0016136

Kostova, Z., Wolf, D.H., 2005. Importance of carbohydrate positioning in the recognition of mutated CPY for ER-associated degradation. J. Cell Sci. 118, 1485–92. doi:10.1242/jcs.01740

Kramer, G., Boehringer, D., Ban, N., Bukau, B., 2009. The ribosome as a platform for co-translational processing, folding and targeting of newly synthesized proteins. Nat. Struct. Mol. Biol. 16, 589–97. doi:10.1038/nsmb.1614

Law, G.L., Raney, A., Heusner, C., Morris, D.R., 2001. Polyamine Regulation of Ribosome Pausing at the Upstream Open Reading Frame of S-Adenosylmethionine Decarboxylase. J. Biol. Chem. doi:10.1074/jbc.M105944200

Lee, H.H., Kim, Y.-S., Kim, K.H., Heo, I., Kim, S.K., Kim, O., Kim, H.K., Yoon, J.Y., Kim, H.S., Kim, D.J., Lee, S.J., Yoon, H.J., Kim, S.J., Lee, B.G., Song, H.K., Kim, V.N., Park, C.-M., Suh, S.W., 2007. Structural and Functional Insights into Dom34, a Key Component of No-Go mRNA Decay. Mol. Cell 27, 938–950. doi:10.1016/j.molcel.2007.07.019

Lee, J.-H., Choi, J.M., Lee, C., Yi, K.J., Cho, Y., 2005. Structure of a peptide:N-glycanase-Rad23 complex: insight into the deglycosylation for denatured glycoproteins. Proc. Natl. Acad. Sci. U. S. A. 102, 9144–9. doi:10.1073/pnas.0502082102

Letzring, D.P., Wolf, A.S., Brule, C.E., Grayhack, E.J., 2013. Translation of CGA codon repeats in yeast involves quality control components and ribosomal protein L1. RNA. doi:10.1261/rna.039446.113

Li, E., Pedraza, A., Bestagno, M., Mancardi, S., Sanchez, R., Burrone, O., 1997. Mammalian cell expression of dimeric small immune proteins (SIP). Protein Eng. 10, 731–6.

Li, W., Schulman, S., Boyd, D., Erlandson, K., Beckwith, J., Rapoport, T.A., 2007. The Plug Domain of the SecY Protein Stabilizes the Closed State of the Translocation Channel and Maintains a Membrane Seal. Mol. Cell 26, 511–521. doi:10.1016/j.molcel.2007.05.002

Liao, S., Lin, J., Do, H., Johnson, A.E., 1997. Both Lumenal and Cytosolic Gating of the Aqueous ER Translocon Pore Are Regulated from Inside the Ribosome during Membrane Protein Integration 90, 31–41.

Lilley, B.N., Ploegh, H.L., 2004. A membrane protein required for dislocation of misfolded proteins from the ER. Nature 429, 834–40. doi:10.1038/nature02592

Lim, P.J., Danner, R., Liang, J., Doong, H., Harman, C., Srinivasan, D., Rothenberg, C., Wang, H., Ye, Y., Fang, S., Monteiro, M.J., 2009. Ubiquilin and p97/VCP bind erasin, forming a complex involved in ERAD. J. Cell Biol. 187, 201–17. doi:10.1083/jcb.200903024

Liu, Y., Choudhury, P., Cabral, C.M., Sifers, R.N., 1999. Oligosaccharide modification in the early secretory pathway directs the selection of a misfolded glycoprotein for degradation by the proteasome. J. Biol. Chem. 274, 5861–7.

Liu, Y., Hu, Y., Li, X., Niu, L., Teng, M., 2010. The crystal structure of the human nascent polypeptide-associated complex domain reveals a nucleic acid-binding region on the NACA subunit . Biochemistry 49, 2890–6. doi:10.1021/bi902050p

Lu, J., Deutsch, C., 2008. Electrostatics in the Ribosomal Tunnel Modulate Chain Elongation Rates. J. Mol. Biol. 384, 73–86. doi:10.1016/j.jmb.2008.08.089

Luke, G.A., Escuin, H., Felipe, P. De, Ryan, M.D., 2009. 2A to the Fore – Research, Technology and Applications. Biotechnol. Genet. Eng. Rev. 26, 223–260. doi:10.5661/bger-26-223

Lykke-Andersen, J., Bennett, E.J., 2014. Protecting the proteome: Eukaryotic cotranslational quality control pathways. J. Cell Biol. 204, 467–476. doi:10.1083/jcb.201311103

Lyumkis, D., Doamekpor, S.K., Bengtson, M.H., Lee, J.-W., Toro, T.B., Petroski, M.D., Lima, C.D., Potter, C.S., Carragher, B., Joazeiro, C.A.P., 2013. Single-particle EM reveals extensive conformational variability of the Ltn1 E3 ligase. Proc. Natl. Acad. Sci. U. S. A. 110, 1702–7. doi:10.1073/pnas.1210041110

Lyumkis, D., Oliveira dos Passos, D., Tahara, E.B., Webb, K., Bennett, E.J., Vinterbo, S., Potter, C.S., Carragher, B., Joazeiro, C.A.P., 2014. Structural basis for translational surveillance by the large ribosomal subunit-associated protein quality control complex. Proc. Natl. Acad. Sci. 111, 15981–15986. doi:10.1073/pnas.1413882111

Malsburg, K. von der, Shao, S., Hegde, R.S., 2015. The ribosome quality control pathway can access nascent polypeptides stalled at the Sec61 translocon. Mol. Biol. Cell 26, 2168–2180. doi:10.1091/mbc.E15-01-0040

Margottin, F., Bour, S.P., Durand, H., Selig, L., Benichou, S., Richard, V., Thomas, D., Strebel, K., Benarous, R., 1998. A Novel Human WD Protein, h-βTrCP, that Interacts with HIV-1 Vpu Connects CD4 to the ER Degradation Pathway through an F-Box Motif. Mol. Cell 1, 565–574. doi:10.1016/S1097-2765(00)80056-8

Matheisl, S., Berninghausen, O., Becker, T., Beckmann, R., 2015. Structure of a human translation termination complex 43, 8615–8626. doi:10.1093/nar/gkv909

Matsuo, Y., Ikeuchi, K., Saeki, Y., Iwasaki, S., Schmidt, C., Udagawa, T., Sato, F., Tsuchiya, H., Becker, T., Tanaka, K., Ingolia, N.T., Beckmann, R., Inada, T., 2017. Ubiquitination of stalled ribosome triggers ribosome-associated quality control. Nat. Commun. 8, 159. doi:10.1038/s41467-017-00188-1

Mbonye, U.R., Wada, M., Rieke, C.J., Tang, H.-Y., Dewitt, D.L., Smith, W.L., 2006. The 19-amino acid cassette of cyclooxygenase-2 mediates entry of the protein into the endoplasmic reticulum-associated degradation system. J. Biol. Chem. 281, 35770–8. doi:10.1074/jbc.M608281200

Meinecke, M., Cizmowski, C., Schliebs, W., Krüger, V., Beck, S., Wagner, R., Erdmann, R., 2010. The peroxisomal importomer constitutes a large and highly dynamic pore. Nat. Cell Biol. 12, 273–7. doi:10.1038/ncb2027

Melnikov, S., Ben-Shem, A., Garreau de Loubresse, N., Jenner, L., Yusupova, G., Yusupov, M., 2012. One core, two shells: bacterial and eukaryotic ribosomes. Nat. Struct. Mol. Biol. 19, 560–7. doi:10.1038/nsmb.2313

Metzger, M.B., Pruneda, J.N., Klevit, R.E., Weissman, A.M., 2014. RING-type E3 ligases: Master manipulators of E2 ubiquitin-conjugating enzymes and ubiquitination. Biochim. Biophys. Acta - Mol. Cell Res. doi:10.1016/j.bbamcr.2013.05.026

Misaghi, S., Pacold, M.E., Blom, D., Ploegh, H.L., Korbel, G.A., 2004. Using a small molecule inhibitor of peptide: N-glycanase to probe its role in glycoprotein turnover. Chem. Biol. 11, 1677–1687. doi:10.1016/j.chembiol.2004.11.010

Molinari, M., Calanca, V., Galli, C., Lucca, P., Paganetti, P., 2003. Role of EDEM in the release of misfolded glycoproteins from the calnexin cycle. Science 299, 1397–400. doi:10.1126/science.1079474

Morisaki, T., Lyon, K., DeLuca, K.F., DeLuca, J.G., English, B.P., Zhang, Z., Lavis, L.D., Grimm, J.B., Viswanathan, S., Looger, L.L., Lionnet, T., Stasevich, T.J., 2016. Real-time quantification of single RNA translation dynamics in living cells. Science (80-.). aaf0899. doi:10.1126/science.aaf0899

Morris, D.R., Geballe, A.P., 2000. Upstream open reading frames as regulators of mRNA translation. Mol. Cell. Biol. 20, 8635–42.

Mueller, B., Klemm, E.J., Spooner, E., Claessen, J.H., Ploegh, H.L., 2008. SEL1L nucleates a protein complex required for dislocation of misfolded glycoproteins. Proc. Natl. Acad. Sci. U. S. A. 105, 12325–30. doi:10.1073/pnas.0805371105

Nadav, E., Shmueli, A., Barr, H., Gonen, H., Ciechanover, A., Reiss, Y., 2003. A novel mammalian endoplasmic reticulum ubiquitin ligase homologous to the yeast Hrd1. Biochem. Biophys. Res. Commun. 303, 91–97. doi:10.1016/S0006-291X(03)00279-1

Nakatogawa, H., Ito, K., 2002. The Ribosomal Exit Tunnel Functions as a Discriminating Gate. Cell 108, 629–636. doi:10.1016/S0092-8674(02)00649-9

Nakatsukasa, K., Brodsky, J.L., 2009. The Recognition and Retrotranslocation of Misfolded Proteins from the Endoplasmic Reticulum 9, 861–870. doi:10.1111/j.1600-0854.2008.00729.x.The

Nakatsukasa, K., Huyer, G., Michaelis, S., Brodsky, J.L., 2008. Dissecting the ER-Associated Degradation of a Misfolded Polytopic Membrane Protein. Cell 132, 101–112. doi:10.1016/j.cell.2007.11.023

Neuber, O., Jarosch, E., Volkwein, C., Walter, J., Sommer, T., 2005. Ubx2 links the Cdc48 complex to ER-associated protein degradation. Nat. Cell Biol. 7, 993–8. doi:10.1038/ncb1298

Nissen, P., Hansen, J., Ban, N., Moore, P.B., Steitz, T.A., 2000. The structural basis of ribosome activity in peptide bond synthesis. Science 289, 920–30. doi:10.1126/science.289.5481.920

Nürenberg, E., Tampé, R., 2013. Tying up loose ends : ribosome recycling in eukaryotes and archaea. Trends Biochem. Sci. 38. doi:10.1016/j.tibs.2012.11.003

Nyathi, Y., Wilkinson, B.M., Pool, M.R., 2013. Co-translational targeting and translocation of proteins to the endoplasmic reticulum. Biochim. Biophys. Acta - Mol. Cell Res. 1833, 2392–2402. doi:10.1016/j.bbamcr.2013.02.021

Oda, Y., Okada, T., Yoshida, H., Kaufman, R.J., Nagata, K., Mori, K., 2006. Derlin-2 and Derlin-3 are regulated by the mammalian unfolded protein response and are required for ER-associated degradation. J. Cell Biol. 172, 383–93. doi:10.1083/jcb.200507057

Ohsaki, Y., Cheng, J., Fujita, A., Tokumoto, T., Fujimoto, T., 2006. Cytoplasmic lipid droplets are sites of convergence of proteasomal and autophagic degradation of apolipoprotein B. Mol. Biol. Cell 17, 2674–83. doi:10.1091/mbc.E05-07-0659

Okuda-Shimizu, Y., Hendershot, L.M., 2007. Characterization of an ERAD Pathway for Nonglycosylated BiP Substrates, which Require Herp. Mol. Cell 28, 544–554. doi:10.1016/j.molcel.2007.09.012

Olivari, S., Cali, T., Salo, K.E.H., Paganetti, P., Ruddock, L.W., Molinari, M., 2006. EDEM1 regulates ER-associated degradation by accelerating de-mannosylation of folding-defective polypeptides and by inhibiting their covalent aggregation. Biochem. Biophys. Res. Commun. 349, 1278–1284. doi:10.1016/j.bbrc.2006.08.186

Otto, H., Conz, C., Maier, P., Wölfle, T., Suzuki, C.K., Jenö, P., Rücknagel, P., Stahl, J., Rospert, S., 2005. The chaperones MPP11 and Hsp70L1 form the mammalian ribosome-associated complex. Proc. Natl. Acad. Sci. U. S. A. 102, 10064–9. doi:10.1073/pnas.0504400102

Oyadomari, S., Yun, C., Fisher, E.A., Kreglinger, N., Kreibich, G., Oyadomari, M., Harding, H.P., Goodman, A.G., Harant, H., Garrison, J.L., Taunton, J., Katze, M.G., Ron, D., 2006. Cotranslocational Degradation Protects the Stressed Endoplasmic Reticulum from Protein Overload. Cell 126, 727–739. doi:10.1016/j.cell.2006.06.051

Panasenko, O.O., 2014. The role of the E3 ligase Not4 in cotranslational quality control. Front. Genet. 5, 1–5. doi:10.3389/fgene.2014.00141

Parks, T.D., Howard, E.D., Wolpert, T.J., Arp, D.J., Dougherty, W.G., 1995. Expression and purification of a recombinant tobacco etch virus NIa proteinase: biochemical analyses of the full-length and a naturally occurring truncated proteinase form. Virology. doi:10.1006/viro.1995.1331

Pechmann, S., Willmund, F., Frydman, J., 2013. The Ribosome as a Hub for Protein Quality Control. Mol. Cell 49, 411–421. doi:10.1016/j.molcel.2013.01.020

Petris, G., Bestagno, M., Arnoldi, F., Burrone, O.R., 2014a. New tags for recombinant protein detection and O-glycosylation reporters. PLoS One 9, e96700. doi:10.1371/journal.pone.0096700

Petris, G., Casini, A., Sasset, L., Cesaratto, F., Bestagno, M., Cereseto, A., Burrone, O.R., 2014b. CD4 and BST-2/tetherin proteins retro-translocate from endoplasmic reticulum to cytosol as partially folded and multimeric molecules. J. Biol. Chem. doi:10.1074/jbc.M113.512368

Petris, G., Vecchi, L., Bestagno, M., Burrone, O.R., 2011. Efficient detection of proteins retro-translocated from the ER to the cytosol by In Vivo biotinylation. PLoS One 6, e23712. doi:10.1371/journal.pone.0023712

Pickart, C.M., Cohen, R.E., 2004. Proteasomes and their kin: proteases in the machine age. Nat. Rev. Mol. Cell Biol. 5, 177–187. doi:10.1038/nrm1336

Pickart, C.M., Eddins, M.J., 2004. Ubiquitin: structures, functions, mechanisms. Biochim. Biophys. Acta - Mol. Cell Res. 1695, 55–72. doi:10.1016/j.bbamcr.2004.09.019

Pilon, M., Schekman, R., Römisch, K., 1997. Sec61p mediates export of a misfolded secretory protein from the endoplasmic reticulum to the cytosol for degradation. EMBO J. 16, 4540–8. doi:10.1093/emboj/16.15.4540

Pisarev, A. V., Hellen, C.U.T., Pestova, T. V., 2007. Recycling of Eukaryotic Posttermination Ribosomal Complexes. Cell 131, 286–299. doi:10.1016/j.cell.2007.08.041

Pisarev, A. V., Skabkin, M.A., Pisareva, V.P., Skabkina, O. V., Rakotondrafara, A.M., Hentze, M.W., Hellen, C.U.T., Pestova, T. V., 2010. The Role of ABCE1 in Eukaryotic Posttermination Ribosomal Recycling. Mol. Cell 37, 196–210. doi:10.1016/j.molcel.2009.12.034

Pisareva, V.P., Skabkin, M.A., Hellen, C.U.T., Pestova, T. V, Pisarev, A. V, 2011. Dissociation by Pelota,

Hbs1 and ABCE1 of mammalian vacant 80S ribosomes and stalled elongation complexes. EMBO J. 30, 1804–1817. doi:10.1038/emboj.2011.93

Plemper, R.K., Böhmler, S., Bordallo, J., Sommer, T., Wolf, D.H., 1997. Mutant analysis links the translocon and BiP to retrograde protein transport for ER degradation. Nature 388, 891–5. doi:10.1038/42276

Ploegh, H.L., 2007. A lipid-based model for the creation of an escape hatch from the endoplasmic reticulum. Nature 448, 435–438. doi:10.1038/nature06004

Prakash, S., Tian, L., Ratliff, K.S., Lehotzky, R.E., Matouschek, A., 2004. An unstructured initiation site is required for efficient proteasome-mediated degradation. Nat. Struct. Mol. Biol. 11, 830–7. doi:10.1038/nsmb814

Predonzani, A., Arnoldi, F., López-Requena, A., Burrone, O.R., 2008. In vivo site-specific biotinylation of proteins within the secretory pathway using a single vector system. BMC Biotechnol. 8, 41. doi:10.1186/1472-6750-8-41

Preissler, S., Deuerling, E., 2012. Ribosome-associated chaperones as key players in proteostasis. Trends Biochem. Sci. 37, 274–283. doi:10.1016/j.tibs.2012.03.002

Quan, E.M., Kamiya, Y., Kamiya, D., Denic, V., Weibezahn, J., Kato, K., Weissman, J.S., 2008. Defining the Glycan Destruction Signal for Endoplasmic Reticulum-Associated Degradation, Molecular Cell. doi:10.1016/j.molcel.2008.11.017

Rabl, J., Leibundgut, M., Ataide, S.F., Haag, A., Ban, N., 2011. Crystal structure of the eukaryotic 40S ribosomal subunit in complex with initiation factor 1. Science 331, 730–6. doi:10.1126/science.1198308

Ramu, H., Vázquez-Laslop, N., Klepacki, D., Dai, Q., Piccirilli, J., Micura, R., Mankin, A.S., 2011. Nascent Peptide in the Ribosome Exit Tunnel Affects Functional Properties of the A-Site of the Peptidyl Transferase Center. Mol. Cell 41, 321–330. doi:10.1016/j.molcel.2010.12.031

Rape, M., Hoppe, T., Gorr, I., Kalocay, M., Richly, H., Jentsch, S., 2001. Mobilization of Processed, Membrane-Tethered SPT23 Transcription Factor by CDC48UFD1/NPL4, a Ubiquitin-Selective Chaperone. Cell 107, 667–677. doi:10.1016/S0092-8674(01)00595-5

Rapoport, T.A., 2007. Protein translocation across the eukaryotic endoplasmic reticulum and bacterial plasma membranes. Nature 450, 663–9. doi:10.1038/nature06384

Rapoport, T.A., Jungnickel, B., Kutay, U., 1996. Protein transport across the eukaryotic endoplasmic reticulum and bacterial inner membranes. Annu. Rev. Biochem. 65, 271–303. doi:10.1146/annurev.bi.65.070196.001415

Re, A., Waldron, L., Quattrone, A., 2016. Control of Gene Expression by RNA Binding Protein Action on Alternative Translation Initiation Sites. PLoS Comput. Biol. 12, e1005198. doi:10.1371/journal.pcbi.1005198

Reits, E.A., Benham, A.M., Plougastel, B., Neefjes, J., Trowsdale, J., 1997. Dynamics of proteasome distribution in living cells. EMBO J. 16, 6087–94. doi:10.1093/emboj/16.20.6087

Richly, H., Rape, M., Braun, S., Rumpf, S., Hoege, C., Jentsch, S., 2005. A Series of Ubiquitin Binding Factors Connects CDC48/p97 to Substrate Multiubiquitylation and Proteasomal Targeting. Cell 120, 73–84. doi:10.1016/j.cell.2004.11.013

Ron, D., Walter, P., 2007. Signal integration in the endoplasmic reticulum unfolded protein response. Nat. Rev. Mol. Cell Biol. doi:10.1038/nrm2199

Roux, K.J., Kim, D.I., Burke, B., 2013. BioID: A screen for protein-protein interactions. Curr. Protoc. Protein Sci. doi:10.1002/0471140864.ps1923s74

Ruan, H., Shantz, L.M., Pegg, A.E., Morris, D.R., 1996. The upstream open reading frame of the mRNA encoding S-adenosylmethionine decarboxylase is a polyamine-responsive translational control element. J. Biol. Chem. 271, 29576–82.

Rumpf, S., Jentsch, S., 2006. Functional Division of Substrate Processing Cofactors of the Ubiquitin-Selective Cdc48 Chaperone. Mol. Cell 21, 261–269. doi:10.1016/j.molcel.2005.12.014

Rutishauser, J., Spiess, M., 2002. Endoplasmic reticulum storage diseases. Swiss Med. Wkly. 132, 211–222.

Ryan, M.D., Donnelly, M., Lewis, A., Mehrotra, A.P., Wilkie, J., Gani, D., 1999. A Model for Nonstoichiometric, Cotranslational Protein Scission in Eukaryotic Ribosomes. Bioorg. Chem. 27, 55–79. doi:10.1006/bioo.1998.1119

Saito, S., Hosoda, N., Hoshino, S.I., 2013. The Hbs1-Dom34 protein complex functions in non-stop mRNA decay in mammalian cells. J. Biol. Chem. 288, 17832–17843. doi:10.1074/jbc.M112.448977

Sasset, L., 2013. Protein quality control: from ribosome to proteasome. PhD thesis.

Sasset, L., Petris, G., Cesaratto, F., Burrone, O.R., 2015. The VCP/p97 and YOD1 proteins have different substrate-dependent activities in endoplasmic reticulum-associated degradation (ERAD). J. Biol. Chem. 290, 28175–28188.

Sato, B.K., Schulz, D., Do, P.H., Hampton, R.Y., 2009. Misfolded Membrane Proteins Are Specifically Recognized by the Transmembrane Domain of the Hrd1p Ubiquitin Ligase. Mol. Cell 34, 212–222. doi:10.1016/j.molcel.2009.03.010

Schäfer, A., Wolf, D.H., 2009. Sec61p is part of the endoplasmic reticulum-associated degradation machinery. EMBO J. 28, 2874–84. doi:10.1038/emboj.2009.231

Schatz, P.J., 1993. Use of peptide libraries to map the substrate specificity of a peptide-modifying enzyme: a 13 residue consensus peptide specifies biotinylation in Escherichia coli. Biotechnology. (N. Y). 11, 1138–43.

Schmitz, A., Herrgen, H., Winkeler, A., Herzog, V., 2000. Cholera toxin is exported from microsomes by the Sec61p complex. J. Cell Biol. 148, 1203–12.

Schröder, M., Kaufman, R.J., 2005. ER stress and the unfolded protein response. Mutat. Res. Mol. Mech. Mutagen. 569, 29–63. doi:10.1016/j.mrfmmm.2004.06.056

Schubert, U., Antón, L.C., Gibbs, J., Norbury, C.C., Yewdell, J.W., Bennink, J.R., 2000. Rapid degradation of a large fraction of newly synthesized proteins by proteasomes. Nature 404, 770–4. doi:10.1038/35008096

Schulze, A., Standera, S., Buerger, E., Kikkert, M., van Voorden, S., Wiertz, E., Koning, F., Kloetzel, P.-M., Seeger, M., 2005. The Ubiquitin-domain Protein HERP forms a Complex with Components of the Endoplasmic Reticulum Associated Degradation Pathway., Journal of Molecular Biology. doi:10.1016/j.jmb.2005.10.020

Shan, S., Walter, P., 2005. Co-translational protein targeting by the signal recognition particle. FEBS Lett. 579, 921–926. doi:10.1016/j.febslet.2004.11.049

Shao, S., Brown, A., Santhanam, B., Hegde, R.S., 2015. Structure and assembly pathway of the ribosome quality control complex. Mol. Cell 57, 433–445. doi:10.1016/j.molcel.2014.12.015

Shao, S., Von der Malsburg, K., Hegde, R.S., 2013. Listerin-dependent nascent protein ubiquitination relies on ribosome subunit dissociation. Mol. Cell 50, 637–648. doi:10.1016/j.molcel.2013.04.015

Sharma, P., Yan, F., Doronina, V.A., Escuin-Ordinas, H., Ryan, M.D., Brown, J.D., 2012. 2A peptides provide distinct solutions to driving stop-carry on translational recoding. Nucleic Acids Res. 40, 3143–3151. doi:10.1093/nar/gkr1176

Shcherbik, N., Chernova, T.A., Chernoff, Y.O., Pestov, D.G., 2016. Distinct types of translation termination generate substrates for ribosome-associated quality control. Nucleic Acids Res. 44, 6840–6852. doi:10.1093/nar/gkw566

Shcherbik, N., Haines, D.S., 2007. Cdc48pNpl4p/Ufd1p Binds and Segregates Membrane-Anchored/Tethered Complexes via a Polyubiquitin Signal Present on the Anchors. Mol. Cell 25, 385–397. doi:10.1016/j.molcel.2007.01.024

Shimizu, Y., Okuda-Shimizu, Y., Hendershot, L.M., 2010. Ubiquitylation of an ERAD Substrate Occurs on Multiple Types of Amino Acids. Mol. Cell 40, 917–926. doi:10.1016/j.molcel.2010.11.033

Shoemaker, C.J., Green, R., 2012. Translation drives mRNA quality control. Nat. Struct. Mol. Biol. 19, 594–601. doi:10.1038/nsmb.2301

Shoemaker, C.J., Green, R., 2011. Kinetic analysis reveals the ordered coupling of translation termination and ribosome recycling in yeast. Proc. Natl. Acad. Sci. U. S. A. 108, E1392-8. doi:10.1073/pnas.1113956108

Sitron, C.S., Park, J.H., Brandman, O., 2017. Asc1, Hel2, and Slh1 couple translation arrest to nascent chain degradation. RNA. doi:10.1261/rna.060897.117

Smith, D.M., Chang, S.-C., Park, S., Finley, D., Cheng, Y., Goldberg, A.L., 2007. Docking of the Proteasomal ATPases' Carboxyl Termini in the 20S Proteasome's α Ring Opens the Gate for Substrate Entry. Mol. Cell 27, 731–744. doi:10.1016/j.molcel.2007.06.033

Song, H., Mugnier, P., Das, A.K., Webb, H.M., Evans, D.R., Tuite, M.F., Hemmings, B.A., Barford, D., 2000. The Crystal Structure of Human Eukaryotic Release Factor eRF1—Mechanism of Stop Codon Recognition and Peptidyl-tRNA Hydrolysis. Cell 100, 311–321. doi:10.1016/S0092-8674(00)80667-4

Spevak, C.C., Ivanov, I.P., Sachs, M.S., 2010. Sequence requirements for ribosome stalling by the arginine attenuator peptide. J. Biol. Chem. 285, 40933–42. doi:10.1074/jbc.M110.164152

Spreter, T., Pech, M., Beatrix, B., 2005. The crystal structure of archaeal nascent polypeptide-associated complex (NAC) reveals a unique fold and the presence of a ubiquitin-associated domain. J. Biol. Chem. 280, 15849–54. doi:10.1074/jbc.M500160200

Steitz, T.A., 2008. A structural understanding of the dynamic ribosome machine. Nat. Rev. Mol. Cell Biol. 9, 242–253. doi:10.1038/nrm2352

Stricher, F., Macri, C., Ruff, M., Muller, S., 2013. HSPA8/HSC70 chaperone protein: Structure,

function, and chemical targeting. Autophagy 9, 1937–1954. doi:10.4161/auto.26448

Suzuki, T., 2007. Cytoplasmic peptide:N-glycanase and catabolic pathway for free N-glycans in the cytosol. Semin. Cell Dev. Biol. 18, 762–769. doi:10.1016/j.semcdb.2007.09.010

Suzuki, T., Huang, C., Fujihira, H., 2016. The cytoplasmic peptide:N-glycanase (NGLY1) - Structure, expression and cellular functions. Gene 577, 1–7. doi:10.1016/j.gene.2015.11.021

Suzuki, T., Park, H., Anderson Till, E., Lennarz, W.J., 2001. The PUB Domain: A Putative Protein–Protein Interaction Domain Implicated in the Ubiquitin-Proteasome Pathway. Biochem. Biophys. Res. Commun. 287, 1083–1087. doi:10.1006/bbrc.2001.5688

Swanson, R., Locher, M., Hochstrasser, M., 2001. A conserved ubiquitin ligase of the nuclear envelope/endoplasmic reticulum that functions in both ER-associated and Matalpha2 repressor degradation. Genes Dev. 15, 2660–74. doi:10.1101/gad.933301

Szathmary, R., Bielmann, R., Nita-Lazar, M., Burda, P., Jakob, C.A., 2005. Yos9 Protein Is Essential for Degradation of Misfolded Glycoproteins and May Function as Lectin in ERAD. Mol. Cell 19, 765–775. doi:10.1016/j.molcel.2005.08.015

Takeda, Y., Totani, K., Matsuo, I., Ito, Y., 2009. Chemical approaches toward understanding glycan-mediated protein quality control. Curr. Opin. Chem. Biol. 13, 582–591. doi:10.1016/j.cbpa.2009.09.011

Taxis, C., Hitt, R., Park, S.-H., Deak, P.M., Kostova, Z., Wolf, D.H., 2003. Use of modular substrates demonstrates mechanistic diversity and reveals differences in chaperone requirement of ERAD. J. Biol. Chem. 278, 35903–13. doi:10.1074/jbc.M301080200

Tirosh, B., Furman, M.H., Tortorella, D., Ploegh, H.L., 2003. Protein unfolding is not a prerequisite for endoplasmic reticulum-to-cytosol dislocation. J. Biol. Chem. doi:10.1074/jbc.M210158200

Tsuboi, T., Kuroha, K., Kudo, K., Makino, S., Inoue, E., Kashima, I., Inada, T., 2012. Dom34:Hbs1 Plays a General Role in Quality-Control Systems by Dissociation of a Stalled Ribosome at the 3′ End of Aberrant mRNA. Mol. Cell 46, 518–529. doi:10.1016/j.molcel.2012.03.013

Uchiyama-Kadokura, N., Murakami, K., Takemoto, M., Koyanagi, N., Murota, K., Naito, S., Onouchi, H., 2014. Polyamine-responsive ribosomal arrest at the stop codon of an upstream open reading frame of the AdoMetDC1 gene triggers nonsense-mediated mRNA decay in Arabidopsis thaliana. Plant Cell Physiol. doi:10.1093/pcp/pcu086

van Wijk, S.J.L., Timmers, H.T.M., 2010. The family of ubiquitin-conjugating enzymes (E2s): deciding between life and death of proteins. FASEB J. 24, 981–93. doi:10.1096/fj.09-136259

Vashist, S., Ng, D.T.W., 2004. Misfolded proteins are sorted by a sequential checkpoint mechanism of ER quality control. J. Cell Biol. 165, 41–52. doi:10.1083/jcb.200309132

Vecchi, L., Petris, G., Bestagno, M., Burrone, O.R., 2012. Selective targeting of proteins within secretory pathway for endoplasmic reticulum-associated degradation. J. Biol. Chem. 287, 20007–20015. doi:10.1074/jbc.M112.355107

Vembar, S.S., Brodsky, J.L., 2009. One step at a time: endoplasmic reticulum-associated degradation 9, 944–957. doi:10.1038/nrm2546.One

Verma, R., Oania, R.S., Kolawa, N.J., Deshaies, R.J., 2013. Cdc48/p97 promotes degradation of aberrant nascent polypeptides bound to the ribosome. Elife 2013, 1–17.

doi:10.7554/eLife.00308

Voges, D., Zwickl, P., Baumeister, W., 1999. The 26S proteasome: a molecular machine designed for controlled proteolysis. Annu. Rev. Biochem. 68, 1015–68. doi:10.1146/annurev.biochem.68.1.1015

Voorhees, R.M., Fernández, I.S., Scheres, S.H.W., Hegde, R.S., 2014. Structure of the mammalian ribosome-Sec61 complex to 3.4 Å resolution. Cell 157, 1632–43. doi:10.1016/j.cell.2014.05.024

Wahlman, J., DeMartino, G.N., Skach, W.R., Bulleid, N.J., Brodsky, J.L., Johnson, A.E., 2007. Real-Time Fluorescence Detection of ERAD Substrate Retrotranslocation in a Mammalian In Vitro System. Cell 129, 943–955. doi:10.1016/j.cell.2007.03.046

Wallrapp, C., Verrier, S.-B., Zhouravleva, G., Philippe, H., Philippe, M., Gress, T.M., Jean-Jean, O., 1998. The product of the mammalian orthologue of the Saccharomyces cerevisiae HBS1 gene is phylogenetically related to eukaryotic release factor 3 (eRF3) but does not carry eRF3-like activity. FEBS Lett. 440, 387–392. doi:10.1016/S0014-5793(98)01492-6

Walter, J., Urban, J., Volkwein, C., Sommer, T., 2001. Sec61p-independent degradation of the tail-anchored ER membrane protein Ubc6p. EMBO J. 20, 3124–31. doi:10.1093/emboj/20.12.3124

Walter, P., Ron, D., 2011. The unfolded protein response: From stress pathway to homeostatic regulation. Science (80-.). 334, 1081–1086. doi:10.1126/science.1209038

Wang, J., Lee, J., Liem, D., Ping, P., 2017. HSPA5 Gene encoding Hsp70 chaperone BiP in the endoplasmic reticulum. Gene 618, 14–23. doi:10.1016/j.gene.2017.03.005

Wang, Z., Sachs, M.S., 1997. Ribosome stalling is responsible for arginine-specific translational attenuation in Neurospora crassa. Mol. Cell. Biol. 17, 4904–13.

Wei, J., Gaut, J.R., Hendershot, L.M., 1995. In vitro dissociation of BiP-peptide complexes requires a conformational change in BiP after ATP binding but does not require ATP hydrolysis. J. Biol. Chem. 270, 26677–82.

Whitley, P., Nilsson, I., Von Heijne, G., 1996. A nascent secretory protein may traverse the ribosome/endoplasmic reticulum translocase complex as an extended chain. J. Biol. Chem. doi:10.1074/jbc.271.11.6241

Wiedmann, B., Sakai, H., Davis, T.A., Wiedmann, M., 1994. A protein complex required for signal-sequence-specific sorting and translocation. Nature 370, 434–40. doi:10.1038/370434a0

Wiertz, E.J.H.J., Jones, T.R., Sun, L., Bogyo, M., Geuze, H.J., Ploegh, H.L., 1996. The human cytomegalovirus US11 gene product dislocates MHC class I heavy chains from the endoplasmic reticulum to the cytosol. Cell 84, 769–779. doi:10.1016/S0092-8674(00)81054-5

Wilson, D.N., Arenz, S., Beckmann, R., 2016. Translation regulation via nascent polypeptide-mediated ribosome stalling. Curr. Opin. Struct. Biol. 37, 123–33. doi:10.1016/j.sbi.2016.01.008

Wilson, D.N., Beckmann, R., 2011. The ribosomal tunnel as a functional environment for nascent polypeptide folding and translational stalling. Curr. Opin. Struct. Biol. 21, 274–282. doi:10.1016/j.sbi.2011.01.007

Wu, B., Eliscovich, C., Yoon, Y.J., Singer, R.H., 2016. Translation dynamics of single mRNAs in live

cells and neurons. Science (80-.). aaf1084. doi:10.1126/science.aaf1084

Xia, D., Tang, W.K., Ye, Y., 2016. Structure and function of the AAA+ ATPase p97/Cdc48p. Gene 583, 64–77. doi:10.1016/j.gene.2016.02.042

Xie, W., Kanehara, K., Sayeed, A., Ng, D.T.W., 2009. Intrinsic conformational determinants signal protein misfolding to the Hrd1/Htm1 endoplasmic reticulum-associated degradation system. Mol. Biol. Cell 20, 3317–29. doi:10.1091/mbc.E09-03-0231

Yamashita, Y., Takamatsu, S., Glasbrenner, M., Becker, T., Naito, S., Beckmann, R., 2017. Sucrose sensing through nascent peptide-meditated ribosome stalling at the stop codon of *Arabidopsis bZIP11* uORF2. FEBS Lett. 591, 1266–1277. doi:10.1002/1873-3468.12634

Yan, F., Doronina, V. a, Sharma, P., Brown, J.D., 2010. Orchestrating ribosomal activity from inside: effects of the nascent chain on the peptidyltransferase centre. Biochem. Soc. Trans. 38, 1576–1580. doi:10.1042/BST0381576

Yang, J., Hao, X., Cao, X., Liu, B., Nyström, T., 2016. Spatial sequestration and detoxification of huntingtin by the ribosome quality control complex. Elife 5, 1–14. doi:10.7554/eLife.11792

Yao, T., Cohen, R.E., 2002. A cryptic protease couples deubiquitination and degradation by the proteasome. Nature 419, 403–7. doi:10.1038/nature01071

Yap, M.-N., Bernstein, H.D., 2009. The Plasticity of a Translation Arrest Motif Yields Insights into Nascent Polypeptide Recognition inside the Ribosome Tunnel. Mol. Cell 34, 201–211. doi:10.1016/j.molcel.2009.04.002

Ye, Y., Meyer, H.H., Rapoport, T.A., 2001. The AAA ATPase Cdc48/p97 and its partners transport proteins from the ER into the cytosol. Nature 414, 652–6. doi:10.1038/414652a

Ye, Y., Shibata, Y., Kikkert, M., van Voorden, S., Wiertz, E., Rapoport, T.A., 2005. Recruitment of the p97 ATPase and ubiquitin ligases to the site of retrotranslocation at the endoplasmic reticulum membrane. Proc. Natl. Acad. Sci. U. S. A. 102, 14132–8. doi:10.1073/pnas.0505006102

Yordanova, M.M., Loughran, G., Alexander, V., Mariotti, M., Kiniry, S.J., Connor, P.B.F.O., Andreev, D.E., Tzani, I., Saffert, P., Michel, A.M., Gladyshev, V.N., Papkovsky, D.B., Atkins, J.F., Pavel, V., 2018. AMD1 mRNA employs ribosome stalling as a mechanism for molecular memory formation. Nat. Publ. Gr. 19. doi:10.1038/nature25174

Yoshida, Y., Tanaka, K., 2010. Lectin-like ERAD players in ER and cytosol. Biochim. Biophys. Acta - Gen. Subj. 1800, 172–180. doi:10.1016/j.bbagen.2009.07.029

Yu, H., Kopito, R.R., 1999. The role of multiubiquitination in dislocation and degradation of the alpha subunit of the T cell antigen receptor. J. Biol. Chem. 274, 36852–8.

Zhang, J.X., Braakman, I., Matlack, K.E., Helenius, A., 1997. Quality control in the secretory pathway: the role of calreticulin, calnexin and BiP in the retention of glycoproteins with C-terminal truncations. Mol. Biol. Cell 8, 1943–54.

Zhang, Y., Berndt, U., Gölz, H., Tais, A., Oellerer, S., Wölfle, T., Fitzke, E., Rospert, S., 2012. NAC functions as a modulator of SRP during the early steps of protein targeting to the endoplasmic reticulum. Mol. Biol. Cell 23, 3027–40. doi:10.1091/mbc.E12-02-0112

Zhong, X., Shen, Y., Ballar, P., Apostolou, A., Agami, R., Fang, S., 2004. AAA ATPase p97/valosin-containing protein interacts with gp78, a ubiquitin ligase for endoplasmic reticulum-

associated degradation. J. Biol. Chem. 279, 45676–84. doi:10.1074/jbc.M409034200

Zhong, Y., Shen, H., Wang, Y., Yang, Y., Yang, P., Fang, S., 2015. Identification of ERAD components essential for dislocation of the null Hong Kong variant of α-1-antitrypsin (NHK). Biochem. Biophys. Res. Commun. 458, 424–428. doi:10.1016/j.bbrc.2015.01.133

Zhu, K., Zhou, X., Yan, Y., Mo, H., Xie, Y., Cheng, B., Fan, J., 2016. Cleavage of fusion proteins on the affinity resins using the TEV protease variant. Protein Expr. Purif. doi:10.1016/j.pep.2016.02.003